University of Stavanger

Faculty of Science and Technology

MASTER THESIS

Study program/Specialization: MSc Petroleum Geosciences Engineering	Spring semester, 2016 Open / Restricted access
Writer: Ekaterina Gulyaeva	(Writer's signature)

Faculty supervisor: Rodmar Ravnås, University of Stavanger, A/S Norske Shell

External supervisor(s): Jord de Boer, A/S Norske Shell

Thesis title:

Permo-Triassic Rifting and Post-Rift Halokinesis in the Norwegian-Danish Basin

Credits (ECTS): 30

Key words: Norwegian-Danish Basin Tectono-stratigraphic evolution Salt tectonics Halokinesis Sub- and supra-salt plays Salt related trapping styles	Pages: 88 Enclosure: CD Stavanger, 15th June 2016

Permo-Triassic rifting and post-rift halokinesis in the Norwegian-Danish Basin

by

Ekaterina Gulyaeva

MSc Thesis

Presented to the Faculty of Science and Technology

University of Stavanger

University of Stavanger

2016

ACKNOWLEDGEMENTS

First and furthermost, I express my deepest gratitude to my supervisors Rodmar Ravnås and Jord de Boer for their kind supervision, patient guidance, numerous discussion and constructive critics. A/S Norske Shell is gratefully acknowledged for providing access to the seismic and well data, software access along with the workstation during the project.

I extend my gratitude to the whole exploration department of A/S Norske Shell for their help and suggestions. Members of the Norwegian-Danish basin APA 2016 exploration team, Heather Campbell, Kerr Greenaway, Tom Sandison and Ingelin Lunde are gratefully acknowledged for their support, discussions and comments. John Willoughby, Marcela Lorenzo and Morris Becker are thanked for their support, inspiring conversations and sharing their working and life experiences.

Permo-Triassic rifting and post-rift halokinesis in the Norwegian-Danish Basin

ABSTRACT

The area of investigation is located in the Norwegian sector of the Norwegian-Danish Basin (NDB) and covers an area of ~20,000 km^2 between the Stavanger Platform and the Central Graben. This basin is a Late Permian rift-basin, where the Upper Permian evaporite-dominated Zechstein Group was accumulated, followed by the deposition of a thick package of Triassic continental strata. The presence of an extensive and thick salt unit within the NDB has significantly influenced patterns of post-salt sedimentation and tectonics in the area during the Mesozoic to the Cenozoic. Furthermore, halokinetic movements control the distribution and geometry of reservoirs, various structural styles, and trapping mechanisms.

The Norwegian part of the NDB is relatively unexplored primarily due to perceive of working petroleum system, and is related to the little understood trapping configurations and uncertain reservoir distribution. In this study, 2D and 3D seismic surveys, well data and analogues are used to map and investigate the tectono-stratigraphic evolution of the NDB from the Late Permian to the Triassic with emphasis given to salt tectonics and its impact on distribution and characteristics of sub- and supra-salt play potential.

The post-Hercynian structural evolution of the NDB commenced with the formation of interior sag basins in the Middle-Late Permian. Subsequently, East-West extension took place in the Late Permian, producing sub-salt faults and tectonic domains. The Triassic halokinetic movements were a response to differential loading and reactivation of sub-salt normal faults, which in turn resulted in pod-intrapod structural styles and sedimentary architecture.

Halokinesis is a principal mechanism within the NDB controlling generation and distribution of the main elements that comprise plays and petroleum systems. For the sub-salt play potential, salt acts as a regional impermeable caprock. For supra-salt plays, halokinetic movements control the distribution of reservoirs and a wide range of trap styles, provide seal against the salt structures, and control access to charge from sub-salt source rocks to supra-salt plays through salt windows in areas with grounded Triassic pods. Identified sub-salt Upper Permian, supra-salt Lower and Upper Triassic plays are poorly explored plays with a candidate petroleum system. The plays are widely represented within the NDB and can form viable exploration targets in the future.

Contents

List of Figures

List of Tables

List of Appendixes

1. Introduction

1.1. Objectives and Rationale

Salt has played an important role in petroleum exploration by generation of salt related traps, forming a competent seal and as well acting as a heat conductor. Some of the world's largest hydrocarbon discoveries (Figure 1) are related to salt-influenced sedimentary basins between sub- and supra-salt reservoirs (for instance, Campos Basin, Santos Basin, Gulf of Mexico, Zagros Basin, Lower Congo Basin and North Sea). A clear understanding of salt tectonics distribution and its influence on syn- and post-kinematic sedimentation is one of the key elements for successful petroleum exploration in these basins. Semi-regional investigation of salt related structures will give an overview about the supra-salt prospectivity of an area, as salt can control the accommodation space for reservoirs and source rock successions, along with their thermal evolution due to high thermal conductivity parameters of salt. Halokinesis accordingly has a fundamental control on supra-salt hydrocarbon fairways and generation of structural and stratigraphic traps.

The main objectives of this thesis are to investigate salt related structural evolution of the Norwegian-Danish Basin with focusing on:

- Salt structuring, distribution and its variations in thickness;
- Influence on distribution and characteristics of sub- and supra-salt play potential with emphasis given to 1) Rotliegend and 2) Lower and Upper Triassic plays.

The rationale for the study is to eliminate a gap in the present day literature, solve poorly understood problem regarding to salt impact of structural history and play potential within the Norwegian-Danish Basin.

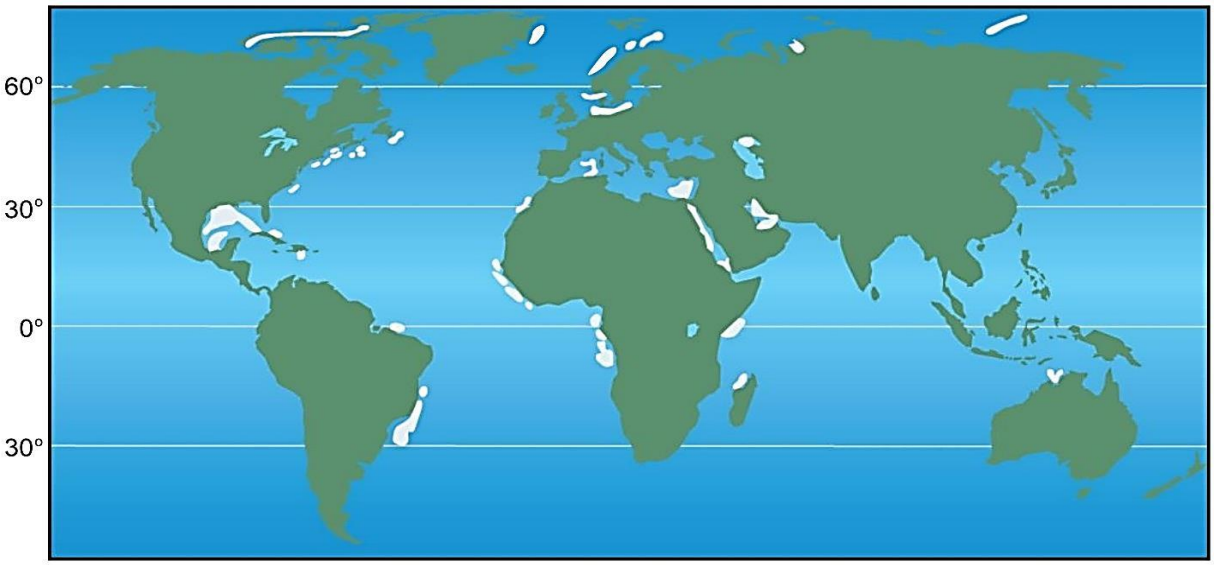

Figure 1. Distribution of offshore basins (modified from Farmer et al., 1996).

1.2. Background of Salt Tectonics

Salt stratigraphic units are fundamentally involved in the structuralization of many sedimentary basins, such as passive margin basins, foreland basins and cratonic basins in various tectonic domains, including contractional, extensional and strike-slip settings. The impact of salt during various deformation refer to the thickness of salt layer, its stratigraphic location and regional distribution, the properties of overburden strata and the intensity of basement-involved strictures (*Fossen, 2010).*

Salt has unique deformation style, occurring on regional scale and creating various salt structures from linear and point source (Figure 2). Elongated structures, rising from line sources, are developing from the salt rollers to salt-wall canopies due to increasing in maturity. This type of structures took their origin due to reactivation of subsalt faults and folding during contractional regime (*Fossen, 2010).* Structures, belonging to point sources, are growing from salt pillows at early stage to reactivated salt sheets at more mature stage (*Hudec and Jackson, 2007).*

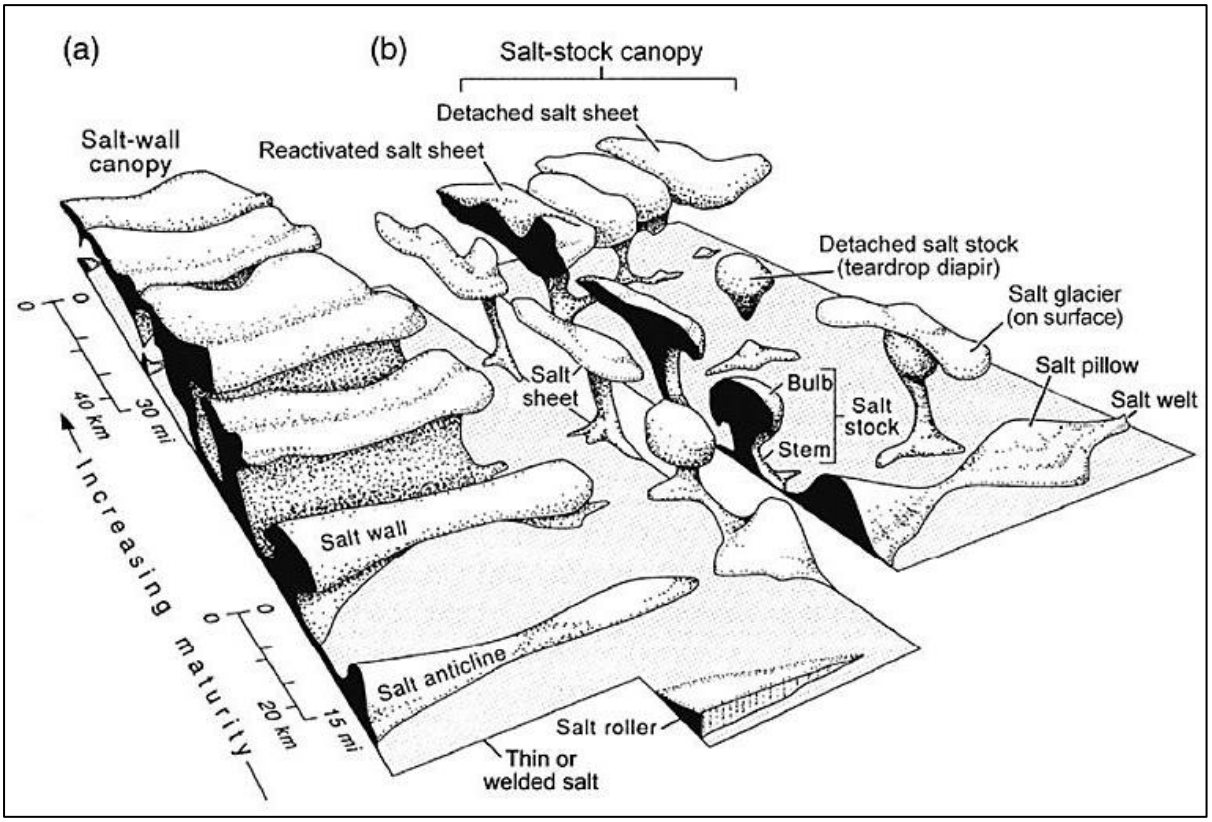

Figure 2. Main types of salt structures from linear sources (A) and from point sources (B) by Hudec and Jackson, 2007.

Salt is a very viscous and rheologically weak material, liable to lateral and upward movements at low temperatures and during relatively long period of time. Hence, halokinetic movements deform surrounding sediments resulting in faulting and folding. Due to impermeable and viscous properties of salt, it forms very efficient seals and caprocks along with juxtaposition to the salt wall. Salt is able to reach hundreds of meters in thickness regarding to seawater evaporation (Fossen, 2010; Farmer et al., 1996).

The density of salt layers is lower than most rocks, 2.160 g/cm^3 even after burial, while surrounding sediments become compacted and increasingly denser then salt. The differences in density between the mother layer of salt and overlying sediments along with buoyant properties of salt buried to a certain depth result in flow of salt toward the surface due to gravitationally unstable situation (Fossen, 2010). Overall, there are four significant mechanisms, which cause salt to move: gravitational and differential loading, displacement loading and thermal loading (Fossen, 2010). In addition, heterogeneity in viscosity, temperature and lateral changes in thickness between the salt and the overlying sediments affects a significant halokinetic movement (Allen and Allen, 2013). For instance, if the overburden sediments resist to halokinesis, so it is sufficient to trigger upward movements and formation of salt domes and pillow structure. From another side, if there is no resistance from overburden strata, salt will mostly create fault arrays and squeeze through the strata (Farmer et al., 1996).

Furthermore, salt has high thermal conductivity. Salt structures behave like heat pipes for conduction, decreasing their temperature and increasing overlying one; therefore, it can vertically shift gas and oil windows in flanks of sediments (Fossen, 2010).

Originally, the seismic velocity of salt is more than twice higher in comparison with velocity of the surrounding rocks, 4400 m/sec (Farmer et al., 1996). This difference affects seismic imaging in irregularly shaped interface between salt and sediments with reflecting and refracting seismic energy along with velocity pull-up below the salt. Extra salt parameters are summarized in the table below (Table 1).

– Low density: 2.160 g/cm^3	– High thermal conductivity
– High seismic wave velocity: 4400 m/sec	– Almost incompressible
– Young's modulus (E): 40 GPa	– Impermeable (good plugs and juxtapositions)
– Poisson's ratio (υ): ~ 0.39	– Behaves as a décollement
– Viscous (like a fluid)	– Influence regional deformations
– Mechanically weak	– Generates structural and stratigraphic traps

Table 1. Summarized information of salt properties (Fossen, 2010, Farmer et al., 1996).

1.3. Play definition

A **play** is defined as a group of fields and prospects having a chance for good quality reservoir, charge from the source rock, regional top seal and trap and belonging to a geologically related stratigraphic unit in a basin. The key elements, comprising play and petroleum system are describing in more details below (Allen and Allen, 2013):

- *a reservoir succession*, characterizing with good porosity and permeability qualities, and accomplished for storage of hydrocarbons and providing commercial rates at the wellbore;
- *a regional top seal for the reservoir unit*, with is sealing the petroleum in the gross reservoir unit;
- *a petroleum charge system*, which comprises source rock capable for generating and expelling hydrocarbons, and a migration pathway toward traps in the gross reservoir unit;
- *the timely relationship*, critical moment or interactive/distractive manner, when all petroleum system elements are available.

A **play segment** is a subdivision of a geological plays, showing an abrupt and significant change in geological model. The boundaries should be consistent with geological controls of the area, that influence chance of success, for example, facies boundaries, structural domains, trapping styles and their distribution, VRE boundary and migration focus area. The subdivision of play segments is based on the hierarchy:

1) Gross Depositional Environment (GDE);

2) Structural style or trap;

3) Business/geopolitical boundaries;

4) Others parameters.

1.4. Previous Studies of the Norwegian-Danish Basin

In the North Sea the evolution of salt structures has been focused on the Central Trough (Stewart and Coward, 1995; Buchanan et al., 1995; Bishop, 1996) and the Danish part of the Norwegian-Danish Basin (Petersen et al., 2008). In contrast, there have been just a few studies covering the Norwegian part of the Norwegian-Danish Basin.

The tectonic development of main structural elements of the southern part of the Norwegian North Sea (Central Graben, Vestland Arch, Norwegian-Danish Basin and Fennoscandian Border Zone) are well known from several publications Ziegler (1981, 1982), Hamar et al. (1980), Rønnevik et al. (1975), and Skjerven et al. (1983), but just presented on the regional scale. Regional mapping of top of Zechstein Group (Late Permian) and major fault was carried in the central North Sea with identifying salt tectonic zones. For instance, Bishop (1996) has proposed three separate salt tectonics zones in the Central Graben: Zone 1, an area of supra-Zechstein Group extensional faulting on the platform west of the Central Graben; Zone 2, a deep basinal region characterized by less faulting above salt and thick salt strata along with formation of salt diapirs; Zone 3, relatively stable region without any fault activity and halokinesis. Recent studies by Karlo et al. (2014) defined five major domains of differing salt tectonic types, related to lateral displacement of combination contractional and extensional structures, which took their origin due to gravity sliding and decoupled rift extension. Possible mechanisms for different salt tectonics domain are extension in the eastern part of the Norwegian-Danish Basin during Triassic, footwall uplift of Central Graben in Triassic, and thermal doming, which have occurred earlier (Karlo et al., 2014). Another research by Pedersen et al. (2006) was aimed to investigate the thermal maturity and source-rock potential of the Paleozoic marine and continental sediments. The study suggests, that the Permian marine Kupferschiefer from Norwegian offshore well 25/10-2 is an oil-prone Type II source rock, with a high petroleum potential (Pedersen et al., 2006).

To summarize all the information that has been mentioned above, there is a significant existing knowledge gap regarding to correlation and connectivity between different salt-tectonics zones and impact on play potential, more specifically on trapping styles, seal characteristics, reservoir distribution and fluid migration from the source rock.

2. Regional Tectonic and Stratigraphic Framework

2.1. Location of the Study Area

This study, related to the salt tectonics and its influence on petroleum elements, is located in the Norwegian-Danish Basin (NDB). This basin belongs to the southern part of the Norwegian Continental Shelf and is situated in the offshore area north-northwest of Denmark, south-southwest of Norway and east of Scotland (Figure 3). The investigated area covers approximately 20,000 km^2. The area is underexplored and no major discoveries have been made in the Norwegian sector of the NDB to date.

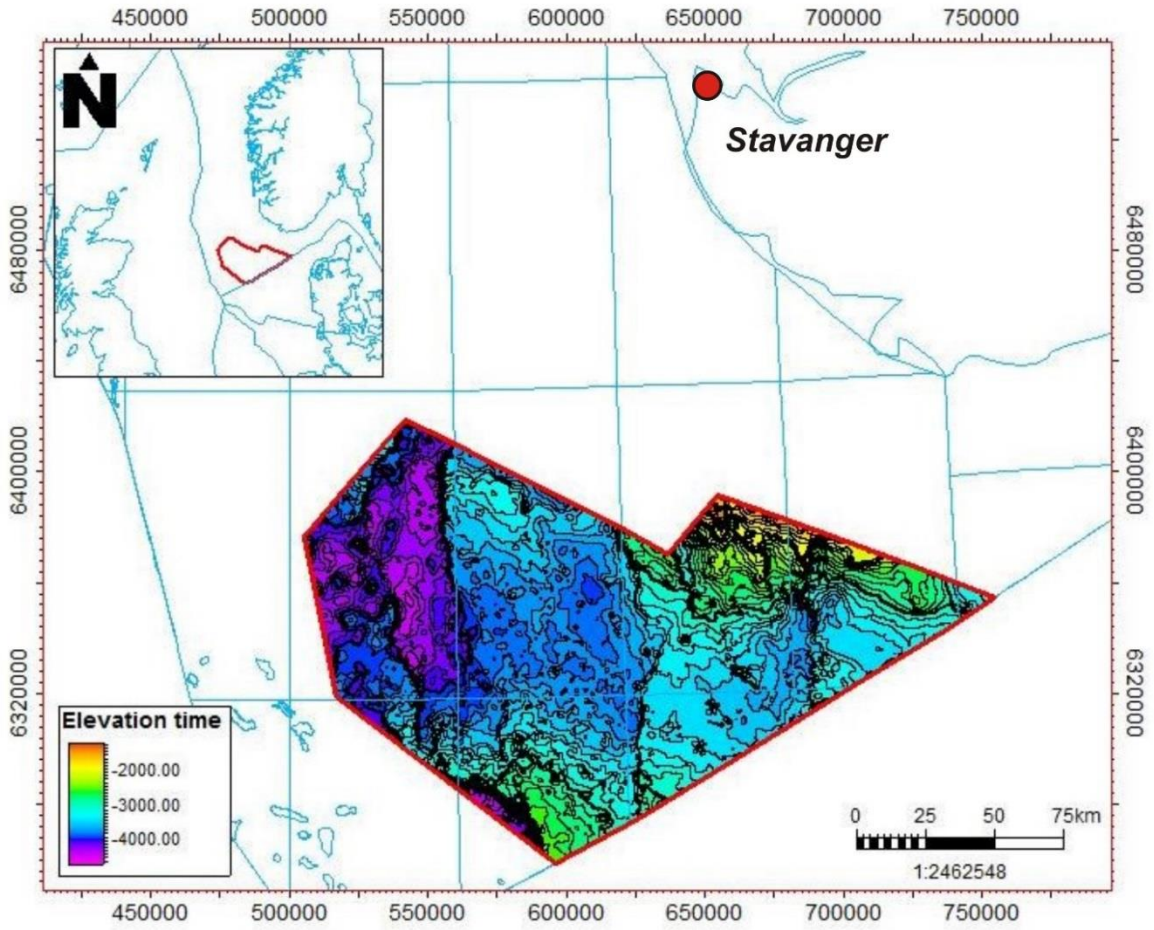

Figure 3. Location of the Norwegian-Danish Basin in the North Sea region, the red line defines the outline of study area and the map is showing interpreted top of Rotliegend Gp.

2.2. Geological Setting

The NDB is a west-northwest – east-southeast epeirogenic subsiding basin formed in the Permian period. It is characterized by thick strata of Permian and Triassic age (Skjerven et al., 1983). The basin is bounded by basement faults from the Fennoscandian Shield to the east-northeast and by the Ryngkøbing-Fyn High to the south-southwest (Figure 4). This Basin derives its origin from the Carboniferous-Permian rifting and belonged to the Northern Permian Basin (NPB), one of two east-west trending basins generated in the north-west Europe region during the Permian. The Southern and Northern Permian basins were divided by the Mid North Sea (Ryngkøbing-Fyn High). The Northern Permian Basin spreads out from the west coast of the southern part of the Swedish mainland to the east of the Grampian Highlands of Scotland. The more explored South Permian Basin extends from the Russo-Polish border to the east coast of England (Evans et al., 2003). The Fennoscandian Border Zone (FBZ) is considered to be an important structural feature for the NDB, separating it from the Fennoscandian Shield. The Fjerritslev Fault is one of the key Permian structural elements linking to the FBZ, it runs from west-northwest to east-southeast and outlines the eastern part of the NDB. The oldest tectonic activity of this fault zone is not well defined, but there is evidence of activity during the Cimmerian Orogeny in the Jurassic Period and Laramide Orogeny in the Late Cretaceous Period (Skjerven et al., 1983).

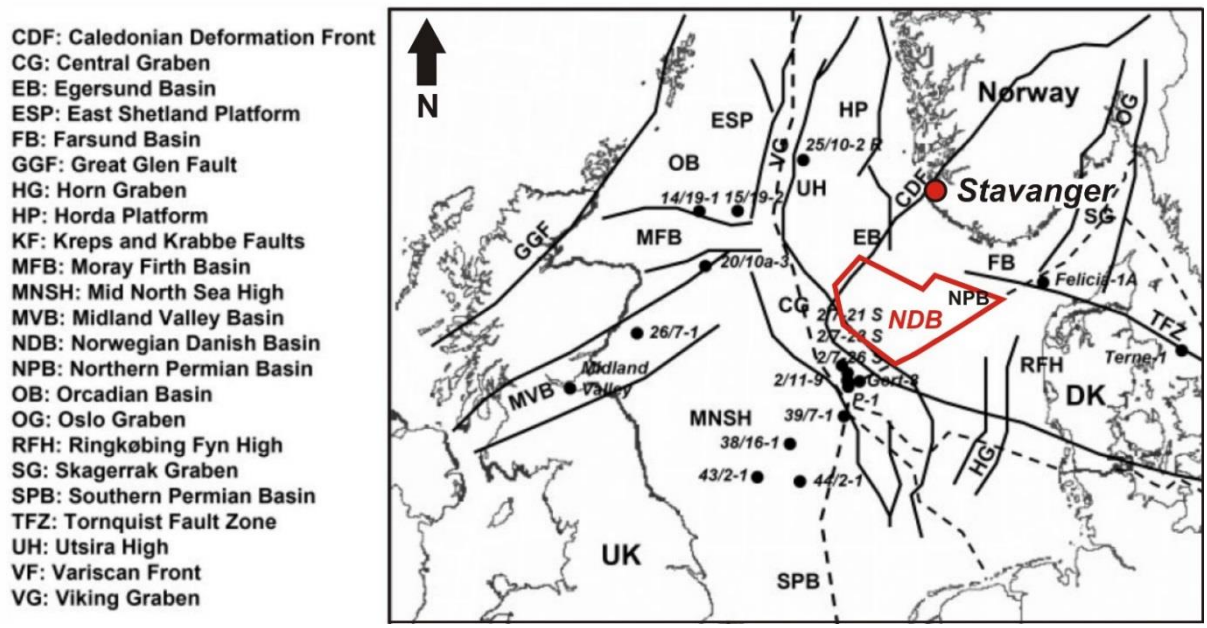

Figure 4. Map showing the main structural elements in the European sector, red outline is the study area (Pedersen et al., 2006).

The Paleozoic structural features are overprinted and obscured by Mesozoic extension and formation of graben structures in the central region of the North Sea (Pedersen et al., 2006a).

Generally, the geological setting of the NDB can be described as six structural levels relating to different tectonic events, changes in relative sea level and its tectono-stratigraphic significance (Figure 5). The first structural level refers to Pre-Devonian basement structures; the second is related to the sub-salt structural level and consists of Early Permian non-marine sediments (the Rotliegend Gp). The next structural level refers to salt tectonics (reactivation and formation of mechanical detachments) and comprises Late Permian evaporate-dominated Zechstein Gp deposited during major marine transgression (Ziegler, 1990; Sørensen et al., 1992). Initial halokinesis of the Zechstein Gp and minibasin formation occured in the following structural level of Triassic age. Halokinesis pods were-filled by clastic continental deposits of the Smith Bank Fm and coarse grained fluvial and alluvial fans systems of Skagerrak Fm. Jurassic-Lower Cretaceous interval is connected to supra-salt syn-rift sedimentation of shallow marine to deep marine depositional environments (Sørensen et al., 1992). The last structural level has a post-rift character and occured in Late Cretaceous to Cenozoic times. It is important to note, that the tectonostratigraphic framework of NDB is taken from the Egersund Basin (Lewis et al., 2013; Tvedt et al., 2013), as these two basins have the same history from Permian to Triassic, while the Egersund Basin also had Triassic-Jurassic influence. The interval of interest is covering the Permian-Triassic succession and includes three major horizons for seismic interpretation: (1) top Skagerrak Fm, (2) top Zechstein Gp, and (3) top Rotliegend Gp (Figure 5C, Figure 8).

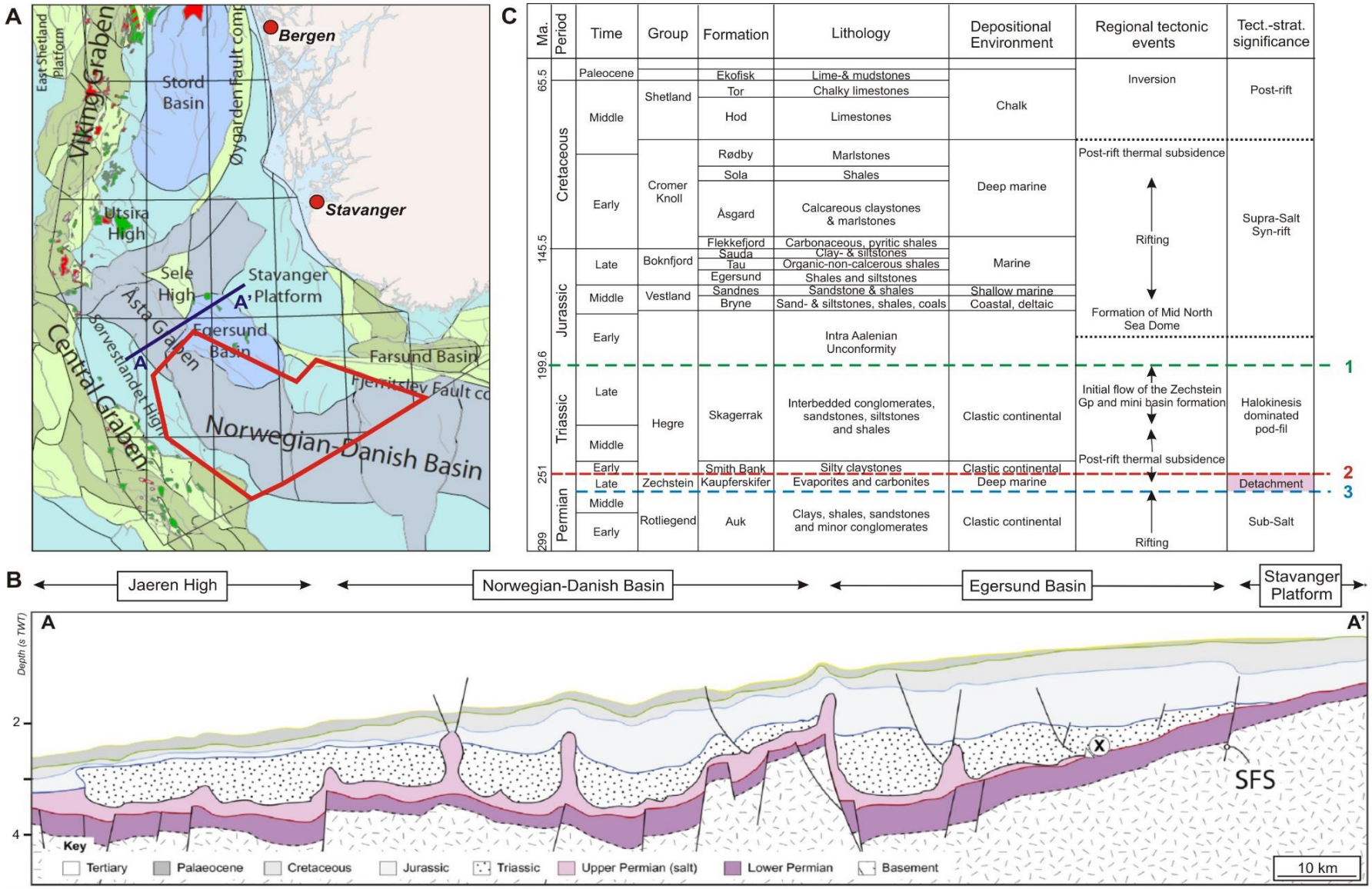

Figure 5. (A) Simplified map showing the distribution of basins and large structural elements related to age of formation (Halland et al., 2011). (B) Simplified regional geo-seismic section and mapped seismic horizons (Lewis et al., 2013). (C) Tectono-stratigraphic framework of NDB (based on Lewis et al., 2013; Tvedt et al., 2013 and NPD, 2014).

2.3. Tectonic evolution

Pre-Carboniferous

The North Sea rift system is situated in a triple-plate collision zone during the Late Ordovician to the Silurian Caledonian Orogeny and to the Cadomian orogeny (Figure 6, Evans et al., 2003). The continental plates of Baltica and Laurentia collided during the Late Silurian closing the Iapetus Ocean and, as an outcome, generating the Laurussia supercontinent resulting in the Caledonian orogeny (Pedersen et al., 2006a). The northeast-southwest trend is common for the Caledonian tectonic stage, especially where fault arrays have separated basement highs (for instance, the Sele High and the Utsira High) in the north, and also the fault zone in the northeast of the Egersund Basin exhibits the same alignment (Skjerven et al., 1983). The Devonian collapse of the Caledonian mountain chain was succeeded in the wide extension lasting into the Carboniferous, followed by reactivation of trusts from Caledonian orogeny and generation of half-graben structures where deposition of continental sediments dominated (Coward, 1995; Evans et al., 2003).

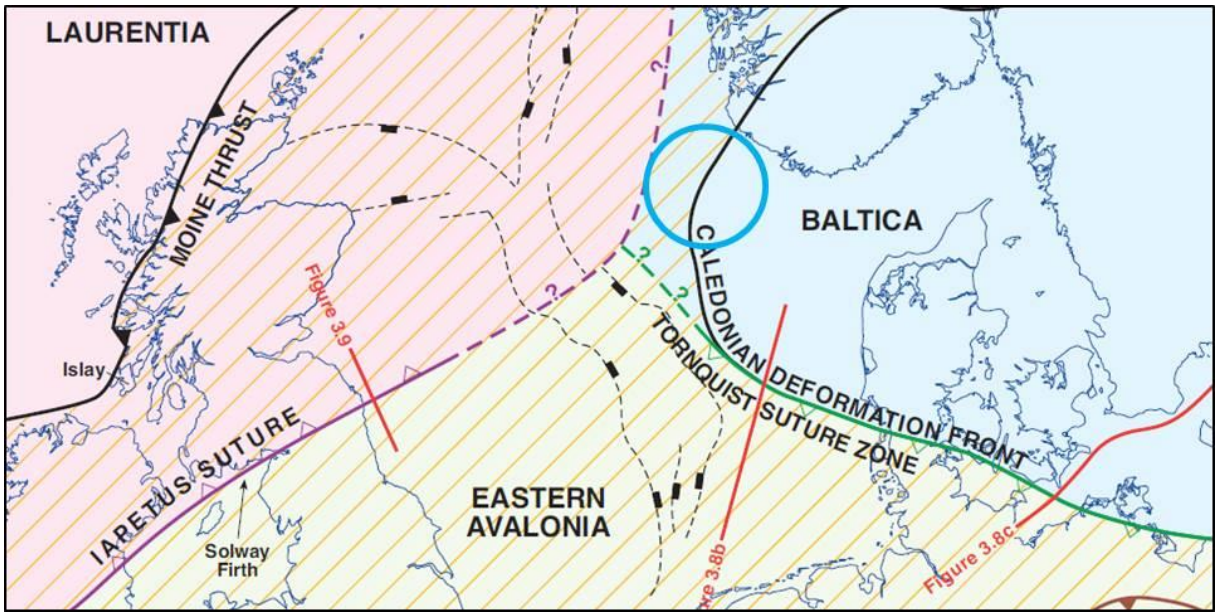

Figure 6. Basement structure (Evans et al., 2003) with study area in a blue circle.

Carboniferous

The Variscan (Hercynian) orogeny, which took place in the Late Carboniferous to Early Permian, mainly influenced the deformation, paleogeography and sedimentation in the southern part of the central North Sea (Ziegler, 1992). Consequently, it resulted in the formation of east-west and northwest-southeast trending major tectonic elements, such as the Ringkøbing-Fyn High and the Mid-North Sea High. The late Variscan orogeny is marked by

an extensional regime and extrusive activity, wide spread in the Northern Permian Basin (Evans et al., 2003); respectively, in formation of the Oslo Graben and the Skagerrak Graben (Husebye et al., 1988; Ro et al., 1990). During Late Variscan compression, the aligned Sorgenfrei-Tornquist deformation Zone has had a significant influence on the east-west extension of the Late Carboniferous-Permian basins (Evans et al., 2003). In the south-western part of the North Sea, the north-south trending Krabbe and Krepps Fault Zones formed in response to the reactivation of old basement lineaments (Pedersen et al., 2006a).

Permian

The extensional tectonic regime took place in Early Permian after the Variscan orogeny, resulting in growth and thermal subsidence of two east-west aligned Northern and Southern Permian sedimentary basins in north-west Europe (Ziegler, 1992; Evans et al., 2003). Late Permian rifting with an east-west extensional directions resulted in formation of north-south aligned systems, accompanied by impact of Sorgenfrei-Tornquist Zone (Evans et al., 2003).

Triassic

At the onset of the Triassic, a triple junction was created by interference of the Arctic and the Atlantic rift systems with different trends of opening (Evans et al., 2003); therefore, the Permian basins and the Arctic Seas became disconnected (Skjerven et al., 1983). Under these circumstances, the north-south trending major structural features were formed, resulting in extension of the Central Graben and formation of several new mini-basins in the NDB. Several minibasins were formed in response to halokinetic movements and to the east-west extension in the Early Triassic (Fraser et al., 1993). These two factors brought sufficiently influenced the evolution of minibasins so that thick Triassic strata accumulated (Fig. 6, Evans et al., 2003). The Triassic tectonic activity together with the overburden strata established halokinetic movements from this time to the Cenozoic in the NDB and in the Central Graben (Skjerven et al., 1983). Coward (1995) states, that the Triassic faults within the Central Graben aligned from north-east to south-west, however the direction of extension is only inferred.

Jurassic

The next intensive tectonic regime is dated to coincide with the Middle Jurassic thermal doming (Ziegler, 1992). During the Early/Mid-Jurassic, salt withdrawal and dissolution led to the generation of intervening depo-axes and north-south oriented salt ridges;

it provided accommodation space for the sediment deposition (Hodgson et al., 1992). In the NDB, two circular depocenters with significant thickening are recognized in the Himmerland Graben and the Fjerritslev Trough (Maystrenko et al., 2013). Understanding of the halokinetic impact on Triassic sedimentation is complicated by Triassic dissolution. As Bishop et al. (1995) defined, around 30 % of the primary salt volume was removed during this period and by major post-Triassic movement.

The major late Jurassic extensional phase in the North Sea created large southwest-northeast trending structural elements; however, some Late Jurassic grabens in the southern part of the NDB were perpendicular to the main direction of extension (Evans et al., 2003).

Cretaceous

The Early Cretaceous was tectonically quiecent, the base is marked by the widespread Base Cretaceous Unconformity (BCU; Figure 7), post-rift succession. The Lower Cretaceous is characterized as a stable basin with uplift of basin margins and halokinetic movements. During the Cretaceous, thermal subsidence was locally increased by the halokinesis in the minibasins, and salt domes with salt diapirs formed in the main areas of Late Jurassic rifting (Hodgson et al., 1992).

Cenozoic

During Early-Middle Paleogene (Paleocene-Early Eocene), north-west Europe was uplifted due to the formation of the North Atlantic hot spot. Subsidence of the North Sea increased, as sediment supply was derived from the uplifted areas (Evans et al., 2003). In addition, salt movements continued in the Paleogene, while halokinesis impacted only local areas in the Neogene.

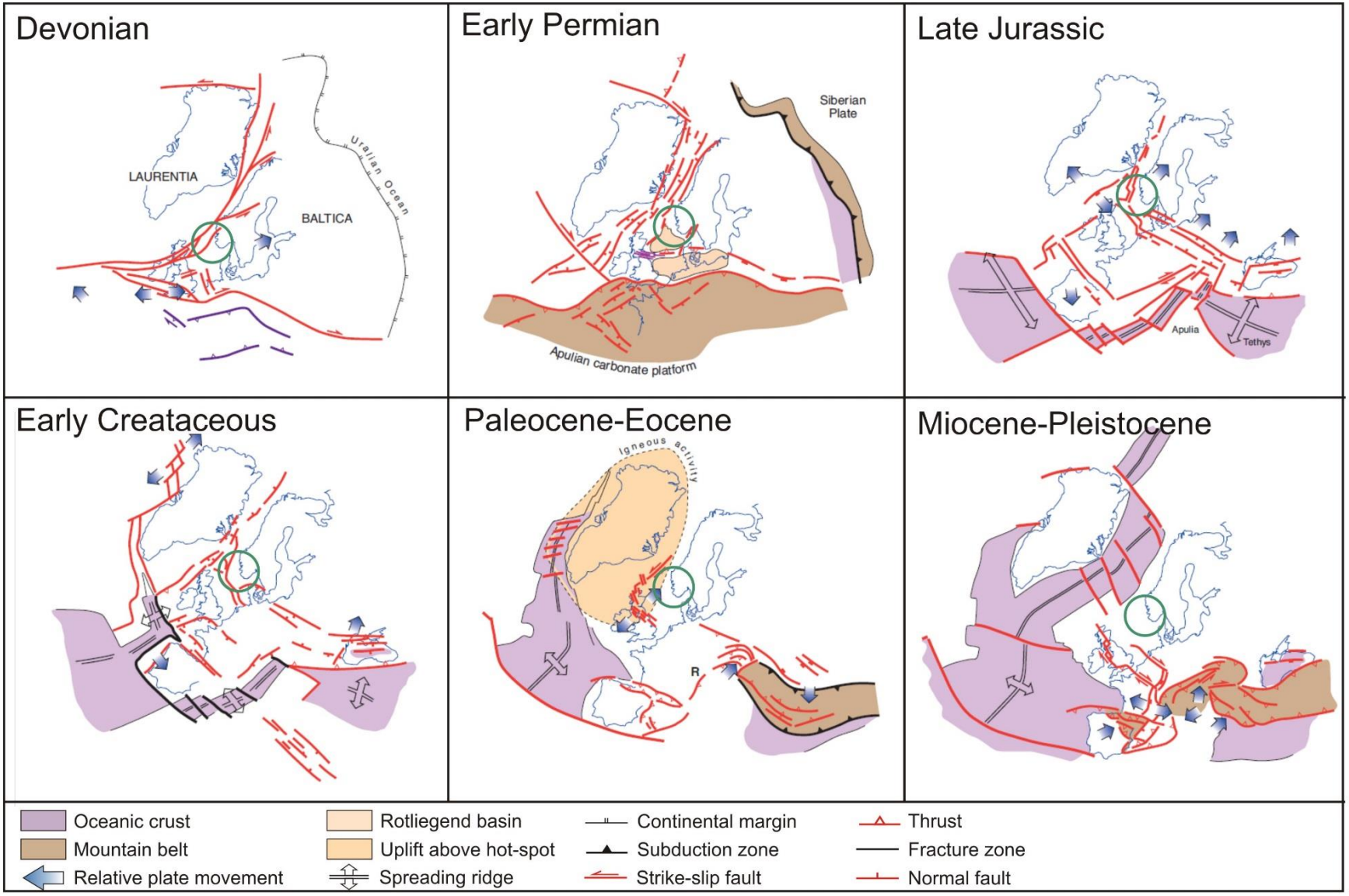

Figure 7. Paleotectonic reconstructions from Devonian to Miocene-Pleistocene times with the study area in a green circle (modified after Evans et al., 2003).

2.4. Stratigraphic evolution

Carboniferous

The Dinantian age represents a widespread transgression during high relative sea level in the southern North Sea, resulting in carbonate platforms building up along with the accumulation of shales and cherts (Ziegler, 1990). The northern North Sea and the Fenno-Scandinavian area comprise extensive land masses. Deltaic and fluvial sediments with marine influence were deposited in the transition zone between land and sea. In the beginning of the Selesian Series, widespread and prolific coals accumulated in the following regressive trend. Lower Carboniferous calcareous marine shales and coals have hydrogen-rich type II kerogen (Grautier, 2003). The Variscan foreland basin comprises a thick non-marine stratigraphic interval of Namurian- Westphalian age with thicknesses up to 9 km (Collinson et al., 1993). Coals and carbonaceous shales accumulated in an extensive fluvial depositional environment in humid conditions with terrestrial plants. Organic matter of the sediments is dominated by type III kerogen, producing natural gas at depth (Cornford, 1998).

Permian

Due to the genesis of the Pangaea supercontinent in the Permian Period, the climate conditions had a dryer character. In the Southern Permian and Northern Permian basins (Figure 8), aeolian sands (the Auk Formation in the Rotliegend Group) were accumulated corresponding to this desert formation. The Mid-Permian time is represented by a large flooding event with deposition of an organic-rich mud (the Kupferschiefer Formation) in the North Sea (Evans et al., 2003). The Kupferschiefer Fm is composed of thin (up to 2 m), grey-black radioactive organic rich shales, locally calcareous, resulting from the anoxic basinal environment and forms a good oil prone source rock (Pedersen et al., 2006a; Pedersen et al., 2006b; Evans et al., 2003). During the Late Permian, the subsidence of the Permian basins significantly increased in the North Sea because of episodic transgressional events, when thick packages of carbonates and salts were precipitated and deposited on the seafloor. The original thickness of these sediments was more than 1000 m (Skjerven et al., 1983). The Zechstein Group consists of salt and gypsum sequences based on seven cycles of salt deposition and evaporation (Figure 8, Ramberg et al., 2008); the entire thickness of the succession is between 1000 and 1500 m (Sørensen et al., 1992). The presence and re-distribution of the Zechstein salt has strongly impacted the evolution of the North Sea Basin and influenced the Triassic sedimentation patterns (Evans et al., 2003).

Triassic

During the Early Triassic, the Smith Bank Fm is widely distributed throughout the Central North Sea and comprises clastic deposits, mainly sandstones (Figure 8). The formation accumulated in a wide range of continental depositional environments (Deegan and Scull, 1977). Middle Triassic stratigraphy comprises claystones, marls and evaporates of the Muschelkalk Fm, mainly located in the Mesozoic basins and their adjacent areas. The depositional setting for Muschelkalk Fm is between shallow-marine and open marine environments with evaporitic episodes (Dinoloket, 2016). The Skagerrak Fm was deposited in prograding fluvial systems and alluvial fans and contains coarse grained clastic continental deposits, mainly sandstones (Figure 8, Deegan and Scull, 1977).

Jurassic

The shallow marine shales from the Fjerritslev Fm, deposited during a widespread transgressional event (Vollset and Doré, 1984), marked the base of the Lower Jurassic and acts as an extensive regional seal for the underlying clastic continental depositional systems (Figure 8).

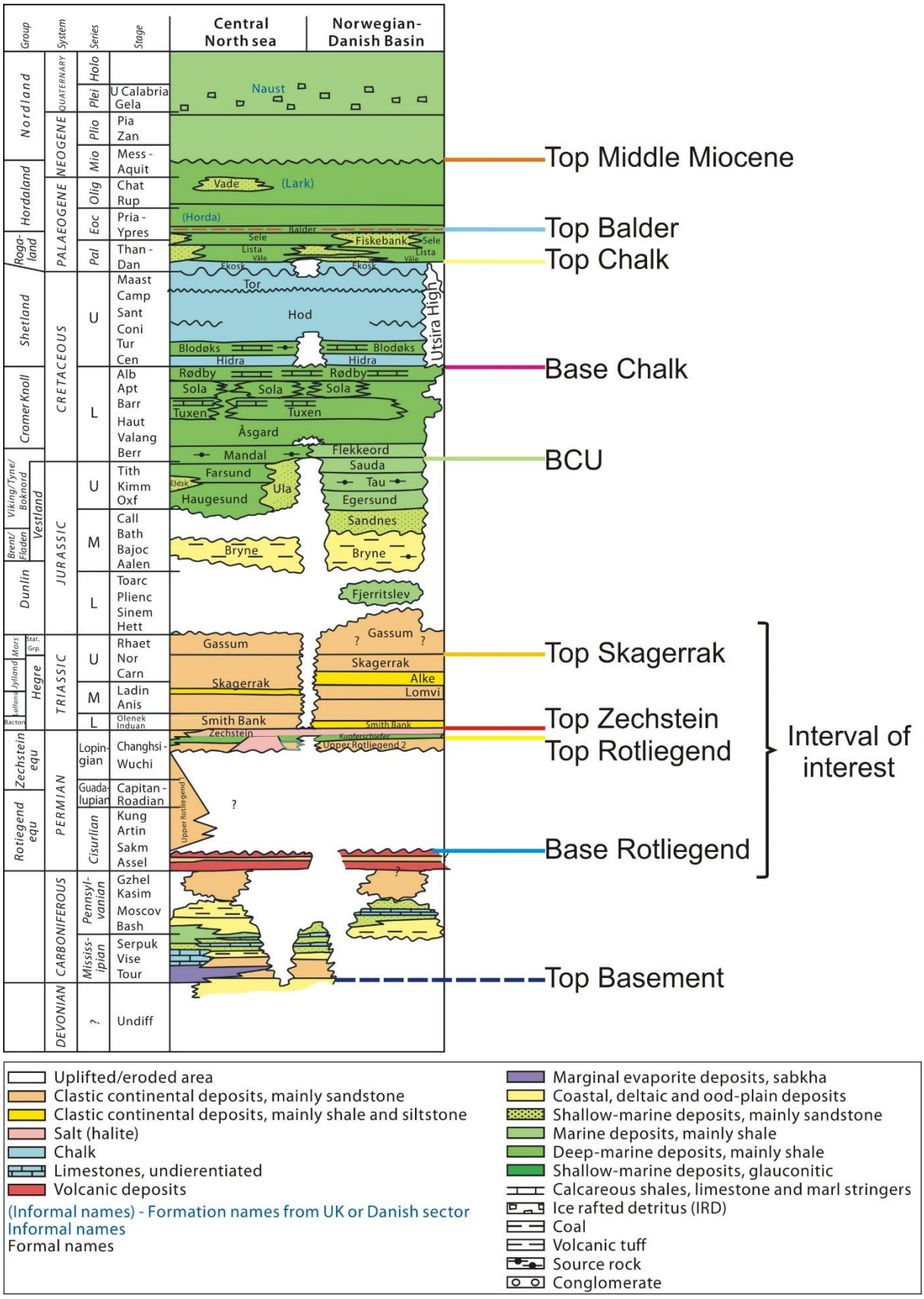

Figure 8. Lithostratigraphic chart of the NDB (modified from NPD, 2014) shows the interval of interest and key horizons, displaying in the regional cross sections (Figure 14-15).

3. Database and Methodology

3.1. Data

A/S Norske Shell has provided all the data and software access.

3.1.1. Seismic Data

The database for this study includes pre-stack time-migrated, two-dimensional reflection seismic surveys (CGME-96, EBS00, SET96, NSR04, and SHD-97) and three-dimensional mega merge reflection survey ST99M1-AREA3, consisting of multiple surveys (ST9602, MC3DQ4, NODAB97-PHASE1 and PHASE2, SH9204, G9603, ST9205) (Figure 9, Table 2). The study area, 20,000 km^2, has contiguous coverage of all seismic surveys. The seismic sections are displayed with SEG reverse polarity (Appendix 1), so that a downward increase in acoustic impedance is represented by a peak (positive reflection event, red on seismic) and downward increase in acoustic impedance is represented by a trough (negative reflection event, blue on seismic). All seismic survey parameters and review of data quality are listed in the table below (Table 2).

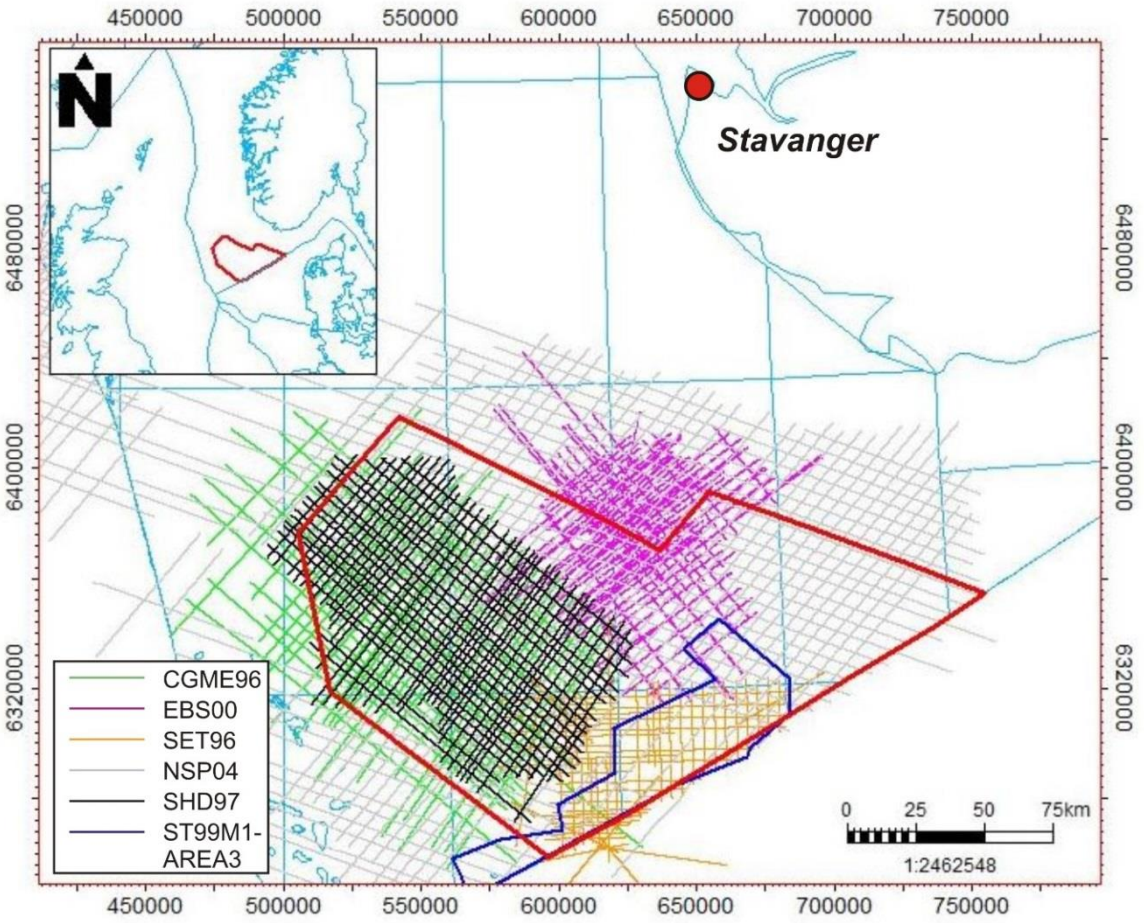

Figure 9. Location of seismic data with study area in red.

	CGME96	*EBS00*	*SET96*	*NSR04*	*SHD97*		*ST99M1-AREA3*
Type of seismic survey	2D					**Type of seismic survey**	3D
Original CRS	ED50 UTM zone 31N					**Original CRS**	ED50 UTM zone 31N
Number of traces	8793	3140	8564	5613	6807	**Number of inlines**	2563
Number of samples per trace	3001	1753	3001	2301	1751	**Number of crosslines**	10988
Sample interval	4	4	4	4	4	**Inline interval**	25
Number of cells total	26387793	5504420	25700564	12915513	11919507	**Crossline interval**	12,5
Storage type	SEG-Y format					**Storage type**	ZGY format
Polarity	Reverse	Reverse	Normal	Reverse	Reverse	**Polarity**	Reverse
Coverage of study area	Western part	Central-Eastern part	Southern part	Entirely except gap in the central part	Western part	**Coverage**	Southern part
Quality of data	Average	Good	Good	Good	Average	**Quality of data**	Very good
Comments	Noisy data, not dense distribution of lines, good for well-tie	Dense distribution of lines, good for well-tie	Blurry in the deep levels, useful for connection SHD97 and ST99M1-Area3 surveys	Good correlation and connectivity with all seismic surveys	Very dense seismic lines, good for well-tie	**Comments**	Clear image, easy for seismic interpretation

Table 2. Seismic survey information table.

3.1.2. Well Data

Thirteen wells from the Norwegian side of the NDB and two wells from the Danish side of the NDB were utilized (Figure 10, Table 3). All the wells comprise check-shot velocity data, joined and raw curves from electrical well log data (for instance, GR, DT, NEU, RHOB, DEN, RES, and CALI), original well reports, chronostratigraphic and lithostratigraphic well tops from Open Works (OW) along with Norwegian Petroleum Directorate (NPD). The majority of the Norwegian wells, eleven out of thirteen, were drilled on structural highs, related to salt walls and salt diapirs, between 1966 and 1978.

The age of the interpreted seismic reflectors and lithological composition were defined to well information. The research was limited to fifteen wells from Norwegian and Danish sector, plus emphasis was on Late Permian-Jurassic interval (Figure 8).

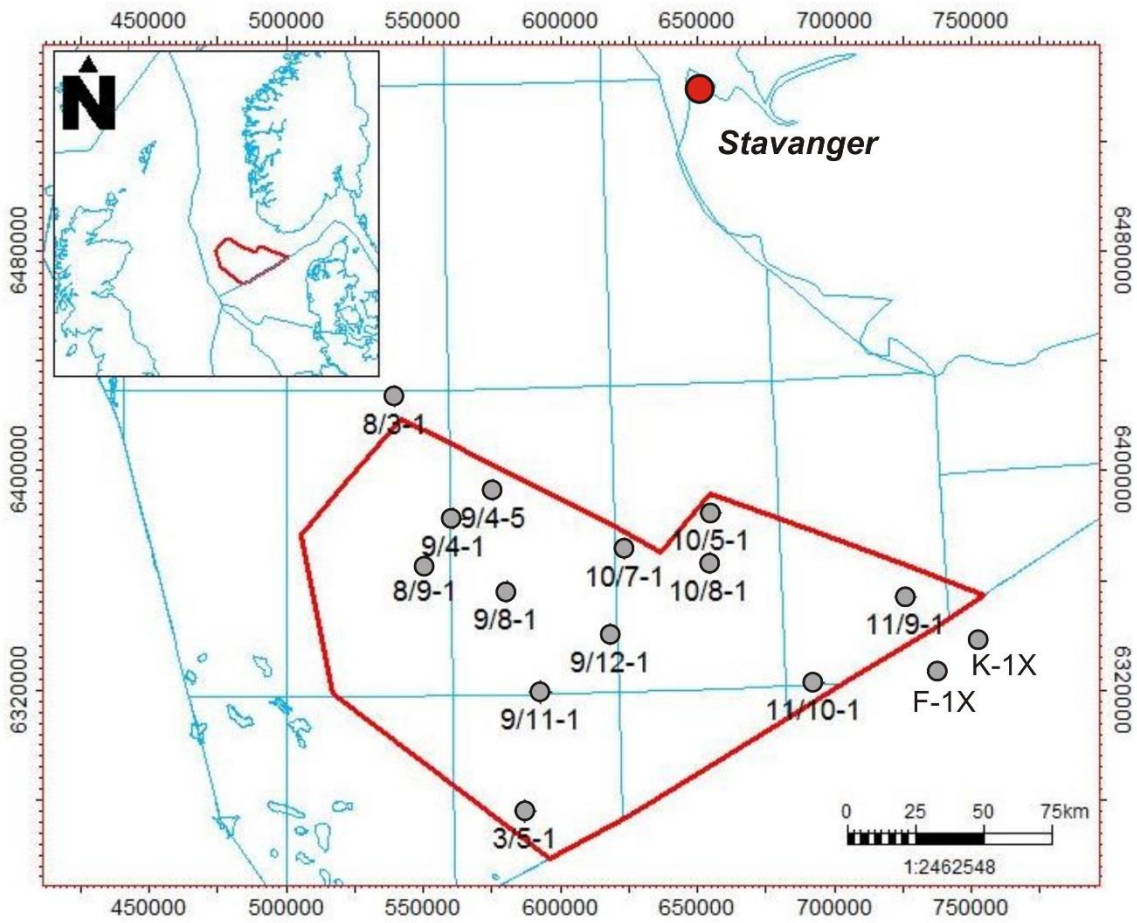

Figure 10. Location of selected wells with study area in red.

Well name	TD (TVD SS)	Completed date	Oldest penetrated age	Oldest penetrated formation	Joined Curves	Checkshots
10/7-1	1865.8	30.07.1992	Late Permian	Sandnes Fm base	Yes	Yes
10/8-1	2844.6	17.01.1971	Late Permian	Zechstein Carbonate top	Yes	Yes
10/5-1	1825.8	26.06.1976	Permian	Rotliegendes Fm top	Yes	Yes
9/12-1	2671.0	06.05.1969	Triassic	Smith Bank Fm top	Yes	Yes
9/11-1	2171.0	19.08.1971	Triassic	Skagerrak Fm top	Yes	Yes
9/8-1	2146.0	29.06.1968	Late Permian	Zechstein Carbonate top	Yes	Yes
8/9-1	2350.6	10.02.1976	Late Permian	Zechstein Carbonate top	Yes	Yes
9/4-1	2933.0	19.05.1968	Late Permian	Zechstein Salt top	Yes	Yes
11/9-1	1947.0	28.02.1976	Late Permian	Zechstein Anhydrite top	Missing	Yes
11/10-1	2402.9	19.08.1969	Triassic	Skagerrak Fm top	Missing	Yes
3/5-1	3408.2	28.06.1978	Permian	Rotliegendes Fm top	Yes	Yes
9/4-5	5830.1	01.08.2006	Triassic	Smith Bank Fm base	Yes	Yes
8/3-1	2989.0	10.10.1966	Pre-Devonian	Basement	Missing	Yes
F-1X	2384.9	20.10.1968	Triassic	Skagerrak Fm base	Missing	Yes
K-1X	2253.9	21.01.1970	Triassic	Skagerrak Fm base	Missing	Yes

Table 3. Well information table (based on NPD and Open Works picks).

3.2. Methodology

3.2.1. Mis-Tie Analysis

Mis-Tie analysis procedure was conducted to reduce mis-picks and to correct mis-tie values within 2D and 3D surveys (Table 4) using Petrel 2014 software. Vertical differences (vertical mis-ties) between the seismic lines from different surveys were corrected with time shift procedure for better matching. Phase mis-ties were identified between 2D seismic surveys after quality check and were adjusted through extracted phase rotation values to minimize the differences in phase between seismic lines.

It was necessary to apply time and phase shift of seismic surveys for reflection alignment for further well-to-seismic tie along with mapping seismic horizons and faults.

	CGME96	***EBS00***	***SET96***	***NSR04***	***SHD97***	***ST99M1-AREA3***
Original/ Modified Data	Original	Modified	Modified	Modified	Original	Original
Phase Shift	No	No	+90°	+180°	No	No
Time Shift	No	+15 ms	No	+20 ms	No	No

Table 4. Time and Phase Shift applied on seismic surveys.

3.2.2. Seismic Well-Tie

The first step of well-to-seismic tie is to calibrate the sonic log with checkshots for each well (Table 5, Figure 11A). Figure 11 shows an example of sonic calibration and synthetic generation for one well, while it has been applied for all wells. The sonic log set and original checkshots were used as the main input in the dialog window, then knee points at checkshots were picked and edited to fit the original data. The outcome of this procedure is a calibrated sonic log, which was used as an input for new time-depth relationships (TDR) and ran for each well.

The second step for proper well-to-seismic ties includes the construction of an appropriate wavelet for each well (Figure 11B). The wavelets have been estimated using a statistical method and an extraction algorithm for every specific well, tied to an exact seismic volume cube or two-dimensional seismic line. The calculated wavelets have a wavelength of 128 ms and sample rate of 2 ms. It is important to note, that all of the seismic wavelets are zero phased and were constructed within a window of correlation for all wells, between Permian and Triassic well tops (Table 5). For a more precise wavelet, the correlation window was set up for 500 ms and less, so as a result it is more fitted to the specific interval of interest for further seismic interpretation.

The third step is to generate a synthetic seismogram for all wells using calculated wavelets, calibrated sonic and original density log set as an input. Generally, a synthetic seismogram is needed to recognize the seismic reflectors representing the geological well tops in advance of horizon and fault interpretation. For each well a window of correlation was identified (the same as for wavelet) and used in the parameters along with some applied methods, like bulk shift and align points procedure. All of these techniques were necessary to achieve maximum cross correlation between the seismic survey and well data. The main result that was obtained after the synthetic generation is a new time-depth relation (TDR), which was used as a final output for calculating the time domain for each well for better correlating well tops and seismic/well data. All the information related to the seismic-well tie is presented in Table 5 along with applied parameters and methods for all 15 wells in the area of investigation. Some of the wells do not have completed density and sonic log joined curves, hence it was not possible to conduct sonic calibration and synthetic generation procedure.

Well name	**Joined Curves**	**Checkshots**	**Sonic calibration**	**Syntethic generation**	**Correlation window (ms)**	**Applied Methods**	
						Bulk Shift	**Allign points**
10/7-1	Yes	Yes	Yes	Yes	1300-1570	+15	Yes
10/8-1	Yes	Yes	Yes	Yes	1600-1985	No	No
10/5-1	Yes	Yes	Yes	Yes	1050-1395	+12	Yes
9/12-1	Yes	Yes	Yes	Yes	1600-2100	+10	Yes
9/11-1	Yes	Yes	Yes	Yes	1800-1950	No	Yes
9/8-1	Yes	Yes	Yes	Yes	1500-1765	-7	Yes
8/9-1	Yes	Yes	Yes	Yes	1700-1880	+7	Yes
9/4-1	Yes	Yes	Yes	Yes	1650-2010	-20	Yes
11/9-1	Missing	Yes	Yes	No	-	-	-
11/10-1	Missing	Yes	Yes	No	-	-	-
3/5-1	Yes	Yes	Yes	Yes	2362-2650	No	Yes
9/4-5	Yes	Yes	Yes	Yes	2150-3500	+30 ms	Yes
8/3-1	Missing	Yes	Yes	No	-	-	-
F-1X	Missing	Yes	Yes	No	-	-	-
K-1X	Missing	Yes	Yes	No	-	-	-

Table 5. Well-to-seismic ties information table.

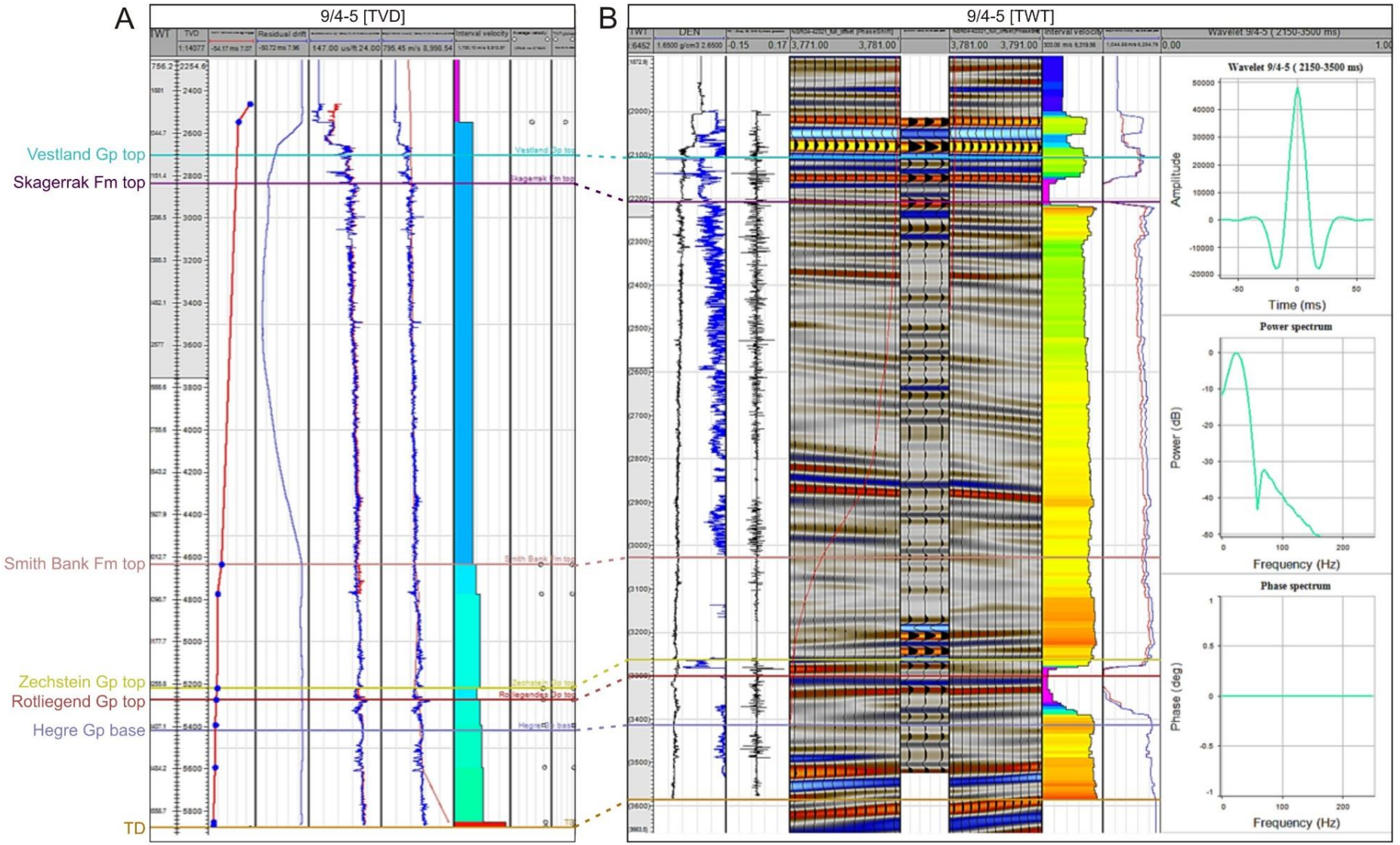

Figure 11. (A) Sonic calibration for well 9/4-5. (B) Synthetic generation and calculation of wavelet for well 9/4-5.

3.2.3. Seismic Interpretation

The stratigraphic interval for regional seismic interpretation is the Permian-Triassic interval and is composed of three key horizons: (1) top of Skagerrak Formation, (2) top of Zechstein Group, and (3) top of Rotliegend Group (Table 6, Figure 5C, Figure 8, Figure 12). Mapping of the top of the Rotliegend Group (Top of Mid-Permian) provides a good overview of the base of salt and sub-salt structures, this horizon is represented by a trough (negative reflection event, blue on seismic) and yields high confidence in interpretation. The top of the Zechstein Group (Top of Late Permian) constrains the upper boundary for the salt interval, but is not well represented in the seismic display window due to salt properties and blurry image, which has significantly influenced level of confidence, resulting in a Medium, and makes interpretation more challenging. The last picked horizon for regional mapping is the Top of Skagerrak Formation (Top of Triassic), which is a major unconformity, as it separates the supra-salt succession, influenced by main phases of halokinetic movements, from the Jurassic strata. This reflector is represented by a peak (positive reflection event, red on seismic) and has medium confidence due to not strong acoustic impedance, discontinuity of reflector, facies changing and widely distributed salt walls along with fault, which have made this reflector difficult to map without enough of well control.

Seismic horizons	Age	Geological feature	Pick (time)	Confidence
Top of Skagerrak	Late Triassic	Unconformity	Positive (soft)	Medium
Top of Zechstein	Late Permian	Top of salt	Top of blurry response	Medium
Top of Rotliegend	Mid-Permian	Base of salt	Negative (hard)	High

Table 6. Information table regarding to selected picks for interpretation.

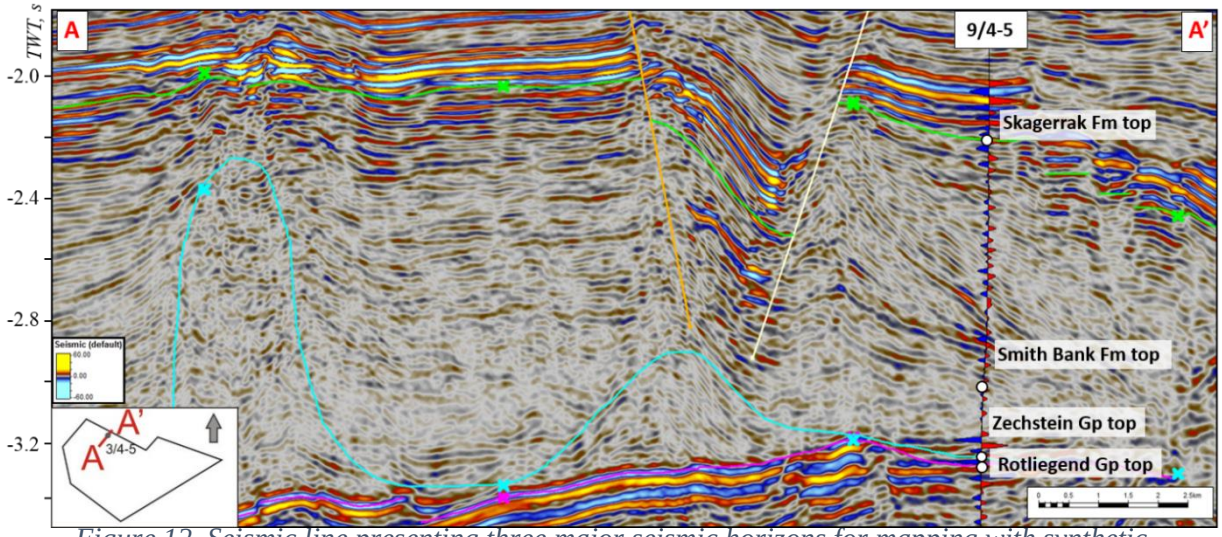

Figure 12. Seismic line presenting three major seismic horizons for mapping with synthetic seismogram

3.2.4. Generation of Time-Structural and Isopach Maps

Time-structural maps (TWT) were constructed for all interpreted seismic horizons (Top of Rotliegend Group, Top of Zechstein Group and Top of Skagerrak Formation). For some of the surfaces it was additional to do some modifications to have reasonably correct maps. As an example showed in Figure 13 for Top of Rotliegend Gp, firstly, the surface was generated just based on the seismic interpretation and bounded by the outline of the area (Figure 13A). The next step was to modify the problem areas near fault planes, considering this the fault polygons and surface were constructed from the original seismic interpretation (Figure 13B). All fault polygons were modified to be used in the algorithm for creating a new surface with centered of fault polygons (Figure 13C). The final step was to cut the completed surface by fault polygons (Figure 13D).

General depth conversion was conducted for all generated time-structural maps in order to transfer data from time domain to depth domain. The velocity model is used NS-1215T-MC_Va_MainCube.

Finally, isopach maps were produced through subtracting depth maps. Isopach maps were used to define differences in thicknesses, growth history, depocentres and fault activity during formation of faults.

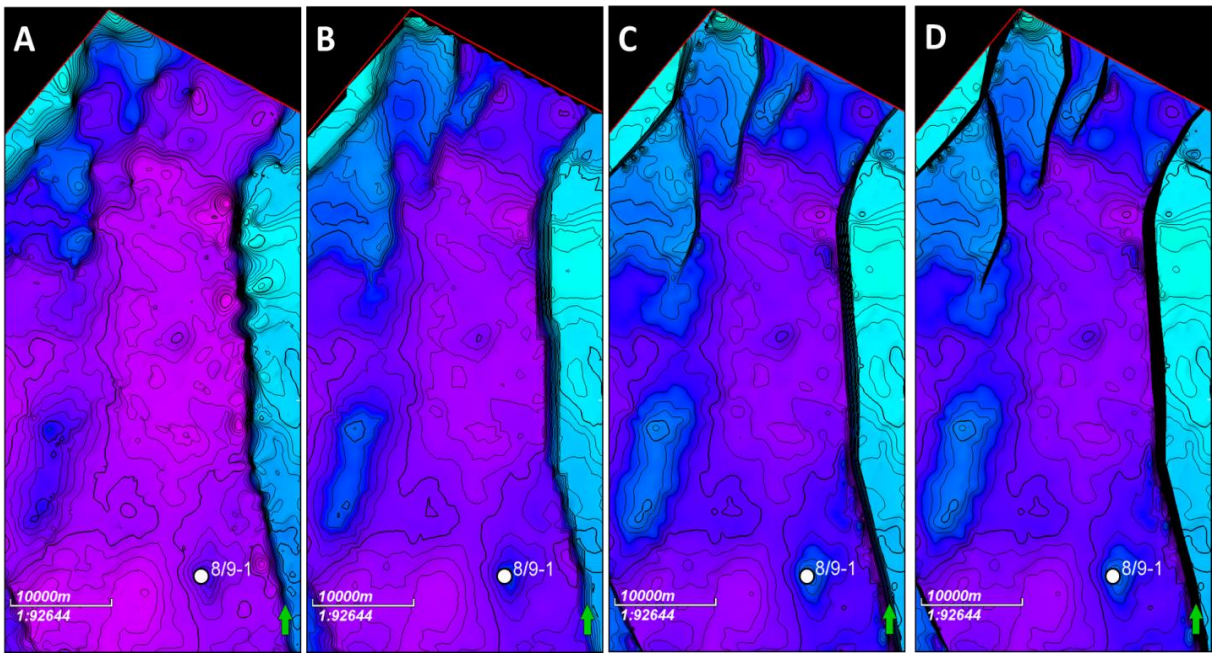

Figure 13. Construction of time-structural maps, Top of the Rotliegend example

4. Observations

In order to describe the observations and support the following discussion two regional cross-sections were constructed across the NDB; one oriented WNW-ESE (Figure 14), the other NNE-SSW (Figure 15).

4.1. Top of the Rotliegend Group

The major structural elements that are identified at the Rotliegend level are the Hummer Fault Zone, Sørvestlandet High, Åsta Graben, Coffee Soil Fault Complex, Sogne Basin, Lista Fault Blocks, Krabbe and Kreps Fault Zones along with the Horn Graben (Figure 14, Figure 15, Figure 16). Overall, 30 regional subsalt-involved normal faults penetrating the top of the Rotliegend level (Figure 16, Figure 17) have been observed in the NDB and can be divided into two principal fault groups based on their orientation (Figure 18).

The first fault array consists of 27 faults mainly oriented north-south (Figure 18C), as the strike varies from 335°-30° to 155°-210° (Appendix 2). All measurements of fault strike were conducted using the right hand rule (RHR) and are presented in Appendix 2. This fault group contains the majority of basin boundary faults, including the Hummer, Krabbe and Kreps Fault zones along with the Horn Graben. All of these faults have 1) influenced the structurization of the basin, and 2) allowed for subdivision into the main structural domains.

The north-west domain includes the Åsta Graben, bounded by the east dipping Hummer Fault Zone and another regional fault dipping to the west. The Hummer Fault Complex comprises 3 segments: the first segment with a length of 73 km and strike direction of 345° RHR is not linked to other segments, while the second, 23 km in length and strike direction of 4° RHR, and the third one, 19 km in length and strike direction of 33° RHR, are soft linked. In addition, smaller offset faults of synthetic nature with normal displacement and lengths between 7.7 km and 15.4 km are represented in the northern part of the Åsta Graben as bounding half-graben structures with a strike of the fault planes varying from 2° to 18° RHR (Appendix 2). The Central part is bounded by the boundary half-graben of the Åsta Graben in the north-west and by the west dipping Krabbe Fault Zone to the east. The Krabbe Fault zone includes two normal faults with lengths of approximately 50 km, strike 180° RHR, and 23 km, strike 201° RHR, respectively (Appendix 2).

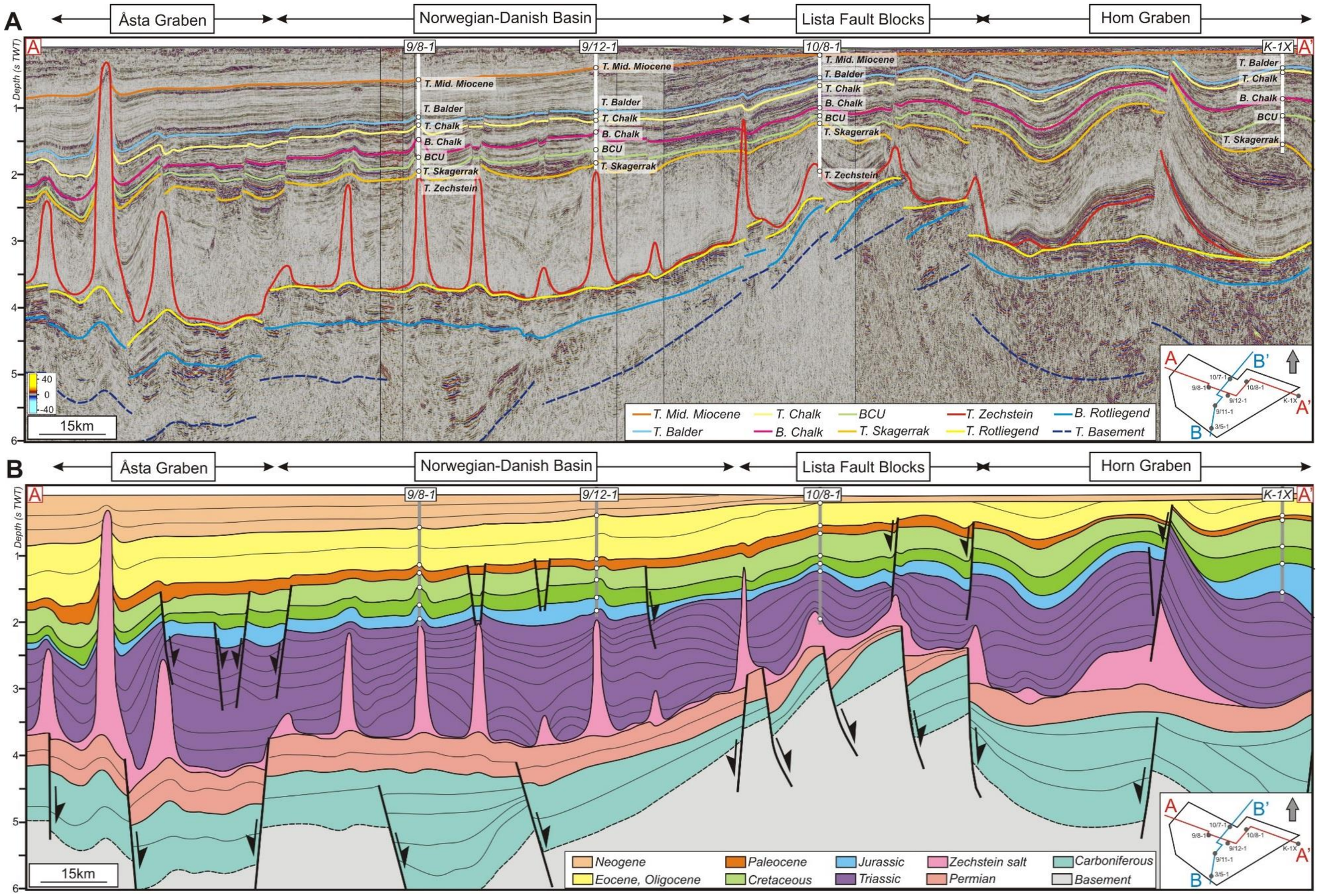

Figure 14. Regional cross-section B-B', vertical exaggeration 1:15.

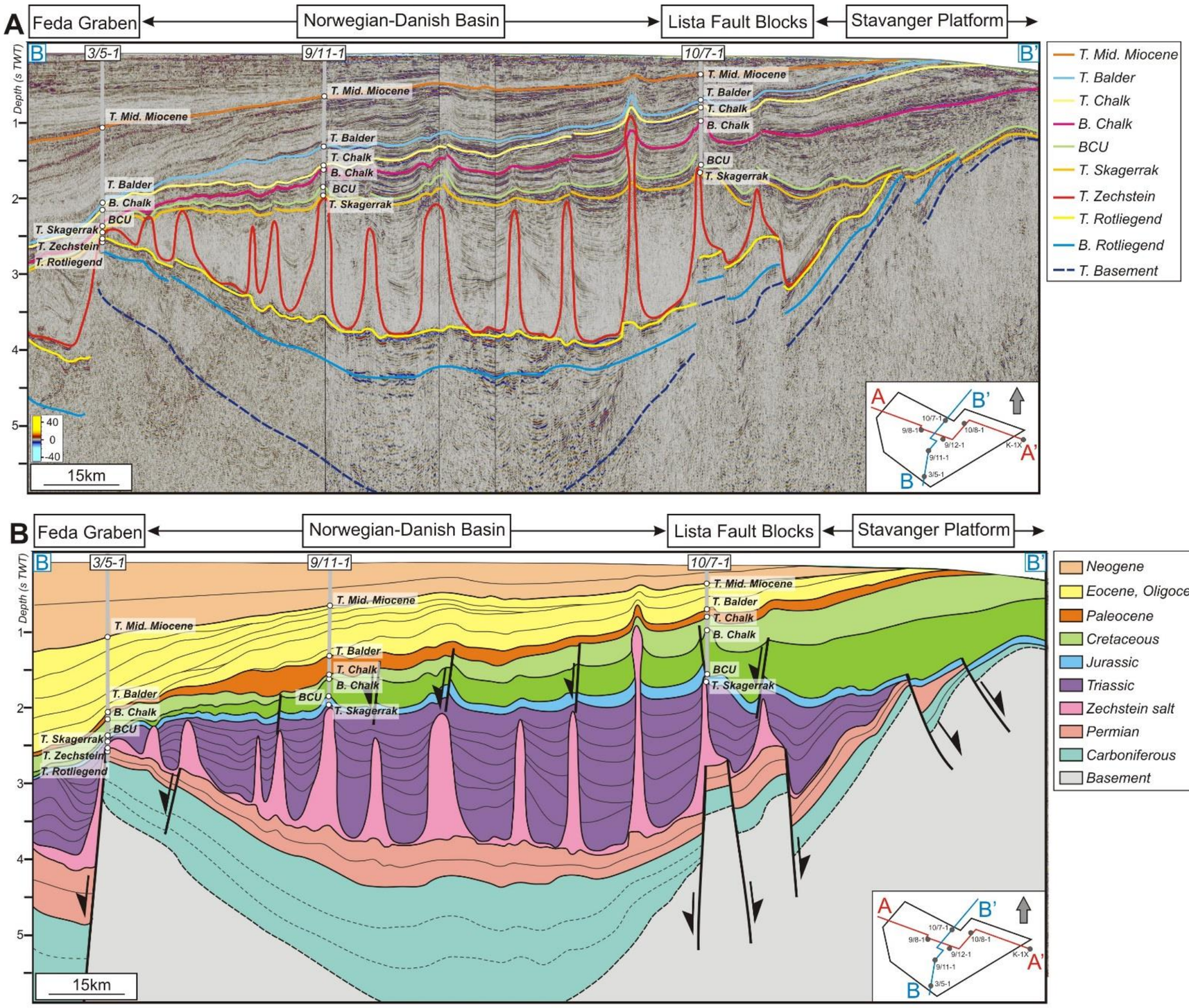

Figure 15. Regional cross-section B-B', vertical exaggeration 1:15.

The next domain is delineated by the Krabbe and Kreps Fault zones and defines a unfaulted area. The Kreps Fault Zone is 42.3 km in length and the strike of the fault plane is 176° RHR. The easternmost zone of the NDB has been distinguished as a structure belonging to the Horn Graben and limited by the Kreps Fault zone and an eastern regional fault with a length of 27 km and strike of 164° RHR. Another important structural feature with a significant difference in deformation and structural style, containing rotated fault blocks, has been recognized as the Lista Fault Blocks area. This region comprises four east dipping regional faults with lengths varying from 15.4 km to 34.6 km and strike direction varying from 339° RHR to 27° RHR and one west-south west dipping normal fault with a length 19.2 km and strike of 167° RHR. Synrift deposition of the Rotliegend Group was identified in a tilted fault block area indicative of fault activity of Lista Fault Block area in the Late Permian (Figure 14).

Another fault array is associated with west-northwest – east-south east alignment (Figure 18C) and contains the regional Coffee Soil Fault Complex in the southern part and two faults in the northern part of the study area. The Coffee Soil Fault Complex defines the southeastern margins of the sedimentary basin at top Rotliegend level. This fault complex includes boundary faults to the Feda Graben, north-eastern part of the Central Graben structure (Figure 15). The fault complex has a curved shape in plan view, a length of 53.8 km and the fault plain trends on average 123° RHR. The activity of this fault zone was multiphased; more specifically the first episode of fault displacement occurred during the Carboniferous rifting where an observed second episode took place during Middle-Late Jurassic rifting, as evident by the presence of Sub-Permian and Upper Jurassic growth strata (Figure 15). A further two faults are distinguished in the northern area, they are 30.8 and 23 km long with strikes of 290˚ RHR and 287˚ RHR, respectively.

These two major fault groups define the distribution of lows and highs at Top Rotliegend Group level (Figure 16, Figure 17). For instance, the low relief (topography) is confined within the Åsta Graben and the subsidence-accompanying the Feda Graben. The low topography is also present in the eastern part of the NDB, and is likely controlled by structural elements situated outside of the area of investigation.

The Central part of the NDB does not exhibit fault activity and significant differences in the paleotopography, it is therefore proposed that it was a sag basin without fault influence. Relatively high relief coincides with footwalls of the Hummer Fault Zone, the Sørvestlandet High, and with the footwall of the Coffee Soil Fault Zone. The Lista Fault Blocks area shows reasonably high relief indicative for rotated fault blocks.

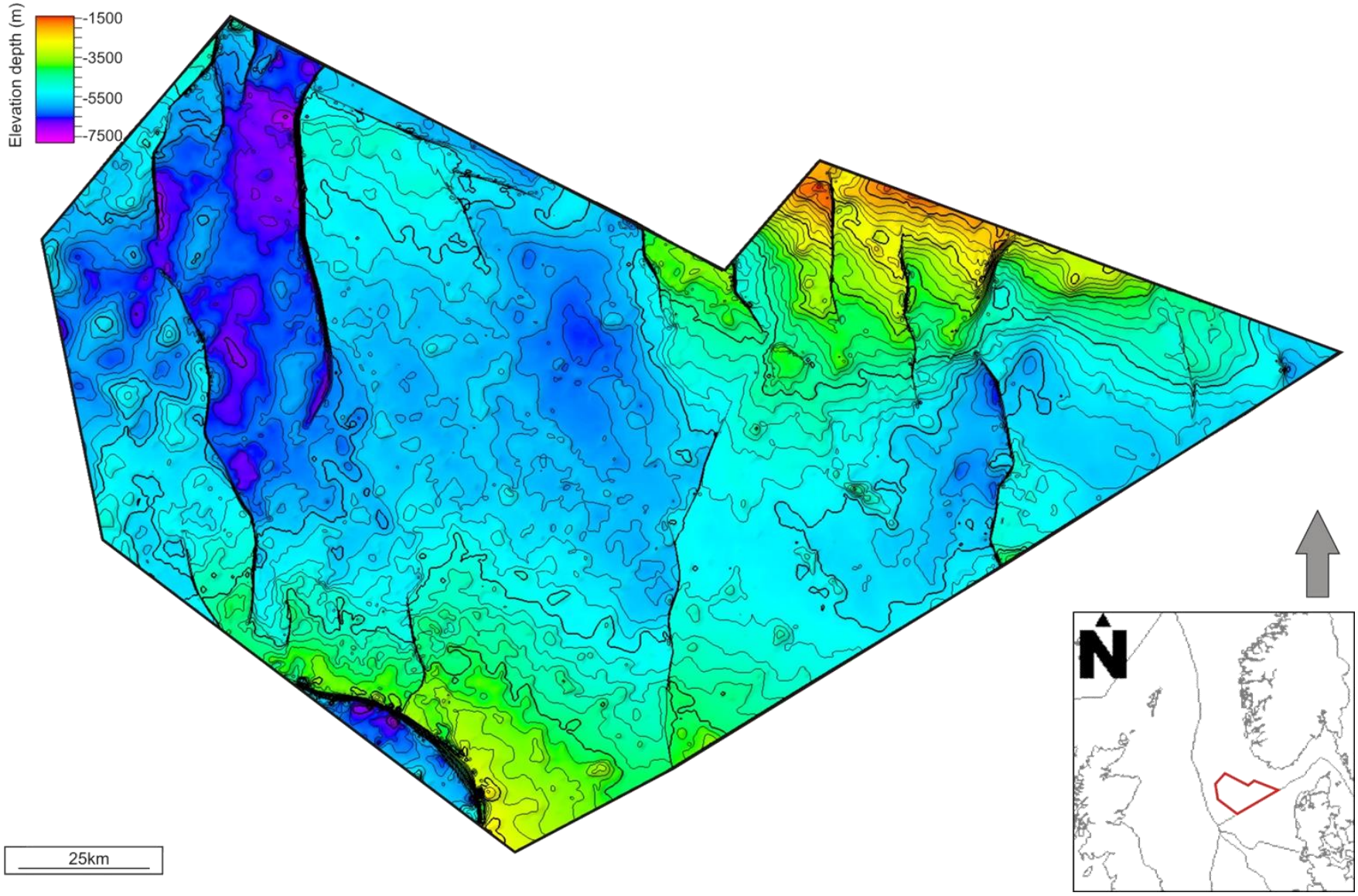

Figure 16. Top structure map of the Rotliegend Group in depth.

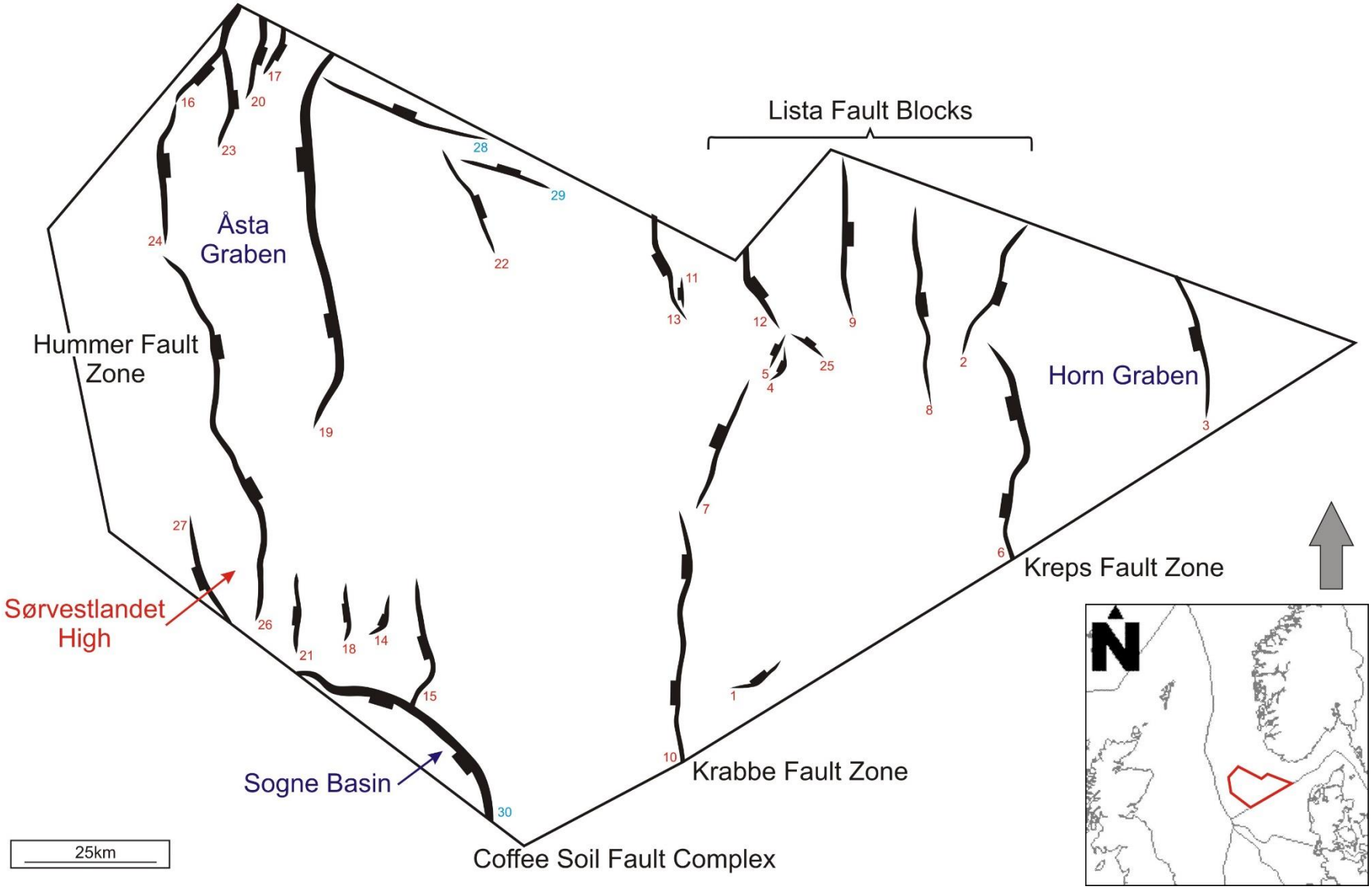

Figure 17. Structural elements map of Top of the Rotliegend Group.

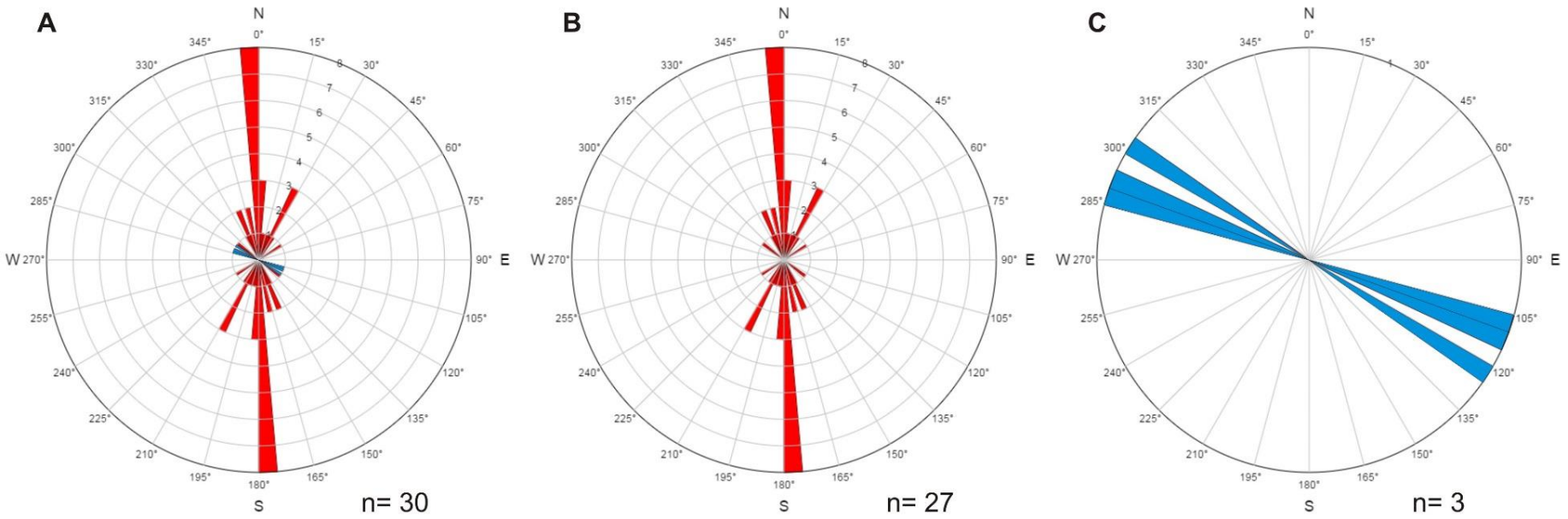

Figure 18. Rose diagrams for faults penetrating the Top of the Rotliegend Group. (A) Rose diagram for all faults, (B) Rose diagram for first fault group, (C) Rose diagram for second fault group.

The Rotliegend Gp isopach suggests presence of two main depocentres (Figure 19); one located in the northern-central part and the other in the eastern part of study area, delineated by two master fault zones, the Krabbe and Kreps Fault zones, respectively. The first depocentre (Figure 20) is interpreted as a sag basin with west-northwest to east-southeast basin axis (120˚-300˚) oriented parallel to the second fault family (Figure 17, Figure 18C). The length of the depocentre is approximately 125 km, while the width is around 75-80 km in the central part. Overall, the maximum thickness of this depocentre varies from 200 m to 600 m in the central part, while the thickness is up to 200 m on the flanks of the identified sag basin. The central depocentre contains the thickest Rotliegend strata in the western part, where isopach thicknesses range from 600 m to 700 m, respectively. The second depocentre is located in the western part of the NDB with a west-northwest to east-southeast trending basin axis (110˚-290˚), similar to the orientation of the first depocentre and the second fault family. The length of the depocentre exceeds 30 km, while the width is around 40 km. The depocentre is limited by the Kreps Fault Zone and the average thickness is 400 m to 600 m up to 700 m in the deepest part. Furthermore, the Rotliegend interval is decreasing in thickness near the northeastern flank.

The Lista Fault Blocks area contains relatively thin Rotliegend strata with thicknesses up to 200 m. The faults were active during deposition of the Rotliegend Group, as evident by variations in thickness along the faults in this region (Figure 19). Hence, the small-scale depocentres were located in the hanging wall of half graben boundary faults (Figure 14) as indicated by thickening in the hanging walls and thinning in the footwalls. Similarly, that the Kreps and Krabbe fault zones were active during Middle to Late Permian with the generation of small-scale depocentres along fault planes in the hanging walls.

The footwall region of the Coffee Soil Fault Complex includes a relatively thin Rotliegend succession with thicknesses up to 100m. It should be also noted that the regional faultsbounding the Åsta Graben, do not exhibit any impact on the deposition of the Rotliegend Group as evident from the absence of variations in thicknesses.

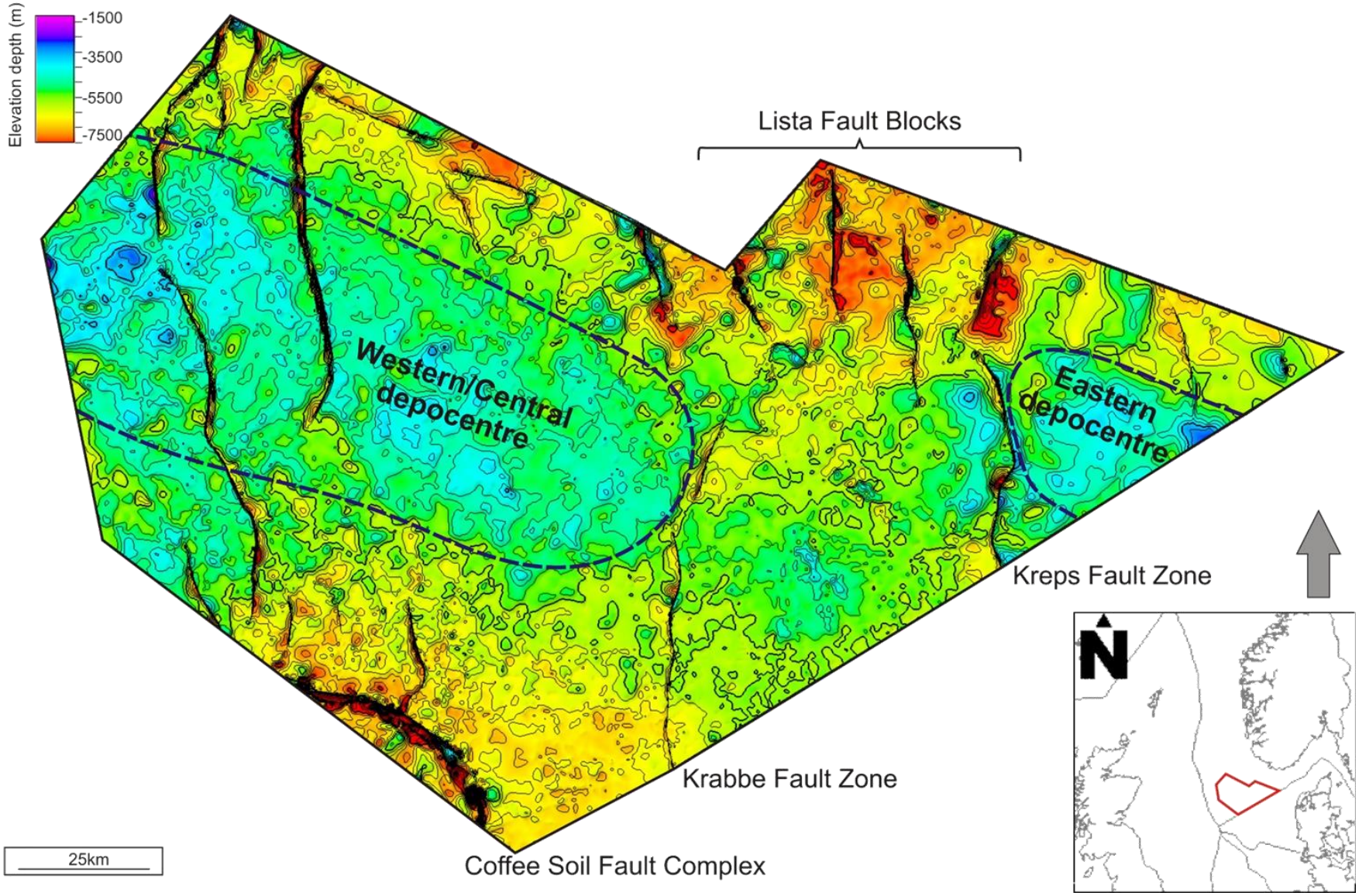

Figure 19. Isopach map of Top of the Rotliegend Group.

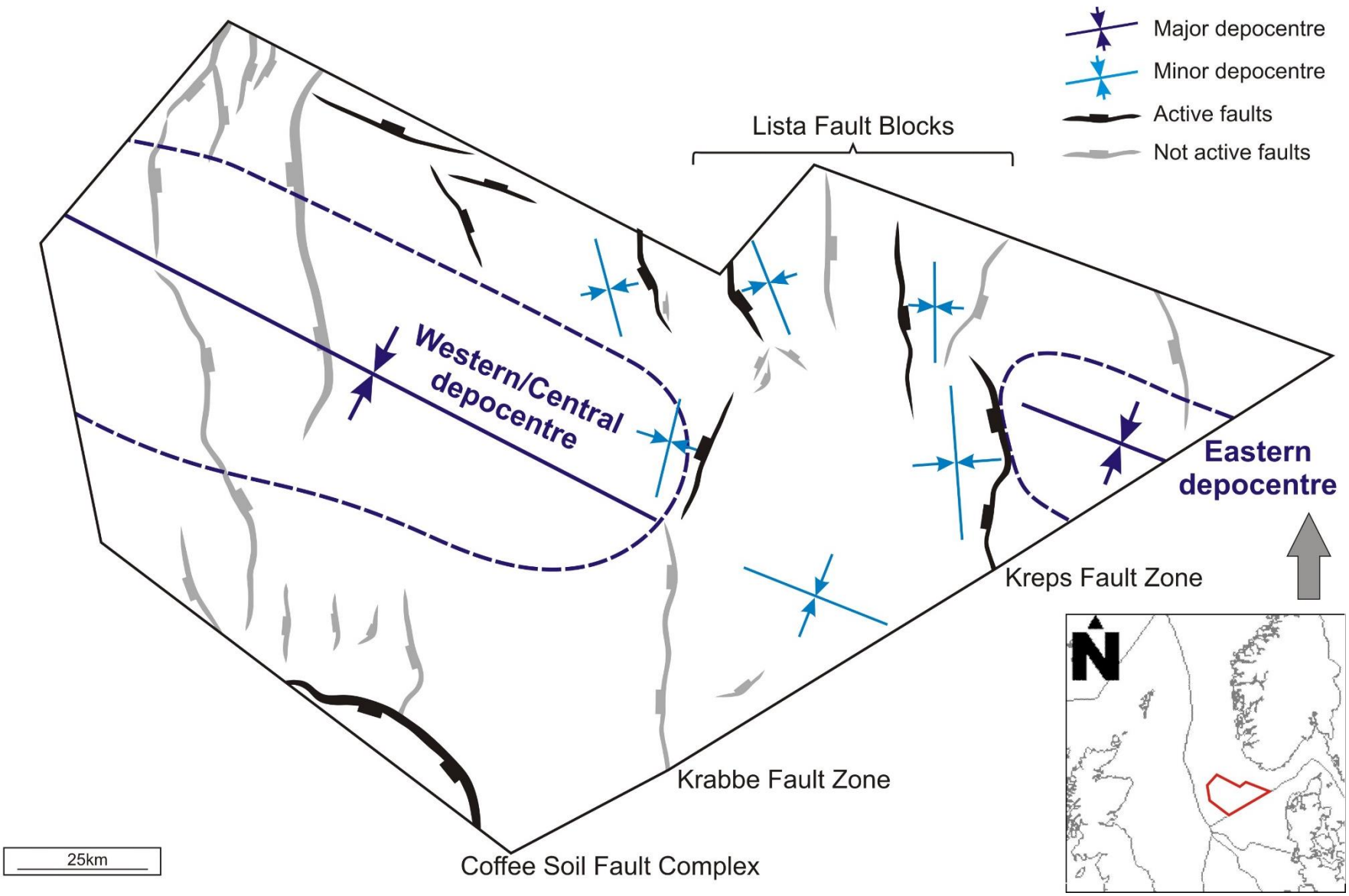

Figure 20. Simplified structural elements map showing the location of the Rotliegend depocentres and fault activity.

4.2. Top of the Zechstein Group

The top of the Zechstein Group mapped within the NDB illustrates the distribution of salt structures and its morphology (Figure 21). The depth-structure map shows the present day distribution of salt. Based on the seismic interpretations and constructed Rose diagrams (Figure 22, Figure 23), six major salt structures within the NDB were observed and listed below:

- Northwest-southeast trending salt walls in the central part;
- Northeast-southwest trending salt walls in the northeastern part;
- Triassic turtle structures in the southeastern part;
- Salt stocks penetrating Cenozoic strata;
- Salt roller and anticline structures in the Lista Fault Blocks area;
- Giant salt roller structure along the Norwegian-Danish border zone.

The isopach map of the Zechstein salt indicates the location of the Late Permian depocentres (Figure 24). According to the salt structure density map, the relatively thick salt intervals are detected in the central and western parts of the NDB (Figure 25). Thick Zechstein salt accordingly focused to the Rotliegend sag basins. Moreover, simplified structural map of the Zechstein isopach and faults, mapped at Rotliegend structural level, shows that variable thickness of salt is consistent with major structural elements at Rotliegend level (Figure 25).

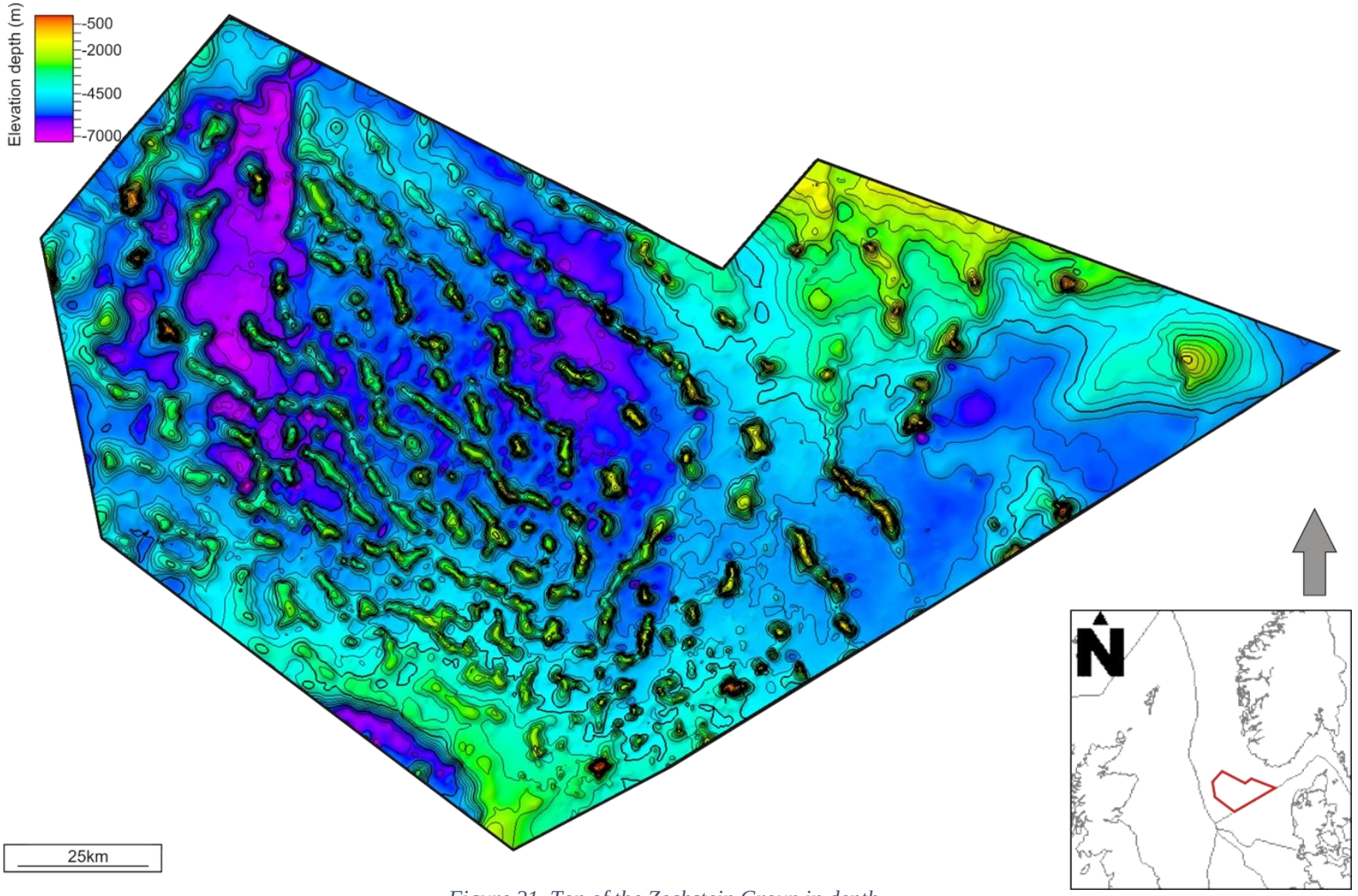

Figure 21. Top of the Zechstein Group in depth.

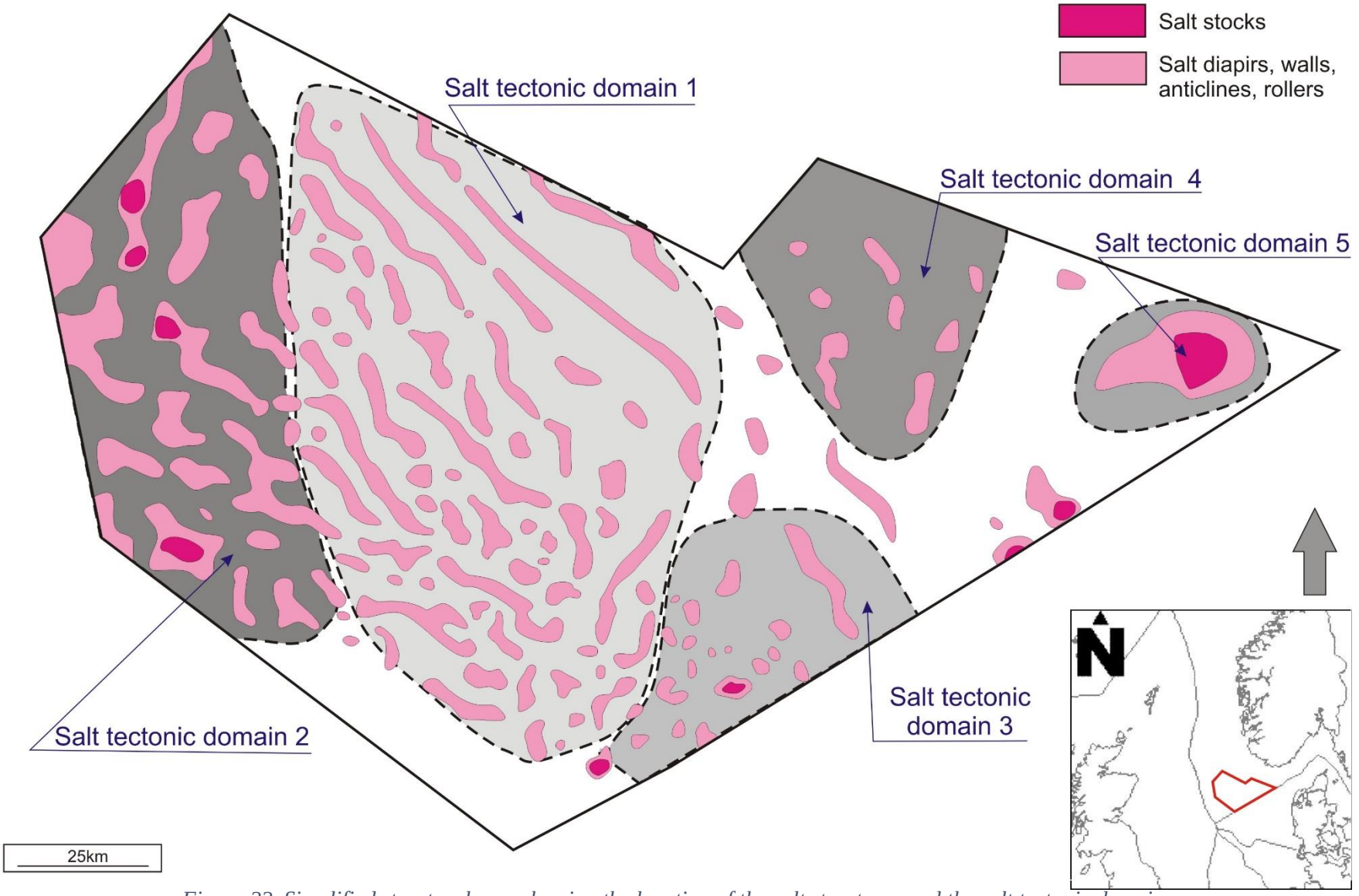

Figure 22. Simplified structural map showing the location of the salt structures and the salt tectonic domains.

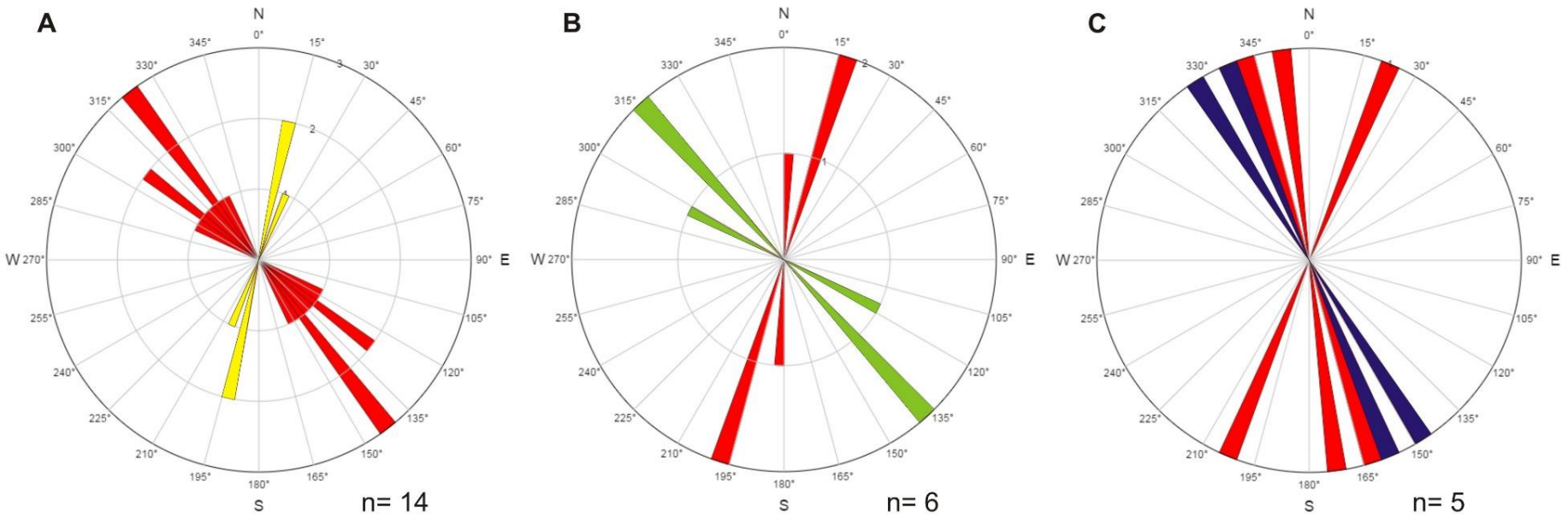

Figure 23. Rose diagram for salt structures. (A) Type 1, NW-SE oriented salt walls; (B) Type 2, NNE-SSW oriented salt walls; (C) Type 5, salt roller structure.

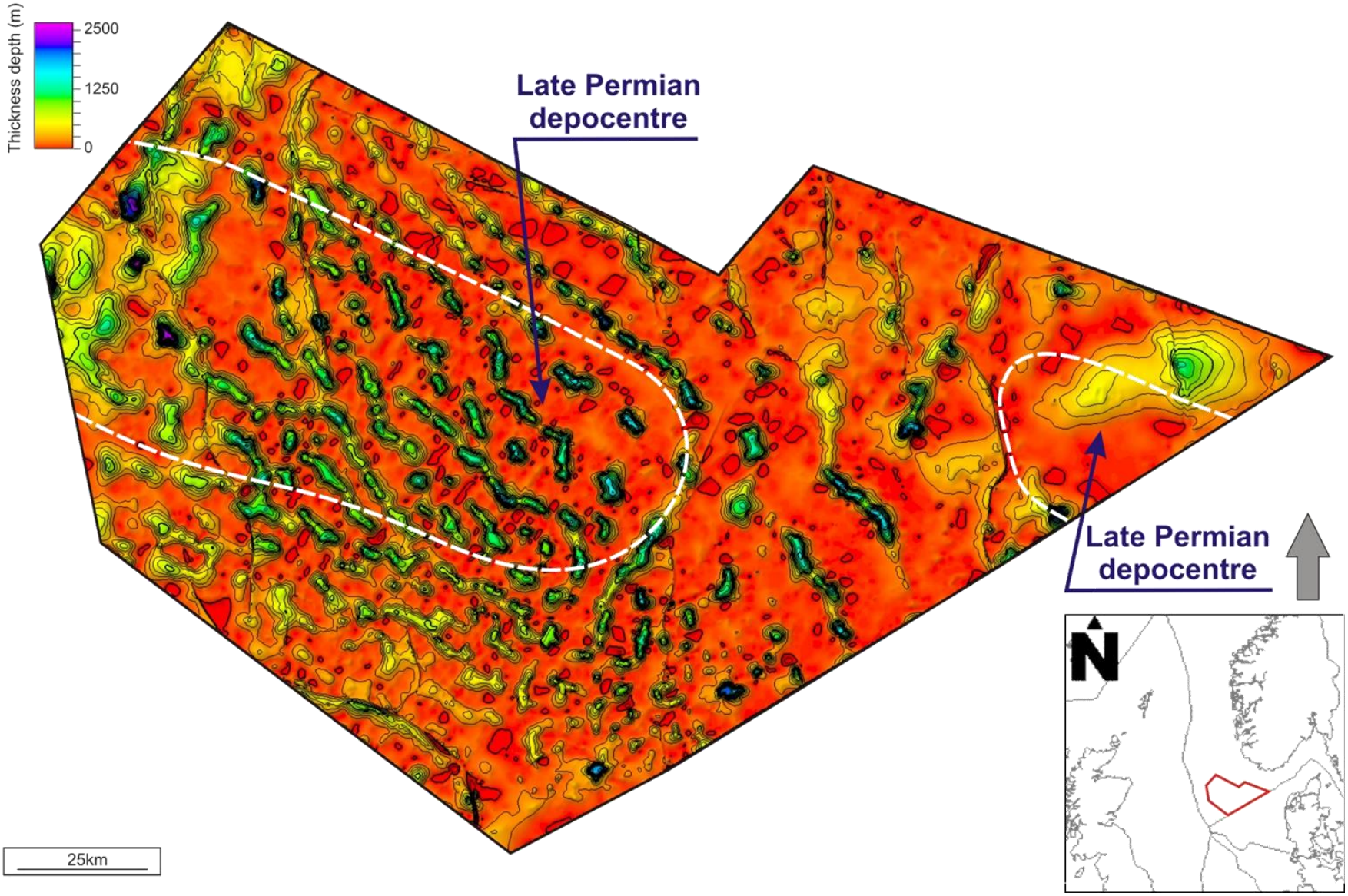

Figure 24. Isopach map of the Zechstein Group.

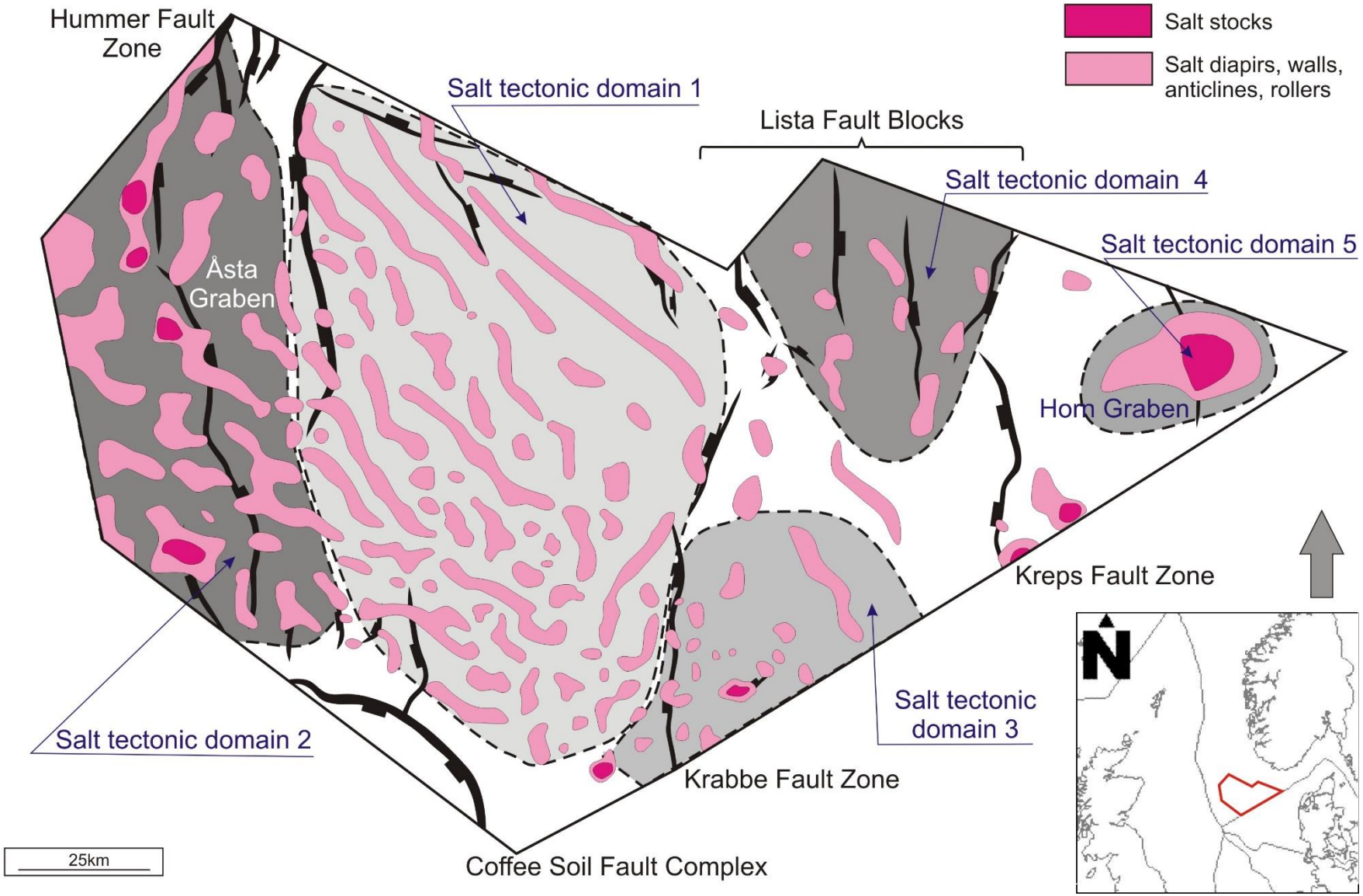

Figure 25. Simplified structural elements map showing the location of the salt tectonic domains and fault activity at the Rotliegend level.

4.2.1. NW-SE trending salt walls

A common salt structural style within the NDB is northwest-aligned salt walls widely located in the central part of the basin (Figure 21, Figure 22). These salt walls limited by the east-dipping fault from the Åsta Graben in the northeastern side and the north-south oriented Krabbe Fault zone in the southeast (Figure 19).

The salt walls have an overall northwest-southeast trend (ranging from 300°-330° to 150°-120°, Figure 23A, Appendix 3), however, the direction changes to north-northeast to south-southwest near the Krabbe Fault Zone (ranging from 12°-23° to 192°-203°, Figure 23A, Appendix 3). The salt features vary in width from 1.5 km to 2.3 km and in length from 9 km in the western part to 75 km in the eastern part. The geometry of salt walls reflects two possible mechanisms: linear source or strong influence from the next tectonic stage. Overall, eight salt walls are identified with the study area.

The timing of salt intrusions varies for different salt walls, which is consistent with sediment loading, reactivation of supra and sub-salt faults along with axial migration and dissolution of salt. This can be noticed from the intra Triassic reflectors (refer to halokinetic movements) as changes of the depocentres of minibasins and rim synclines. Figure 26 shows typical example of the salt walls in cross-section. Underneath the salt, sub-salt normal faults displace Rotliegend Group along with formation of horst and half graben structures. Salt walls symmetrically flanked by strongly dipping intra-Triassic reflectors along with salt welds features, consistent with minimum of salt thickness. The geometry of pod-interpod structures provide information regarding to the growth history of Triassic strata. The stratigraphic packages in the central part of cross-section (Figure 26) have rotated shape sequences with syn-deposition and thickening in opposite directions between two salt walls. Hence, there is an evidence of primarily clockwise rotation of strata from SW to NE and afterwards influenced by counter-clock wise rotation from NW to SE of Triassic succession. Moreover, rim-synclines are widely distributed near propagating upward salt bodies' indicative halokinesis. The overburden strata is relatively subhorizontal, however there are folded strata above the salt structure due to the trigger upward movements of salt. Furthermore, thin-skinned suprasalt crestal normal faults are located on the top of the salt walls resulting of high strengthening and following collapsing of salt structures.

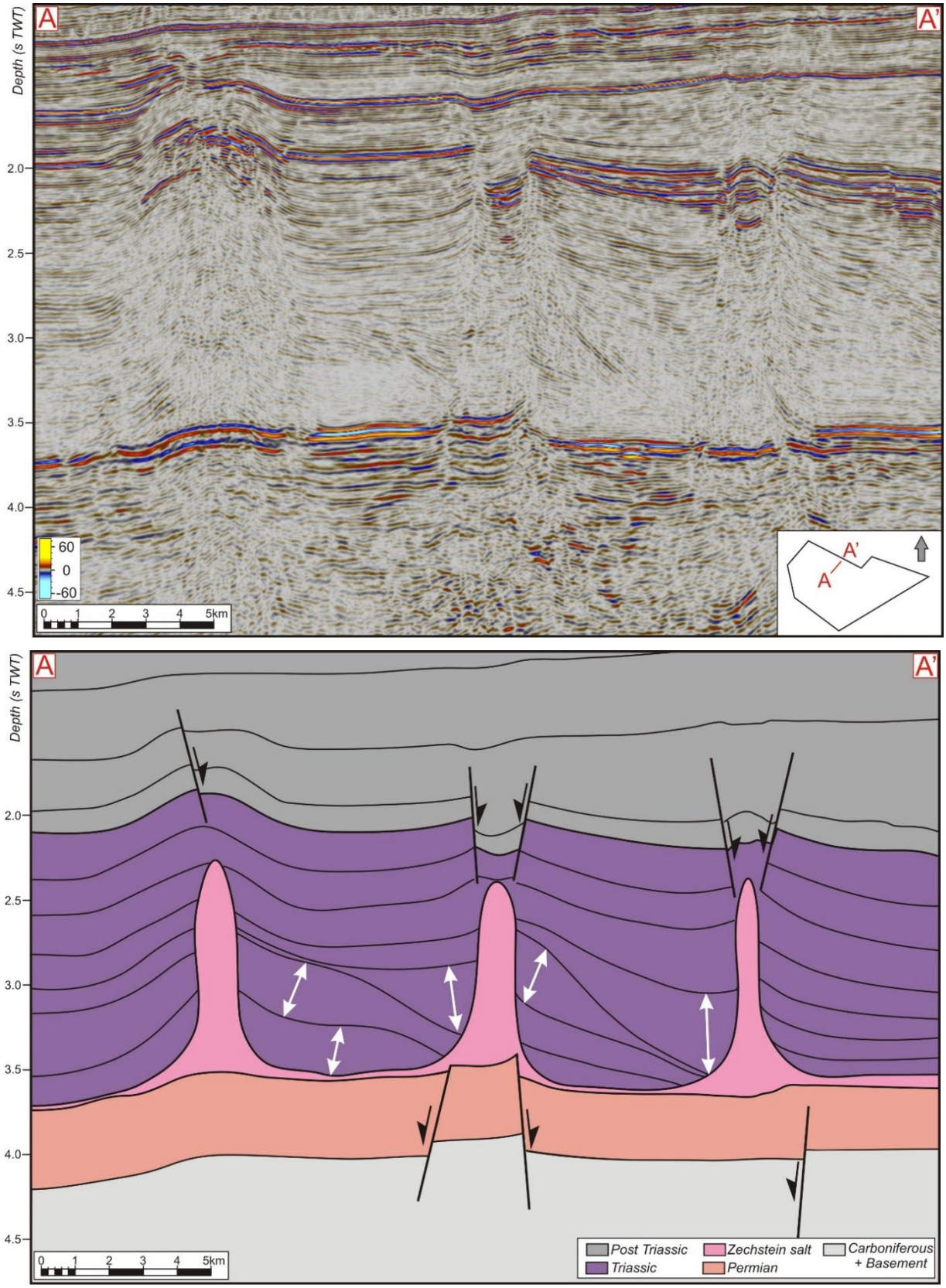

Figure 26. NW-SE trending salt walls, white arrows show the location of depocentres .

4.2.2. NNE-SWW trending salt walls

The subsequent observed salt structures are north-northeast to south-southeast trending salt walls in the western part of the NDB (Figure 21, Figure 22). This salt type is limited to the the Upper Permian Åsta Graben structure, more specifically located within the Hummer fault zone (Figure 22, Figure 25).

The salt walls have principal alignment from north-northeast to south-southeast (varying from 4˚ -19˚ to 184˚ -199˚, Figure 23B, Appendix 3) parallel to the Hummer fault zone and changing the trend to north-west in the southern part (varying from 117˚-136˚ to 227˚-316˚, Figure 23B, Appendix 3. Measurements of salt structures alignment.). The geometry of these salt walls is less linear in comparison with NW-SE trending salt walls, the length is shorter, up to 20-40 km; however, they are larger in width, up to 4-5 km. In addition, the distribution of the salt structure has slightly disordered character in the western part, but it is still possible to observe alignment.

Cross-section illustrates the displaced Rotliegend Group by the subsalt Hummer fault zone, and two salt walls with “drop” and “pyramidal” shape (Figure 27). Salt walls and faults bound the Triassic minibasins with thick strata. Furthermore, the stratigraphic packages are wedge shaped and counter clock wise rotated due to the changes in thickening of different packages. Hence, the synsedimentary deposition and rotation of strata was primarily influenced by salt structure in the southeastern part along with supra-salt fault detaching to the salt wall and secondary by the intrusion of northwestern salt wall and propagation through overburden Triassic strata. It is stated due to the evidence of rim synclines of Triassic strata near salt wall and lack of variations in thickness, hence the intrusion of salt body have post sedimentary character.

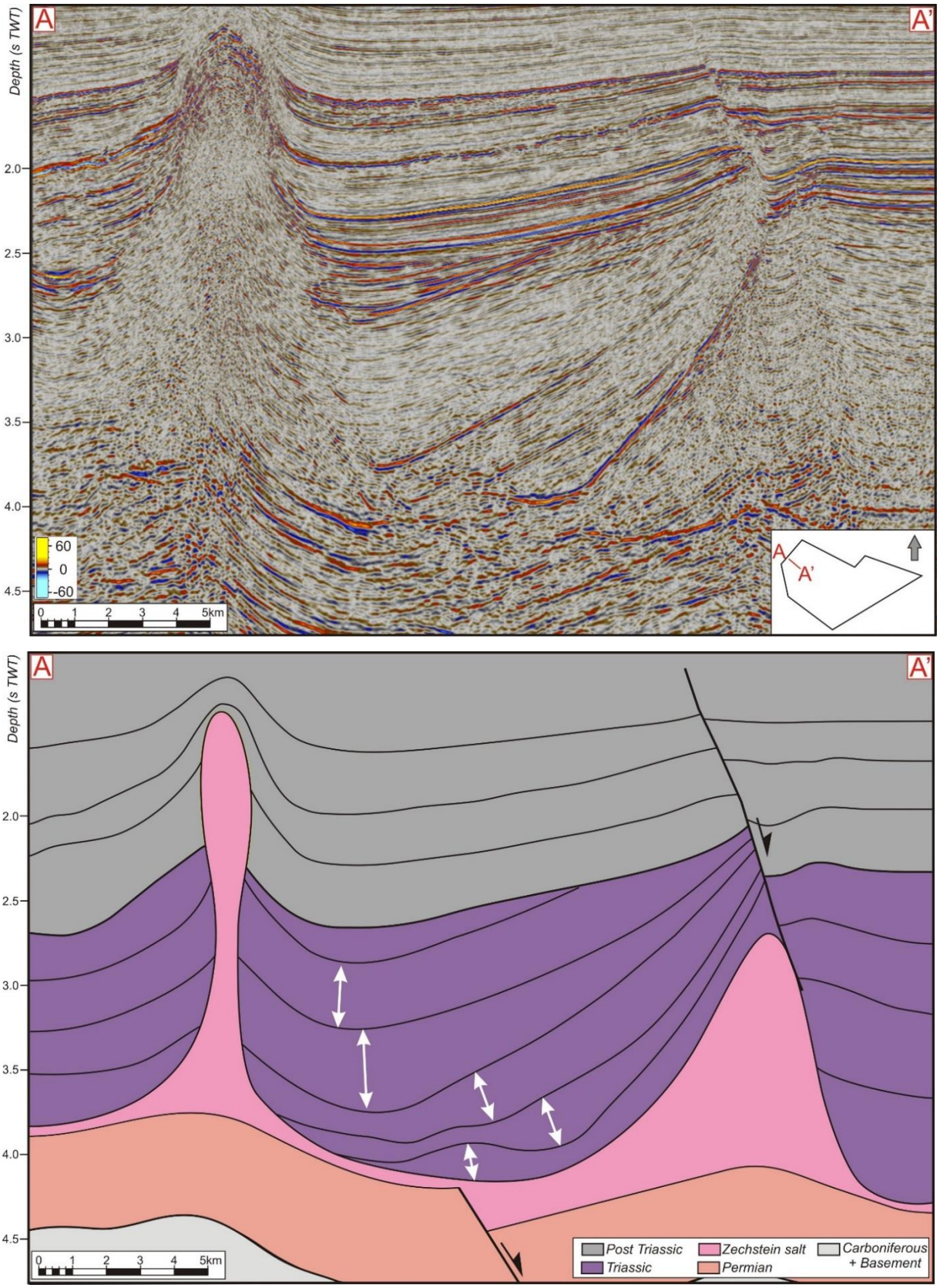

Figure 27. NNE-SSW trending salt walls, white arrows show location of depocentres.

4.2.3. Triassic turtle structures

Triassic turtle structures are identified in the southeastern part of the Norwegian-Danish Basin, and their location is restricted to footwall of the Krabbe fault zone (Figure 21, Figure 22).

The salt diapirs and small-scale salt roller structures have moderately disordered and quite limited distribution in contrast with the distribution of previously discussed salt walls. In addition, salt have relatively thin thickness. Hence, it can be proposed, that point salt source took the place in this region.

The sub-salt involved restricted normal fault is a syn-depositional Carboniferous fault according to the growth strata in the hanging wall and wedge unconformity surface dated as the base of the Rotliegend Group (Figure 28). The Rotliegend Group has homoclinal structure, conformable with no variations in thickness and no tectonic activity. The Zechstein Group comprises salt diapirs in southwestern part of cross-section and salt roller structures in the northeastern part.

The evolution and deposition of Triassic stratigraphic interval began with creation of primary salt-related minibasins (or “pods”), the sequence is marked from the base of Triassic to the more reflective wedge in the middle of Triassic (Figure 28). Generally, the salt diapirs have controlled the deposition of Triassic interval with thinning on the top of salt structures and thickening in depocentres between diapirs or where salt has axially migrated. Subsequently, the salt walls have collapsed (or axial migrated) resulting in inversion of primary depocentres, creating turtle structures and generating synforms above salt walls as a secondary depocentre for overburden Triassic sequence. Along with turtle structures and diapirs, there are salt weld features underneath of primarily depocentres and rim-synclines resulting in vertical halokitetic movements.

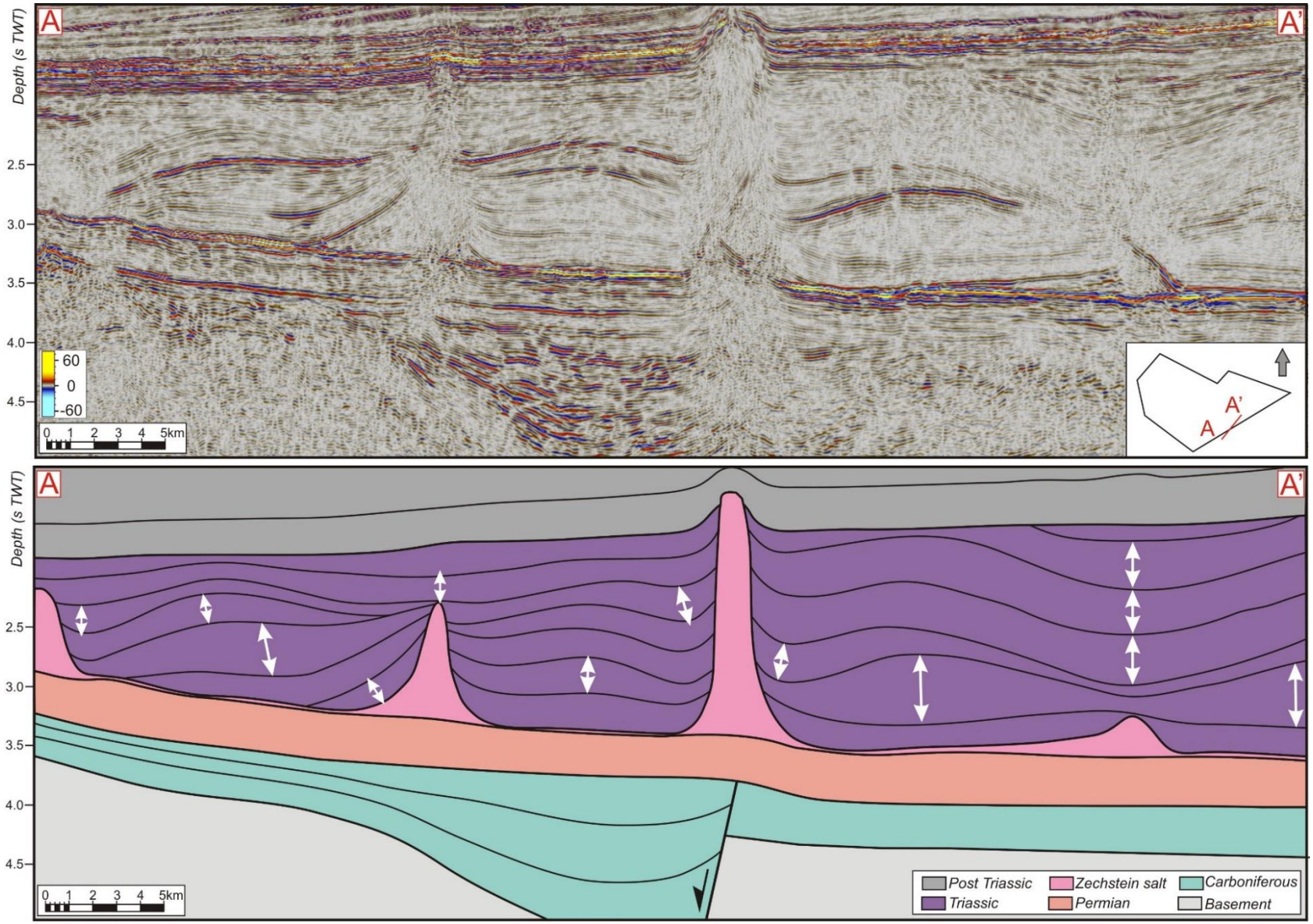

Figure 28. Triassic turtle structures, white arrows show location of depocentres.

4.2.4. Salt stocks penetrating Cenozoic section

Tall salt stocks are chaotically distributed in the southeastern and furthermore western part of investigated area (Figure 21, Figure 22). The tall salt diapirs occupy small areas in the map view, however, they achieve a great high (Figure 29).

These salt structures propagate not only through the Triassic section, but also through the Mesozoic-Cenozoic section and reach the sea floor in some locations. Furthermore, the supra-salt faults are absent in the southern area, in spite of associated listric supra-salt faults in the western part confined with the distribution of Type 4, which can be a possible driving mechanism for halokinesis.

The diapirs have moderately mushroom shape linked by a narrow neck to an underlying salt triangle. The salt welds are distributed where the salt interval is relatively thinner and supra-salt Triassic sediments are quite close to the top of the Rotliegend Group.

The overlaying salt the Triassic succession is symmetrical near salt intrusion and flanked by strongly dipping sediments, whilst several depocentres are distinguished due to the thickening of strata (Figure 29). Distinct stratigraphic packages have wedge shape and thickening in alternative directions on opposite sides of salt stock. Consequently, the Triassic succession in the southern part was clock wise rotated; but it has been observed counter-clock wise rotation in the northern side. Hereafter, the upward halokinetic movements resulted in the rotation of existing Triassic packages along with generation of accommodation space far from the salt diapirs as the upward propagation of the salt allowed more sediments to accumulate in the space that was previously occupied by salt. Meanwhile, it was more reactivated in the Mesozoic-Cenozoic.

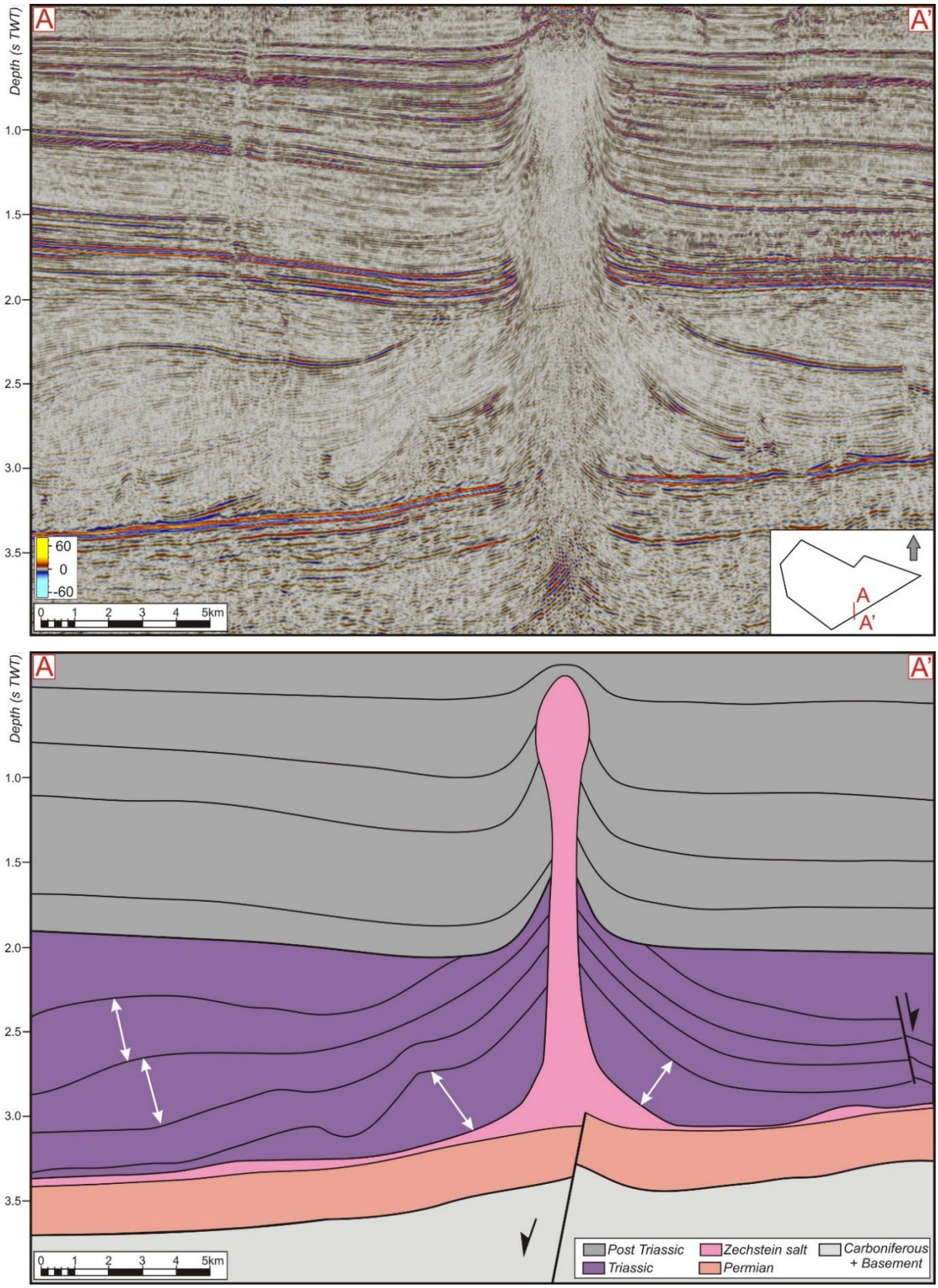

Figure 29. Salt stocks, white arrows show the location of depocentres.

4.2.5 Salt roller and anticline structures

Salt roller and anticline structures distributed in the northeastern region (Figure 21, Figure 22) and limited by the sub-salt normal faults belonging to the Lista Fault Bocks area and the distribution of salt is very indicative with the location of faults from the Rotliegend structural level (Figure 24, Figure 25).

The salt structures have isolated shape with small thickness. Some of the salt structures have more elongated shape (for instance, salt rollers and anticlines); whereas, other structures have more isolated and rounded geometry (for example, isolated diapirs and pillows). Overall, this salt structural domain is quite disorganized and discontinuous; however, the general trend is oriented from north-northwest to south-southeast, mostly varying from 147˚-174˚ to 327˚-354˚ (Figure 23C, Appendix 3).

During seismic interpretation it has been observed, that elongated salt structures developed from salt rollers to salt anticlines due to increasing in maturity and have considerably linear source, while more isolated salt diapirs refer to lack of salt or point salt source. In addition, the salt structural features have triangle shape and associated supra-salt normal faults detached to the salt décollement layer.

The overburden sedimentary cover above the salt has constant thickness in the lower level, displaced by small-offset fault family dipping in southeast direction (Figure 30). Taking into consideration this fact, post-sedimentary tectonics has taken place without any influence on the accommodation potential of lower Triassic stratigraphy contrasting with pod-interpod structural architecture. In the upper Triassic succession, the stratigraphic packages are thickening toward the hanging wall of the southeastern fault, admittedly, that the fault activity and/or halokinetic movements were coexisting with sedimentation. Two supra-salt normal faults displace Triassic interval along with Mesozoic-Cenozoic section and comprises a typical graben structure (Figure 30).

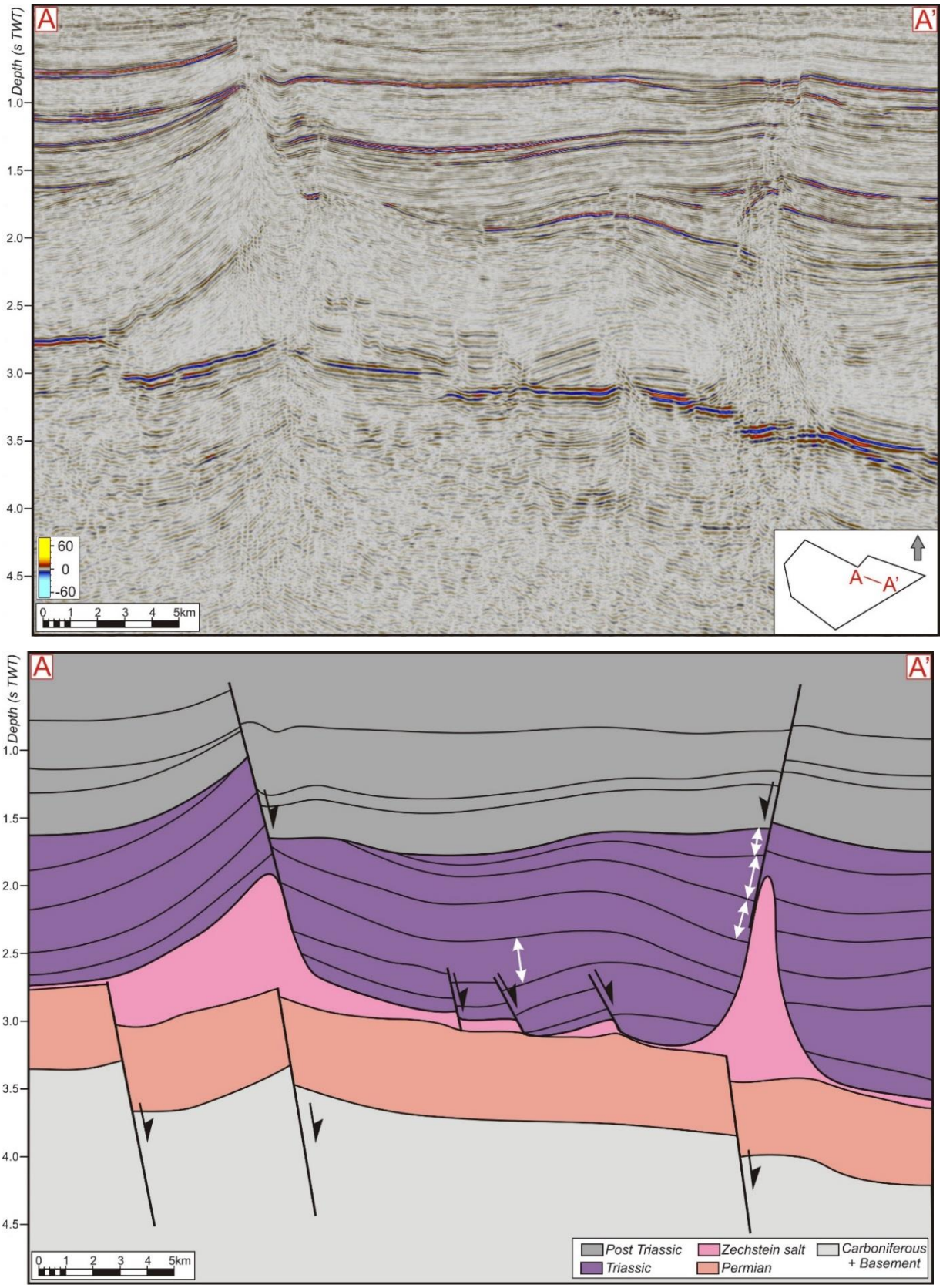

Figure 30. Salt roller and anticline structures, white arrows show depocentres.

4.2.6. Giant salt roller structure

A giant salt roller feature located in the southeastern part of NDB along the Norwegian-Danish border zone, limited to the Horn Graben (Figure 14, Figure 21, Figure 22).

Giant salt roller are characterized in large thickness, around 600 m in the hanging wall and 900 m in the uplifted footwall (Figure 24, Figure 25), also approximately 30 km in length and 15 km in width. The main axis of the structure is aligned from northeast-east to southwest-west (107˚-287˚, Appendix 3).

The salt succession is heterogeneous as suggested by the presence of reflectors within the salt interval (Figure 31). These clearly visible reflectors outline layers within the salt, which can represent diagenetic or primary layering of salt succession.

Underneath the Zechstein Group (Figure 31), the sub-salt regional fault related to the second fault family (described earlier in 4.1) and dipping in west-south west direction has syn-ryft signature resulting in Carboniferous interval due to the evidence of growth strata toward the hanging wall. The Rotliegend structural level has constant thickness of sediments and lack of fault activity impact on structuralization. Along with the giant salt roller structures, another salt feautures were identified, such as salt pillow, around 2 km in length, and salt welds, where the salt layer has minimum thickness or even absent which can provide for hydrocarbons good migration pathways for upper levels.

The overburden Triassic strata has consistent thickness, strongly folded and faulted in agreement with ductile and brittle deformations, caused by halokinetic movements and active supra-salt fault. Overall, it is post-sedimentary tectonics for Triassic interval with not of significant variations in thicknesses identifying the locations of minibasins. Nonetheless, there is turtle structure of upper Triassic sediments in the footwall of fault, indicative with the location of the primarily depocentre and its following inversion with become after a relative high.

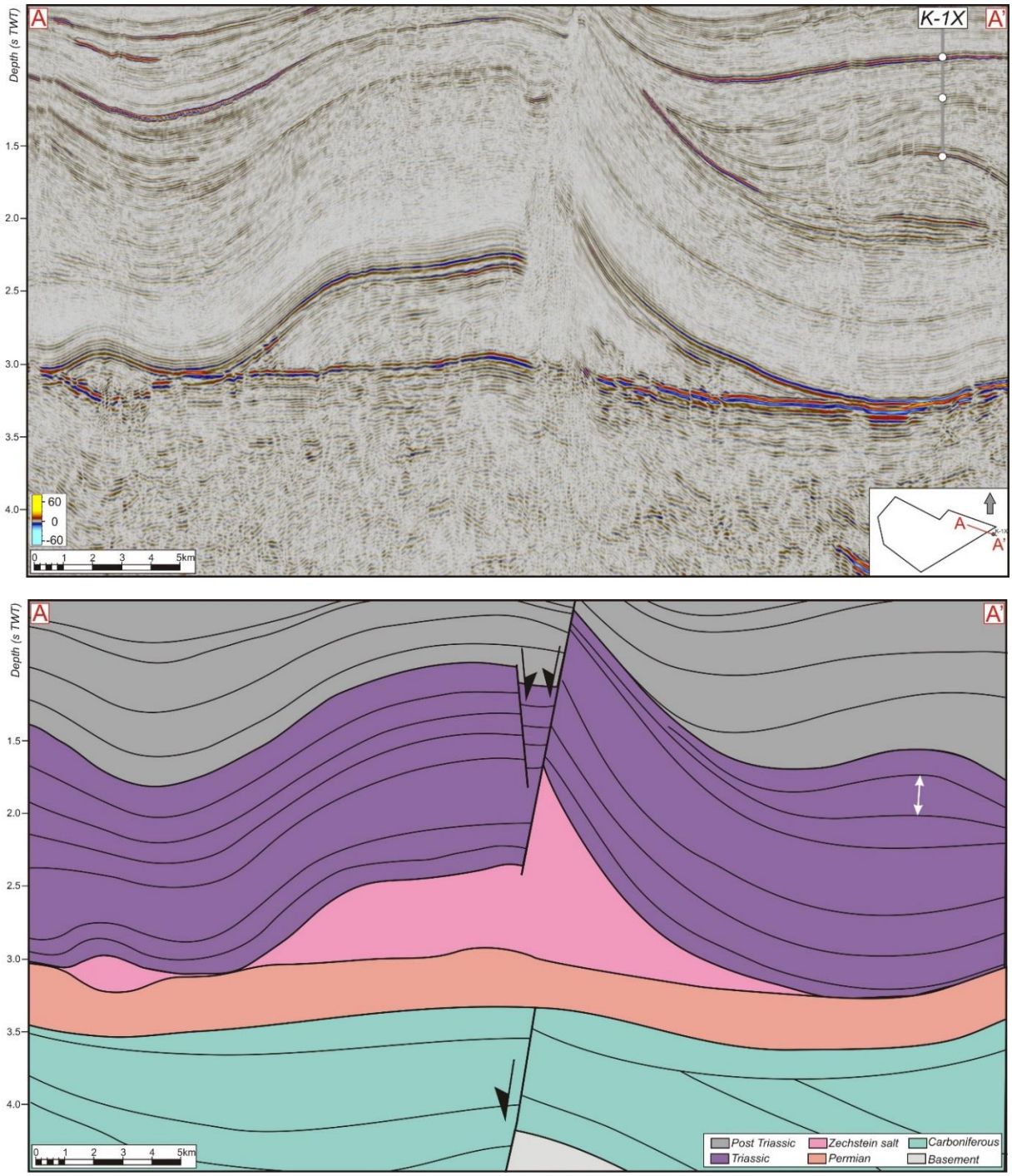

Figure 31. Giant salt roller structure, white arrow show location of depocentre.

4.2.7. Salt tectonic domains

The salt tectonic domains were distinguished according to the geometry and distribution of salt structures, while their complexity is closely connected to the tectono-stratigraphic evolution of the NDB (Figure 25). Possible driving mechanisms include multi-episodic rifting, influence of subsalt-involved normal faults along with supra-salt restricted normal faults, differential loading and local basin inversion in some parts of the basin. Five major salt tectonic domains were carefully identified, mapped and described below:

- **Domain 1** includes NW-SE trending salt walls and salt diapirs in the central part of study area, bounded by the Åsta Graben structure and the Krabbe Fault Zone;
- **Domain 2** comprises NNE-SWW trending salt walls and tall salt stocks in the western part of the NDB, limited to the Åsta Graben structure and the Hummer Fault Zone;
- **Domain 3** contains Triassic turtle structures, tall salt stocks, diapirs, salt anticlines and salt roller structures in the south-eastern region of the NDB, restricted to the footwall of the Krabbe Fault Zone;
- **Domain 4** consists of salt anticlines, salt rollers and diapirs, limited to the Lista Fault Blocks area in the north-eastern part of the study area;
- **Domain 5** is presented by the giant roller structure with associated salt pillows and located in the eastern part of the NDB along the Norwegian-Danish border zone.

4.3. Top of the Skagerrak Formation

The Top of Skagerrak Fm is a relatively smooth surface in the central part of the NDB. A series of faults bounded structural highs and are present over the giant salt roller structures in the north-western part and eastern part of the sedimentary basin. The top Triassic level is bounded to the NE and SW by the Egersund basin and Central Trough, respectively. Within the NDB, 26 crestal supra-salt normal fault have been distinguished in the area and separated into two different fault families according to their strike of fault planes and timing of fault activity (Figure 33, Figure 34A).

The first discerned fault family is limited to the north-west region, confined to the location of the Åsta Graben from the Rotliegend structural level (Figure 32, Figure 33). Overall, this fault family shows a variety in fault plane geometry, changing from a more listric shape to a more planar (Figure 14). Fault activity displays post-sedimentary characteristics displacing all stratigraphic intervals from the Triassic to Cretaceous. The fault family comprises two subgroups with fault planes in perpendicular directions following the structural interpretations and constructed Rose diagrams (Figure 33, Figure 34B). The major alignment of the first subgroup is northwest-southeast, strike direction is ranging from 117˚ to 139˚ RHR and from 277˚ to 334˚ RHR (Appendix 4), whereas the second subgroup has a northwest-southeast trend with strike directions of 55˚ and 234˚ RHR (Appendix 4). In addition, the average length of the fault polygons belonging to the first subgroup is more extensive (around 15 km - 45 km) then the length of polygons of the second subgroup (approximately 10 km).

The second fault family is located in the eastern part of study area, restricted to Lista Fault Blocks and Horn Graben regions (Figure 32, Figure 33). Based on seismic interpretations and constructed Rose diagram (Figure 34C), the main orientation of this fault group is from north-northwest to south-southeast (the strike directions are 341˚-354˚ and 175˚-163˚ RHR, Appendix 4), whereas two faults have a north-northeast to south-southwest trend. The timing of fault activity is linked to Paleocene times, due to the displacement of the top of the Balder Formation (Figure 14), in addition, this fault family has larger offset of displacement then the first family described above.

There is no evidence of hard or soft linkage between the supra salt and the sub-salt faults from different structural levels thought to be related to the existing non-displaced salt (Figure 14, Figure 15, Figure 26, Figure 30, Figure 31). Apart from this, the majority of the supra-salt faults are detached above the Zechstein salt because of the rheological properties of this décollement horizon (Figure 27, Figure 30, Figure 31). Moreover, the distribution of the supra-salt fault families coincides with the location of salt-related structures (Figure 22).

Some of the supra-salt faults comprise a system of peripheral salt-related graben structures, owing their origin to the upward halokinetic movements, followed by squeezing overburden strata and resulting in collapse (for example, Figure 26).

The Triassic isopach map suggests presence of several depocentres (Figure 35, Figure 36). Three major Triassic depocentres with an average thickness of 1400-1600 m are recognized in the Åsta Graben area and in the southeastern area in the Horn Graben and the Kreps Fault Zone. The basin axis of the first depocentre has a north-south trend (178˚-358˚), aligned with the sub-salt Åsta Graben. In the southeastern side, the orientation of two another depocentres, separated by a high, trend from the west-northwest to east-southeast trending basin axis (105˚-295˚), subparallel to the Rotliegend depocentres. In the Central part of the NDB, minor depocentres are observed and proposed to be salt-related mini-basins. However, more detailed seismic interpretations of intra-Triassic reflectors is proposed to have a more precise understanding of the halokinetic movements and influence on accommodation potential. In addition, the Søgne Basin located in the hanging wall of the Coffee Soil Fault Complex has an average thickness of Triassic strata ranging from 800 m to 100 m (Figure 35). Notably, these three depocentres are defined based on a thick gross Triassic succession, as discussed in Chapter 4.2, while laterally shifting intra-Triassic depocentres occurred in the various sub-areas due to diachronous development of salt structures. Hence, this suggests a more complex sedimentary architecture with detailed infill styles, unfortunately it is not represented by the Triassic isopach map.

A relatively thin Triassic interval (0-400 m) covers the southern edge of the NDB, more precisely the footwall of the Coffee Soil Fault Complex. The thin Triassic strata, in the order 0-400 m, is also observed in the northeastern peripheral part that is consistent with the location of the Lista Fault Blocks region. The eastern and the northern flanks have thin Triassic strata, ranging from 600 m to 100 m, and their locations are consistent with the Sørvestlandet High and the footwalls of the Åsta Graben structure. In the entire area, the thin Triassic succession is consistent with the distribution of the Zechstein salt structures.

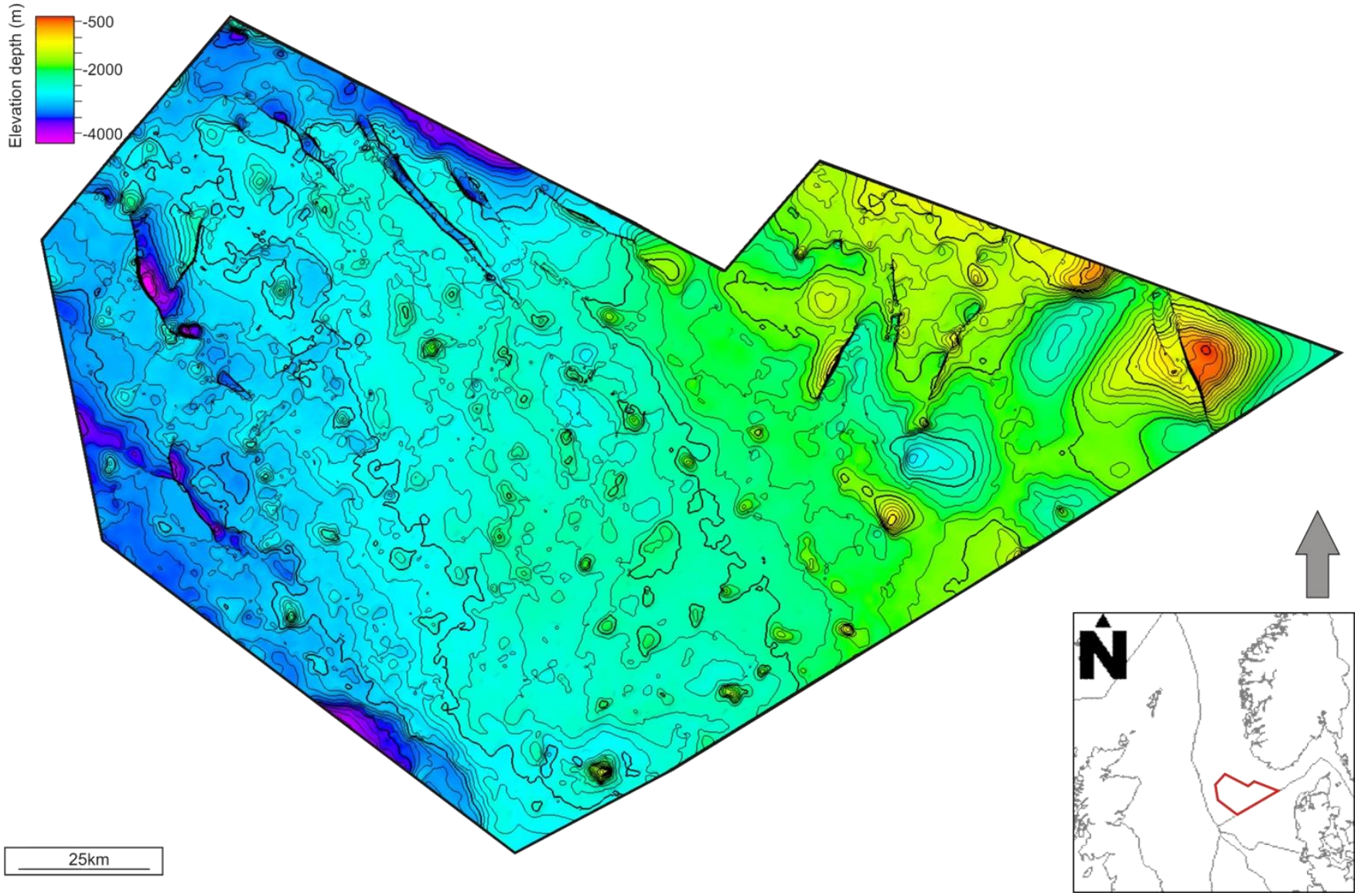

Figure 32. Top of the Skagerrak Formation in depth.

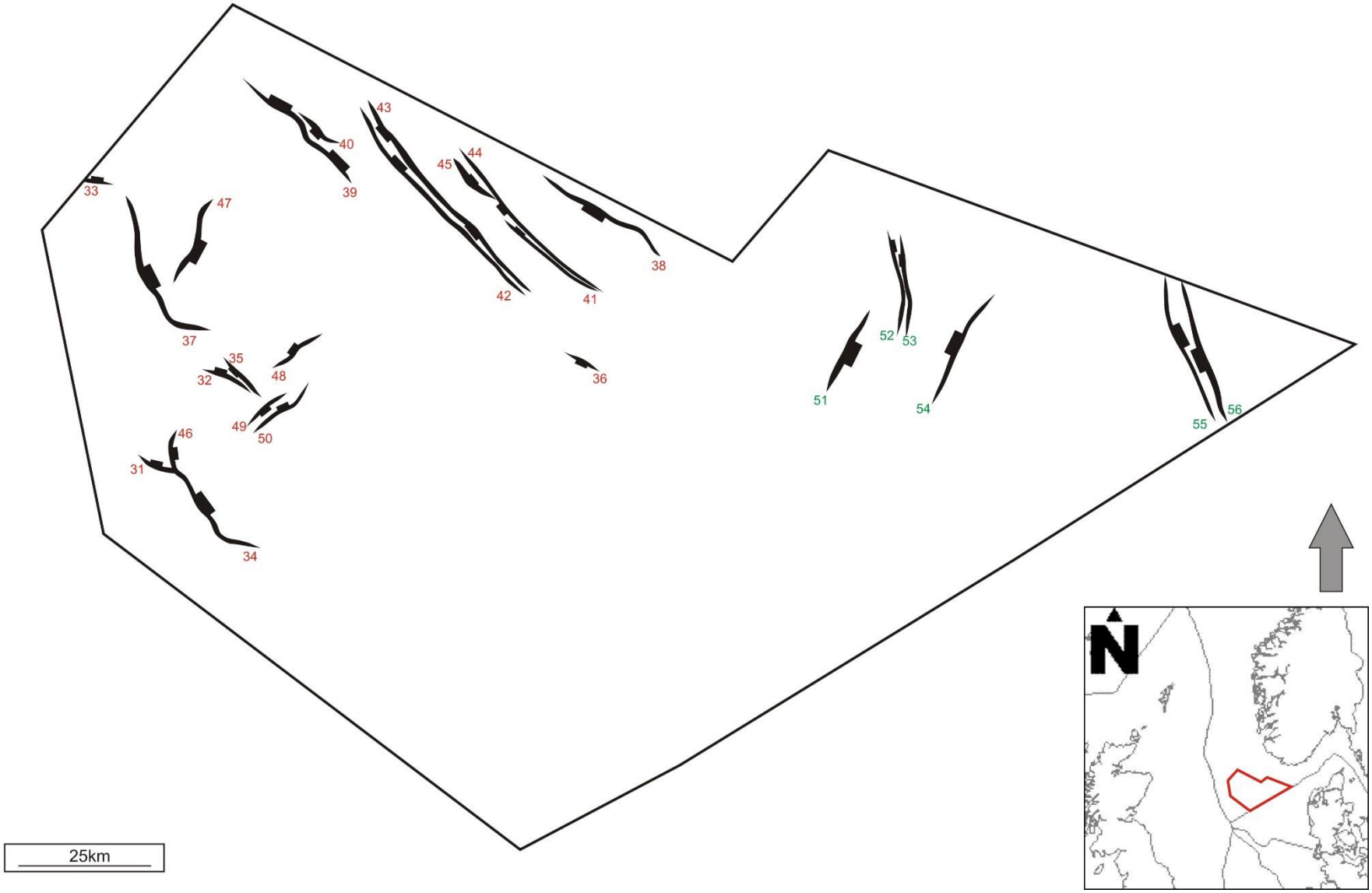

Figure 33. Structural elements map of Top of Skagerrak Formation.

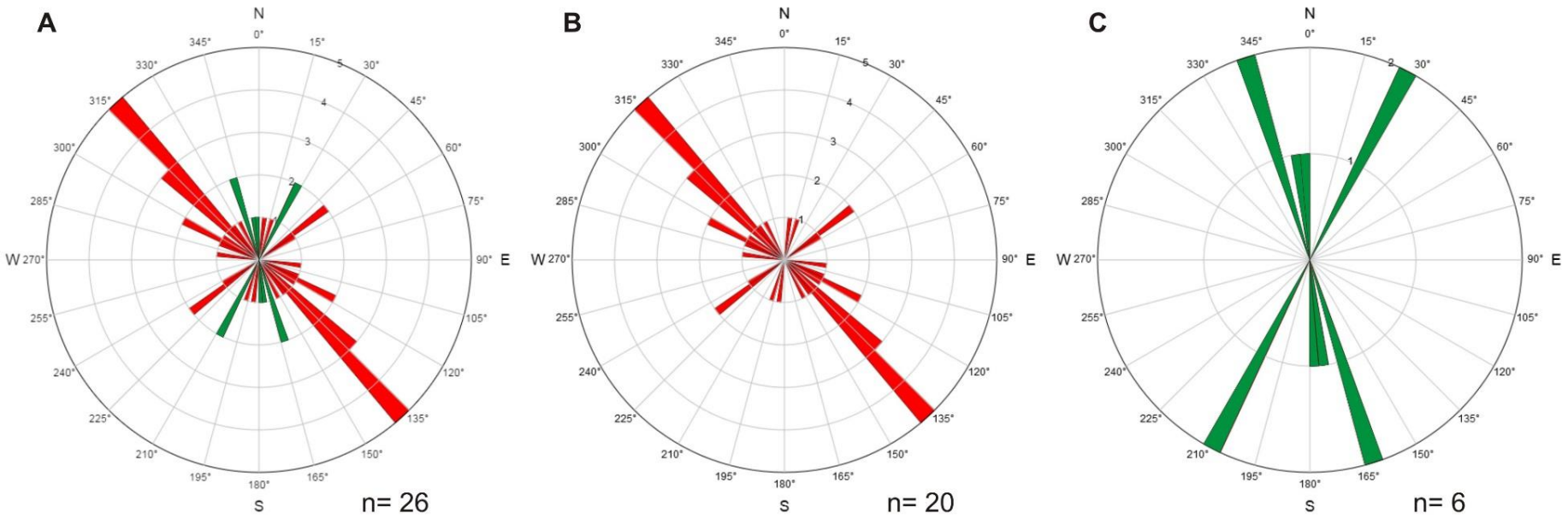

Figure 34. Rose diagram for faults penetrating Top of Skagerrak Formation. (A) Rose diagram for all faults, (B) Rose diagram for first fault group, (C) Rose diagram for second fault group.

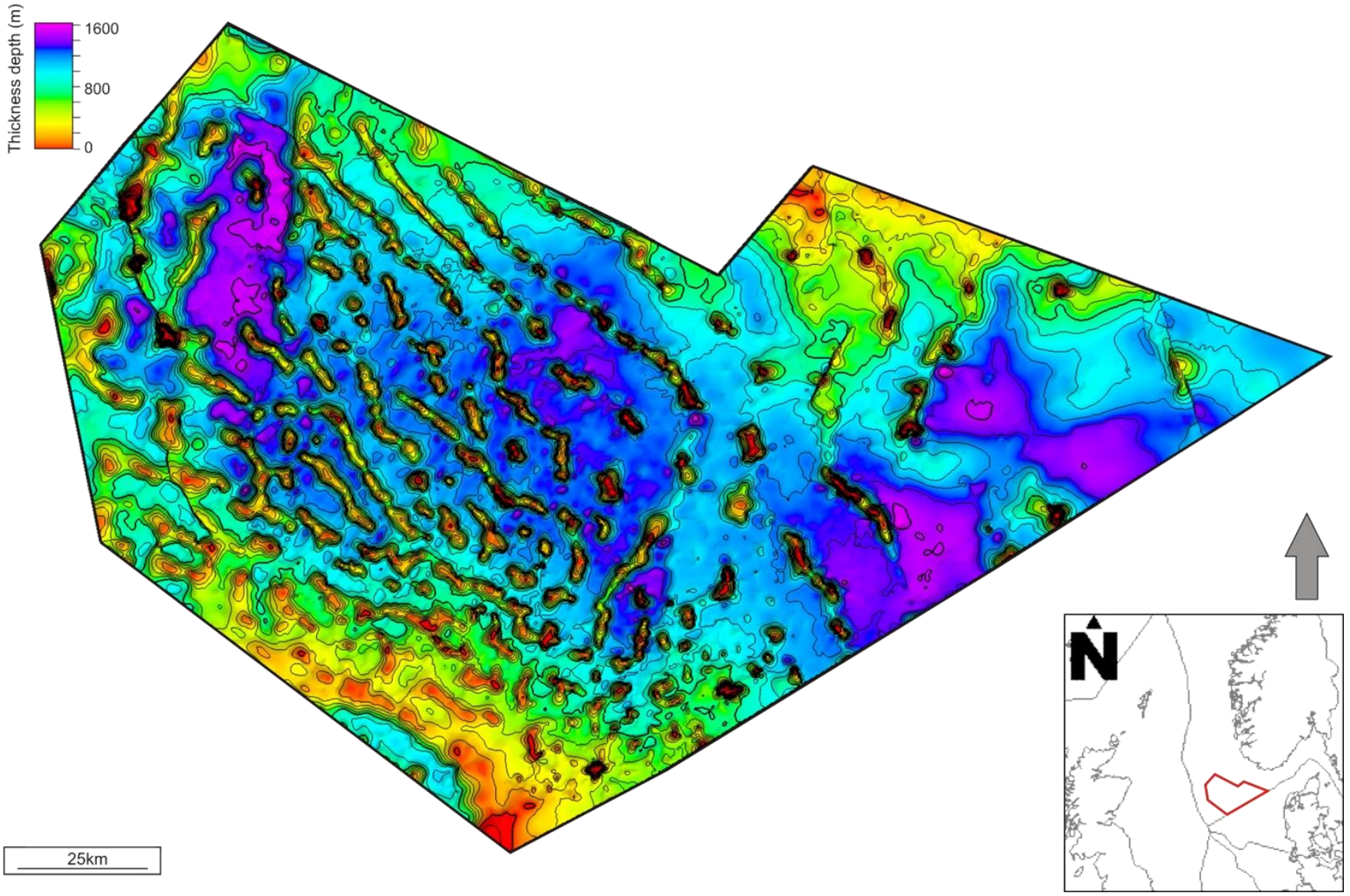

Figure 35, Isopach map of Triassic interval.

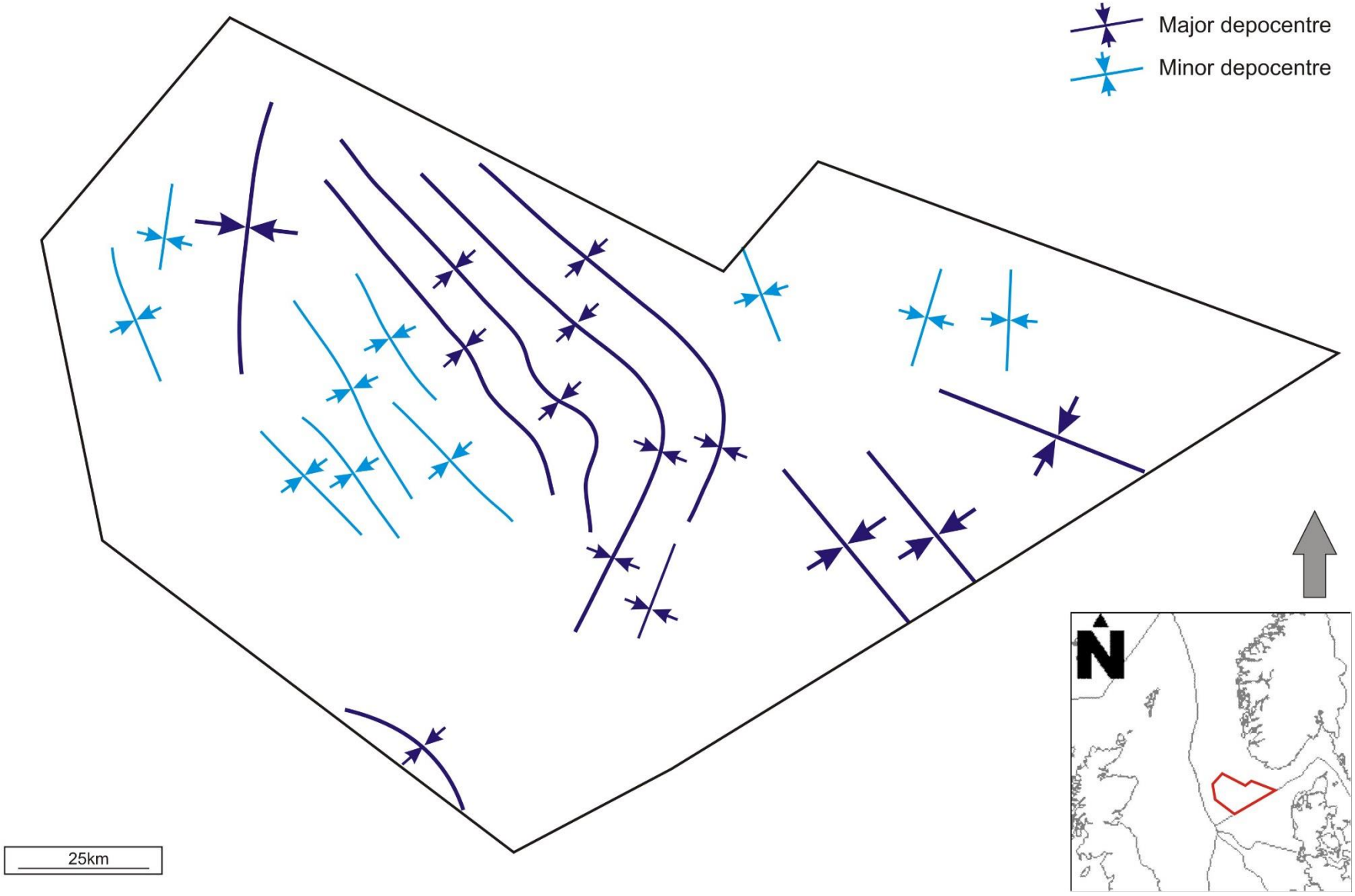

Figure 36. Structural elements map showing the location of Triassic depocentres.

The top of Skagerrak Formation in the reflection-seismic profiles is clearly defined by an unconformable contact between the Triassic and the Jurassic structural levels (Figure 37). In more detail, this angular unconformity separates a folded Triassic stratigraphic unit with inverted turtle structures along with strongly dipping reflectors along the collapsed salt diapir from the Jurassic overburden strata with more parallel horizontal reflectors. The contact is also obvious from crosscutting of Triassic folded sediments and their truncation by erosion.

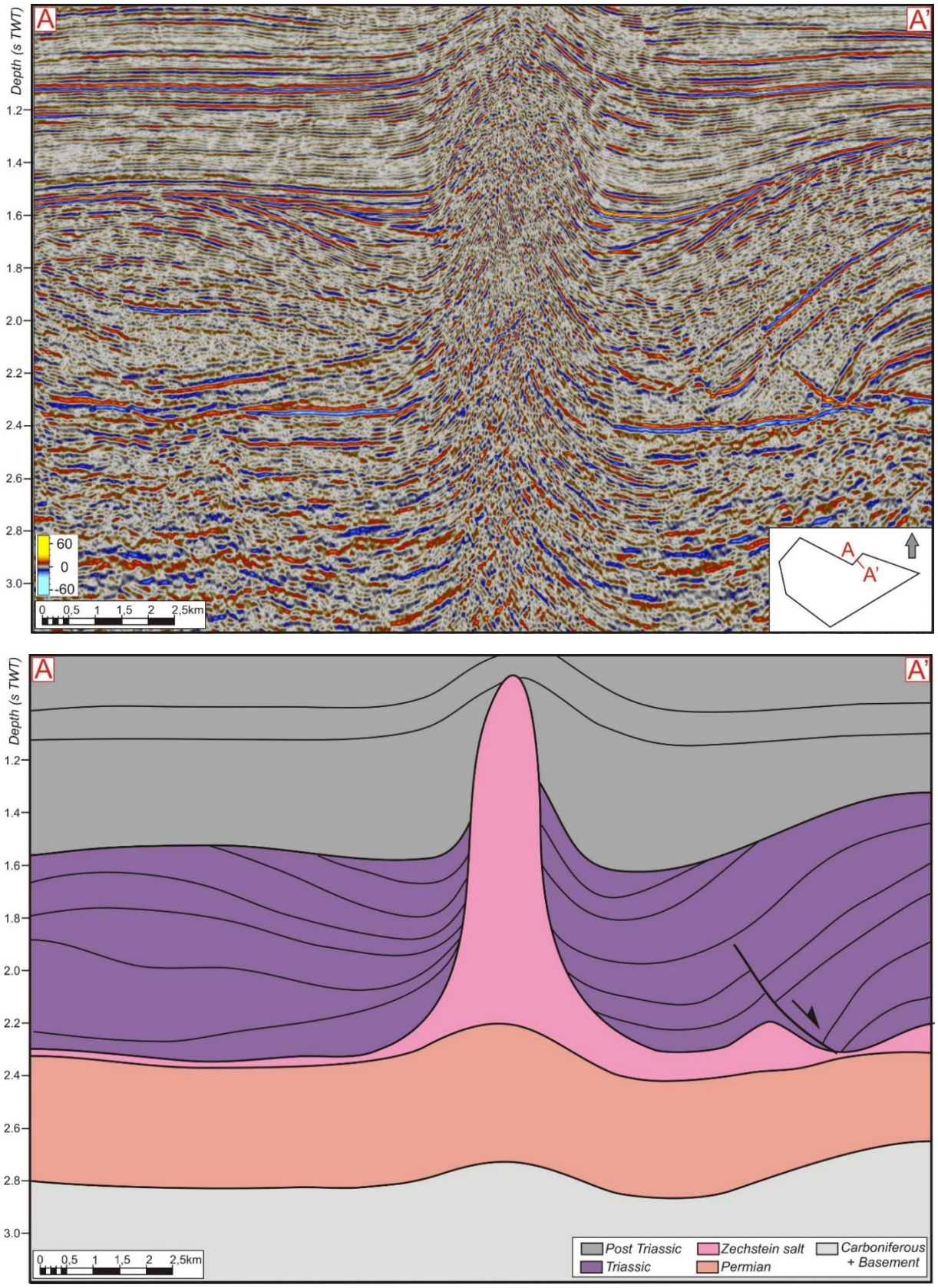

Figure 37. Major Base Jurassic unconformity surface, separating Triassic and Jurassic structural levels.

5. Discussion

5.1. Structural Evolution of the Norwegian-Danish Basin

For the following discussion part, all observations, provided by seismic interpretation and constructed key cross-sections along with previous studies of the area, have been reviewed to generate conceptual tectono-stratigraphic models of the structural evolution of the NDB. During Late Permian to Triassic, three major tectonic regimes have been recognized and proposed as following, 1) Pre-salt structurization, 2) Structural impact on salt, and 3) Salt impact on depocentres.

5.1.1. Pre-salt structurization

The first stage of the NDB evolution occurred in the Middle-Late Permian, more specifically during the Rotliegend interval, and resulted in the formation of two major depocentres with west-northwest to east-southeast oriented basin axis (Figure 38A). Two sub-basins are located in the northern-central part and in the south-eastern part of study area, limited by two master fault zones, the Krabbe and Kreps Fault zones, respectively. These basins have been identified and interpreted as large intracratonic sag basins (Figure 38B), in agreement with a smooth isopach suggesting relatively flat topography (Figure 15), long-term stability and continental depositional systems (Chapter 4.1). This is evident by the accumulation of aeolian sands of the Auk Formation in the Rotliegend Group representing semi-arid conditions. The present day analogue for an interior sag basin is the Lake Eyre Basin in Australia. In addition, major active fault complexes from the second group forming the boundaries, hence a pre-existing northeast-southwest extensional direction can be inferred. Accordingly, the alignment of the sag basins controlled by the Late Carboniferous and Early Permian Hercynian Orogeny (Ziegler, 1992), resulting in the formation of east-west and northwest-southeast trending major tectonic lineaments.

The two depressions with thicknesses in the order of 600-700 m formed the initial sedimentary basin with continued subsidence for a long period of time. In the Late Permian, thick organic-rich shales from the Kupferschiefer Formation accumulated during the transgression and therefore occur within the two depocentres.

The presence of localized synclines in the hanging walls of boundary faults in the Lista Fault Blocks area along with the Krabbe and Kreps Fault Zones seems related to the initiation of west-east extension in the eastern region of the NDB (Figure 38B). According to

Pedersen et al., 2006a, the north-south trending Krabbe and Krepps Fault Zones developed due to the reactivation of old basement structures in the south-eastern part of the North Sea.

The Late Permian stage of the pre-salt structuring coincides with a period of widespread rifting with a continuous west-east extension direction (Figure 38C, Figure 38D) based on seismic interpretation of the top of the Rotliegend Group. This is time equivalent to the extensional regime of the late Hercynian Stephanian-Autunian orogeny in the Northern Permian Basin (Evans et al., 2003). Two general sub-salt fault families with north-south and west-northwest – east-southeast alignments formed in response to this rifting event. In addition, the boundary faults, such as the Hummer Fault Zone and the Krabbe and Kreps Fault Zones, had a significant impact on the development of an echelon imbricate faults with hard linkage to the master faults (Figure 38D). Apart from this, imbricate faults could also form in response to clock-wise rotation of the north-south aligned master faults attributed to their curved shape. Due to intensive Late Permian fault activity, several major structural elements within the NDB were generated with subsequent impact on the evolution of the basin and accommodation potential. These are the Lista Fault Blocks area, Sørvestlandet High, Åsta Graben, Horn Graben, Hummer Fault Zone and the Krabbe and Kreps Fault Zones (Chapter 4.1, Figure 14, Figure 15, Figure 17).

5.1.2. Structural impact on salt

The sedimentation rate significantly increased in the NDB due to accumulation of thick stratigraphic packages of salt and carbonates of the Zechstein Formation during episodic changes in the relative sea level during the Late Permian. According to the present day isopach map of the Zechstein Formation (Figure 39A), the sub-salt basinal faults along with the Rotliegend topographical relief controlled the distribution and thickness variation of the salt stratigraphic interval (Figure 39B) as well as the position of Zechstein evaporate-carbonate facies tracts (Chapter 4.2). The Zechstein salt is generally concentrated in the northwestern and central parts of the study area with less salt represented in the Lista Fault Blocks area and Kreps and Krabbe Fault Zones. The original thickness of these sediments was more 1000 m (Skjerven et al., 1983). In addition, the salt is very thin or absent towards the footwall of the Coffee Soil Fault Complex (Figure 39B). The Rotliegend sag basins dictated the accumulation and preservation of salt, to illustrate this the thickness is up to 1250-2500 m in the western/central depocentre and 900 m in the eastern depocentre. In addition, salt has a relatively small thickness on the flanks of the sag basins.

Regional mapping of the top of the Zechstein Group allows us to distinguish several salt structures within the NDB, comprising the main salt tectonic domains (Figure 39C, Figure 39D). These are 1) Northwest-southeast trending salt walls in the central part; 2) Northeast-southwest trending salt walls in the northeastern part; 3) Triassic turtle structures in the southeastern part; 4) Tall salt stocks penetrating Cenozoic strata; 5) Salt roller and anticline structures in the Lista Fault Blocks area; 6) Giant salt roller structure along the Norwegian-Danish border zone, and 7) Salt diapirs. The salt structure nomenclature proposed in this thesis is in line with the classification of salt bodies suggested by Bishop (1996) in the Central Trough, by Karlo et al. (2014) in the Central North Sea and in the NDB by Hospers et al. (1988). Bishop (1996) identified salt rollers along with salt welds in the platform west of the Central Graben and tall salt stocks penetrating Mesozoic-Cenozoic interval and propagating to the sea floor in the Central part of the North Sea. Karlo et al. (2014) proposed five major salt domains, including 1) Pod-interpod structures; 2) Fault-bounded minibasins; 3) Collapsed-anticline diapirs; 4) Salt welds and 5) Salt walls. Salt walls are recognized by Hospers et al. (1988) and identified by their strong linearity and extending for lengths greater than 50 km. To conclude, the six major salt tectonic domains proposed in this research are in accordance with previous studies and have been identified by geometry, shape, and distribution of salt structures. Furthermore, the salt structures formed due to differential loading of Triassic sediments along with reactivation of basement faults, discussed below.

5.1.3. Salt impact on depocentres

The subsequent tectonic stage of the NDB evolution is related to the accumulation of the Triassic sediments in response to halokinetic movements resulting in formation of salt structures. Deposition of Triassic strata took place during the extensional episodes associated with the breakup of the Pangaea supercontinent (McKie, 2014). According to the isopach map, constructed from the top of the Zechstein Group to the top of the Skagerrak Formation (Figure 40A), three major Triassic depocentres, in the order of 1400-1600 m in thickness, are present within the NDB. Their location, shape and distribution are controlled by sub-salt restricted normal faults (Figure 40B). In other words, normal faults at the Rotliegend structural level in combination with salt withdrawal influenced the accommodation pattern for the Triassic depositional system with a high rate of subsidence. Importantly, the location of Triassic depocentres coincides with the Rotliegend and Zechstein depocentres. Four major entry points of Triassic clastic depositional system into the NDB from the northeastern basin margin are tentatively suggested based on the Triassic depocentre distribution (Figure 40B).

The structural and stratigraphic architecture of Triassic mini-basins above the salt diapirs are linked to the pod-interpod model of extension over collapsing salt walls proposed by Hodgson et al. (1992). The first stage is the initiation of mini-basin subsidence during extension of basement structures and accumulation of overburden strata above the salt (Figure 41A). Secondly, mini-basins continue to subside and salt walls initiate to grow due to gravity driven subsidence of Triassic depocentres into the salt and buoyant properties of the salt (Figure 41B). The distribution and alignment of pod mini-basins is consistent with the strong linear salt walls and presented in the central and less in the northwestern part of study area (Figure 40C). The next stage is related to the mini-basins grounding on sub-salt basement with the development of salt welds due to lack of sediment supply and ending of salt wall propagation (Figure 41C). Finally, salt walls collapse related to inversion of original mini-basins and developing synforms on the top of collapsing walls, acting like a secondary mini-basins (Figure 41D). All the stages of pod-intrapod evolution have been observed in almost all interpreted seismic lines and described in the cross-section in this research (for example, Figure 14, Figure 15, Figure 26-Figure 31, Figure 37). McKie (2014) studied in more detail the Triassic dryland terminal fluvial systems architectures in the central North Sea (Figure 42), which is in accordance with the observed results of this thesis together with proposed pod-intrapod model by Hodgson et al. (1992). Moreover, understanding of the impact of halokinesis on Triassic sedimentation is complicated by Triassic salt dissolution. As Bishop et al. (1995) suggested, around 30 % of the primary salt volume was removed during this period and by major post-Triassic movement.

Halokinetic movements initiated mainly due to differential loading by the overlying strata, reactivated sub-salt basement structures and, possibly, thermal loading. Karlo et al. (2014) proposed that likely mechanisms for halokinesis are uplift of the footwall of the Central Trough in the Triassic, a rifting event in the eastern region of the NDB during Triassic and thermal doming.

The Late Triassic-Early Jurassic stage of evolution of the NDB is represented by a pronounced widespread unconformity. The shallow marine shales from the Fjerritslev Fm marked the unconformity, separating Jurassic and halokinesis influenced the Triassic structural levels. The Late Triassic- Early Jurassic supra-salt faults formed in the eastern and north-wetstern parts of study area (Figure 40D). Based on seismic interpretation, the location of supra-salt faults reveal a correlation between salt halokinetic structures. Hence, the fault activity relates to upward propagation of salt instead of a south-west extensional regime. In general, supra-salt faults are post-sedimentary faults, detached on the salt layer and exhibit a

listric shape of the fault plane (Figure 27, Figure 30, Figure 31). Two fault families, differing in age and orientations, have been recognized within the NDB. The first fault family, located in the north-west region, is older relative to the second fault family and has a predominant northwest-southeast alignment consistent with the trends of the salt walls (Figure 40D). The second fault array, located in the eastern part of the study area, trends from north-northwest to south-southeastand has larger offset then the first fault family. Some of the supra-salt faults above a salt diapir or salt wall form crestal collapsed graben structures with partial intrusion of salt (Figure 26). Overall, the origin of supra-salt faults is related to the upward tectonic movements, resulting in the "pushing" of overlying strata, its strengthening and followed by collapse. Throughout the NDB, individual salt stocks have been reactivated at a later stage and propagate into the Cenozoic succession and in places up to sea floor.

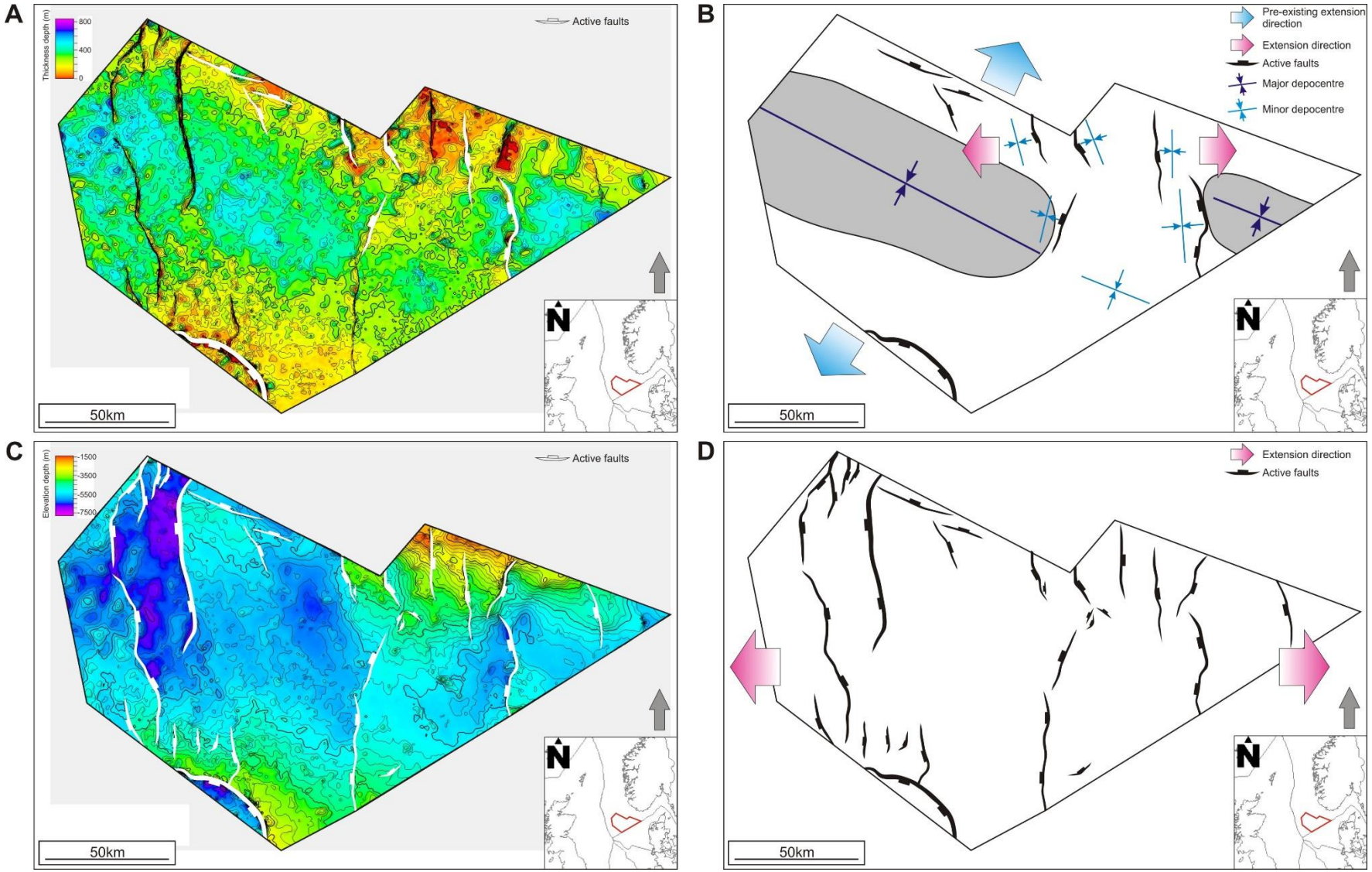

Figure 38. Pre-salt structurization. (A) Isopach map between base Zechstein and base Rotliegend showing the Rotliegend sag basins with active faults; (B) Structural elements map of the Rotliegend interval; (C) Top of the Rotliegend Group with penetrating faults; (D) Structural elements map of Late Permian interval.

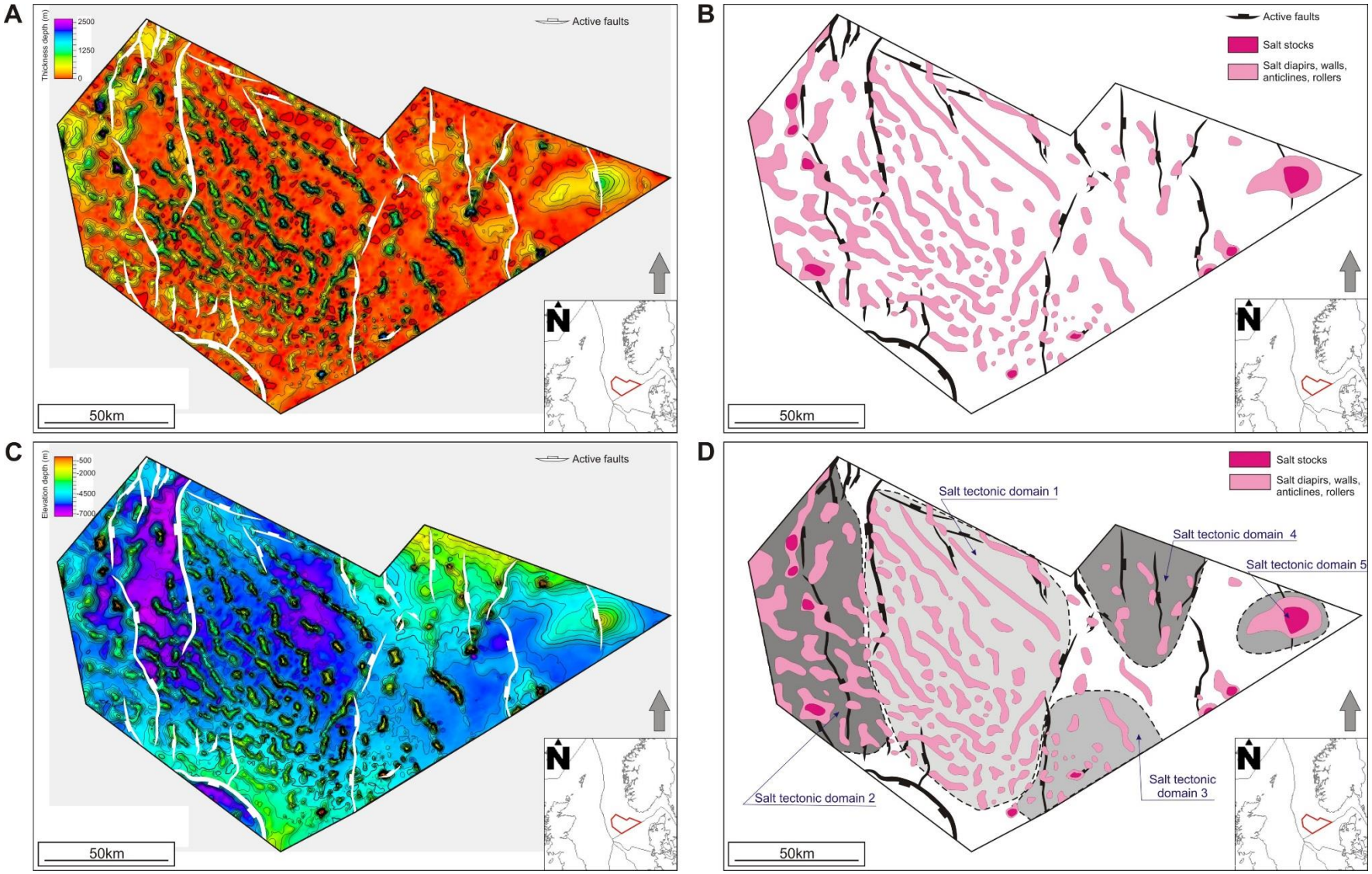

Figure 39. Structural impact on salt distribution. (A) Isopach map of the Zechstein Group; (B) Structural elements map showing the distribution of salt structures with Rotliegend faults; (C) Top of the Zechstein Group with Rotliegend faults; (D) Structural elements map with the location and distribution of major salt tectonic domains.

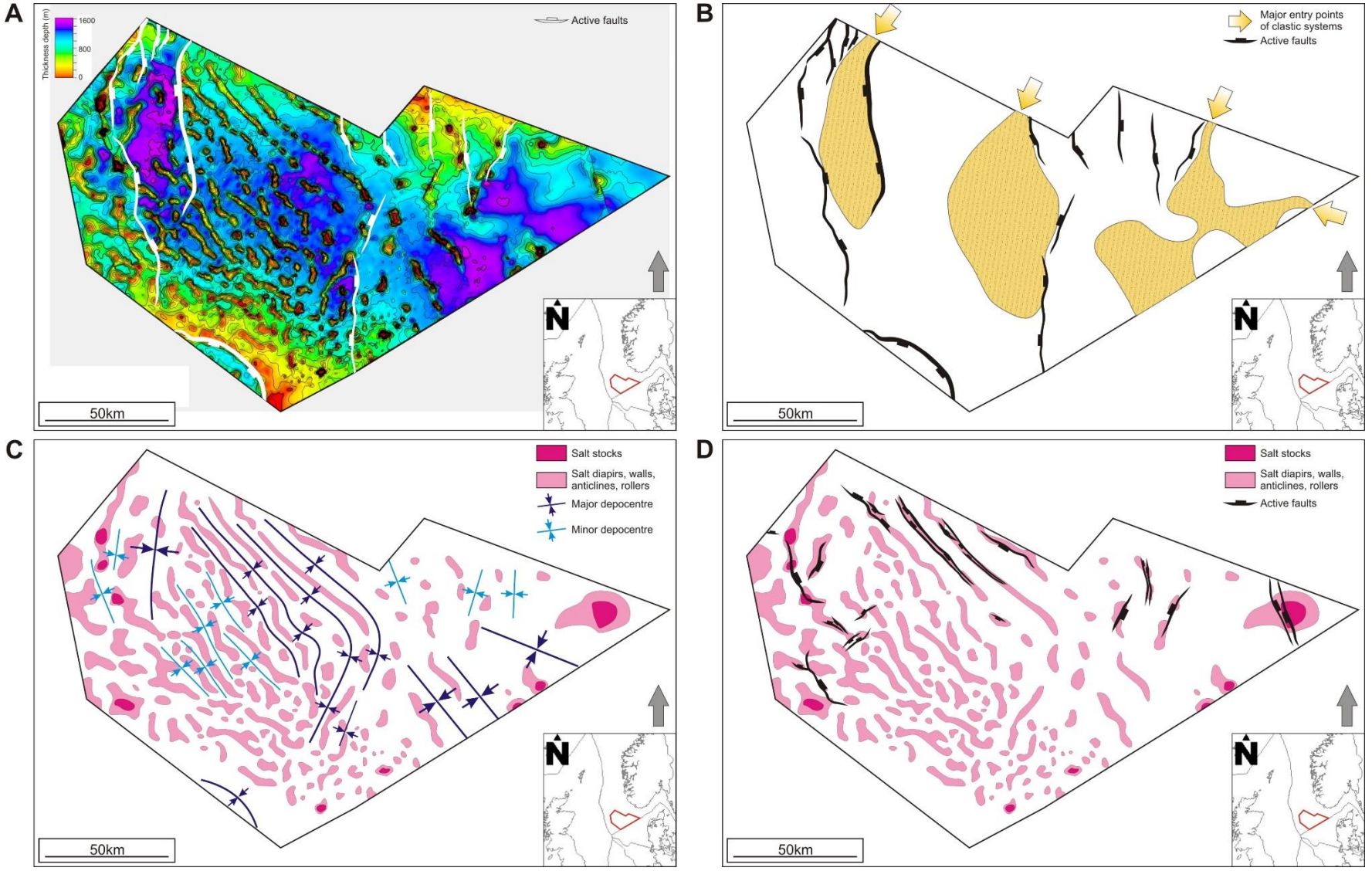

Figure 40. Salt impact on deposition of Triassic succession. (A) Isopach map of the Triassic interval (top Zechstein – Top Skagerak Fm); (B) Structural elements map showing the main entry points for Triassic clastic systems; (C) Structural elements map showing the distribution of Triassic depocentres; (D) Structural elements map with faults penetrating the top of the Skagerrak Formation.

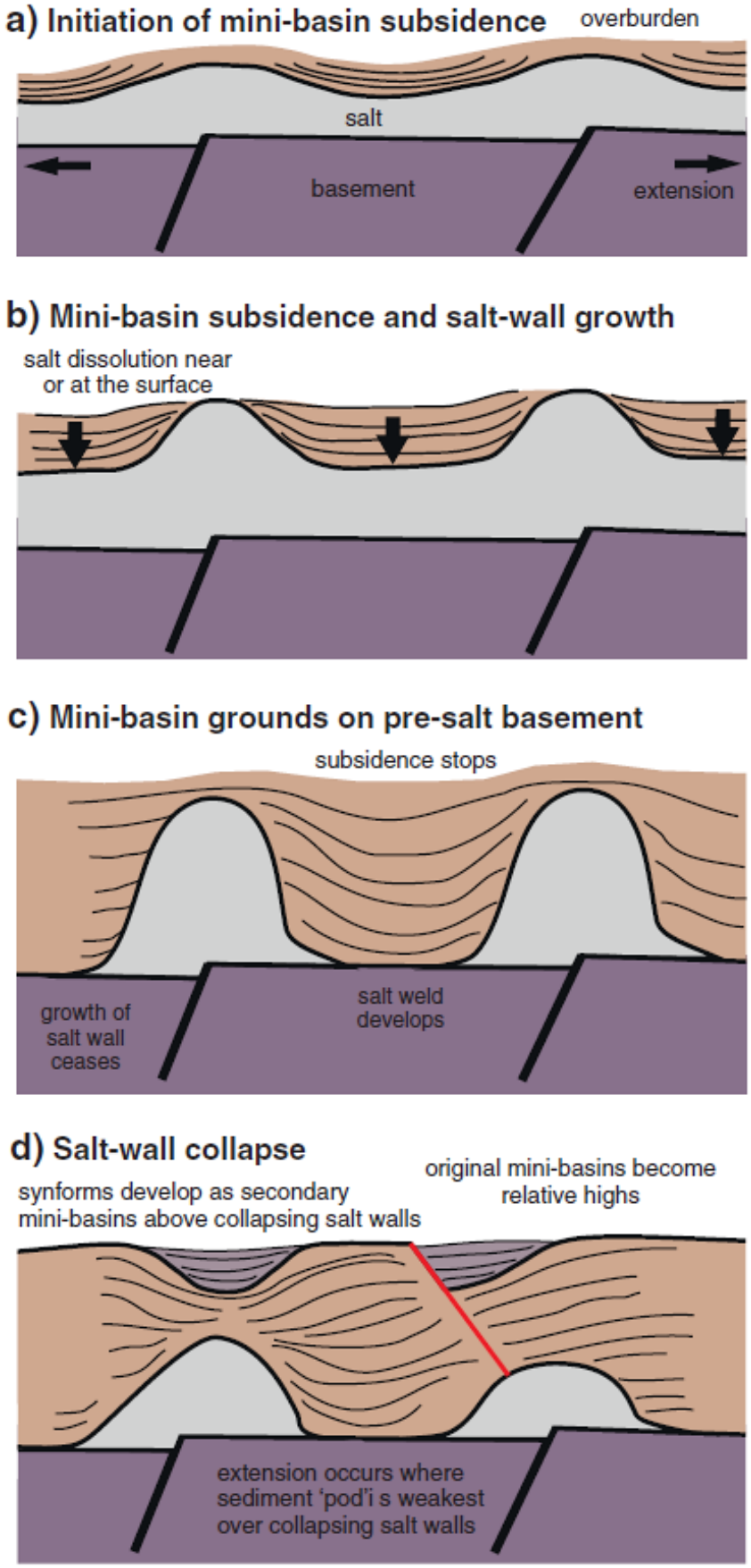

Figure 41. Conceptual model for the structural and stratigraphic evolution of salt-walled minibasins through various stages of evolution (Hogson et al., 1992).

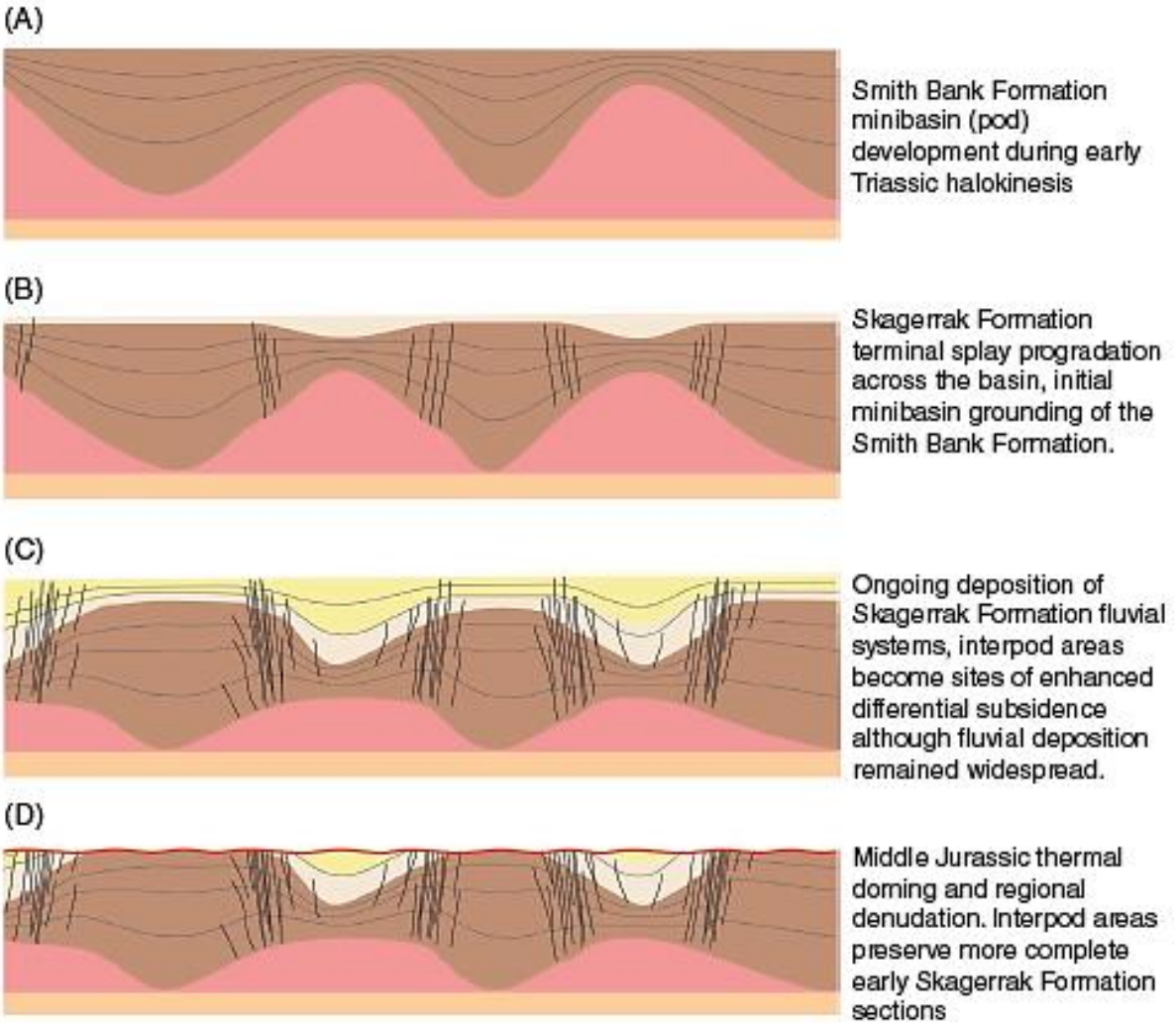

Figure 42. Model for stratigraphic infill of pod-interpod accumulation from Smith Bank Formation to Skagerrak Formation (McKie, 2014).

5.2. Structural impact on Play Elements

An understanding of the NDB framework on a regional scale is essential to the petroleum play assessment of the potential of the basin. Main outcomes of this basin analysis are conceptual geological models of predicted petroleum system elements, such as reservoir, source rock and seal – the critical components of the play definition. The distribution and determination of play elements is the primary step towards categorizing, mapping and quantification of plays within the NDB. Based on the petroleum play assessment, three geological plays with a working petroleum system are proposed, these are the Upper Permian, Upper Triassic and Lower Triassic plays, in the relatively unexplored NDB (Appendix 5, Appendix 6).

5.2.1. Paleozoic Source Rocks

There are three source rock candidates within the NDB (Figure 43), Lower Carboniferous marine shales, Upper Carboniferous coals and Upper Permian organic rich shales. Relatively unexplored and without any well penetrations in the NDB, the Lower Carboniferous (Dinantian) source beds comprise calcareous marine shales with good potential for generating both oil and gas. Source beds of Namurian and Westphalian (Upper Carboniferous) age include dominantly gas prone deltaic and carboniferous shales with coals (Pedersen et al., 2006a). Both of these source rocks accumulated during a pre- and synrift regime in a marginal marine to paralic depositional environment during anoxic conditions with preservation of good quality type II organic matter (Grautier, 2003). The Lower Permian Kupferschiefer Fm contains relatively thin up to 2 m grey-black radioactive organic rich shales deposited in an anoxic basinal environment in the in this study identified Rotliegend depocentres (Figure 19, Figure 20) and is predominantly oil prone (Pedersen et al., 2006a; Pedersen et al., 2006b; Evans et al., 2003).

5.2.2. Permian-Triassic Reservoirs

Potential reservoir rocks, identified in the study area, are of Late Permian age (Rotliegend Gp) and Triassic age (Smith Bank Fm and Skagerrak Fm; Figure 43). Rotliegend reservoirs mainly accumulated in the desert depositional environment during arid climate, resulting in aeolian sands with good to excellent reservoir properties (Evans et al., 2003). Based on observations, two principal WNW-ESE oriented depocentres, are presented as interior sag basins, located in the northern-central part and in the south-eastern part of the NDB (Figure 38A). These depocentres exhibit a WNW-ESE aligned basinal axis and

significant thicknesses of aeolian sands (up to 700 m), making the Rotliegend Gp succession the primary sub-salt reservoir.

Supra-salt reservoir candidates are those of the Lower Triassic Smith Bank Fm and the Upper Triassic Skagerrak Fm (Figure 43). The reservoirs are characterized as clastic semi-arid to dryland (fluvial) continental deposits with a high sandstone content. Halokinetic movements had a fundamental control on the deposition and distribution of the Triassic reservoirs, resulting in pod-itrapod structural and sedimentary architecture (Figure 41, Figure 42) with formation of Triassic mini-basins with a linear shape (Figure 35, Figure 36). Due to salt walls collapse, axial migration and dissolution of salt, primary mini-basins has been inverted resulting in the generation of accommodation space for secondary mini-basins.

5.2.3. Seal

The most effective regional caprock/seal within the NDB is the Zechstein evaporate succession (Figure 43). The Upper Permian Zechstein Group consists of salt and gypsum sequences with seven cycles of salt deposition and evaporation (Ramberg et al., 2008). In addition, salt forms excellent lateral seal for salt flanks traps with reservoir juxtaposed against the salt structures (Figure 43).

Another sealing mechanism is related to juxtaposition by fault movement, linking to various types, such as clay smear potential, Shale Gauge Ratio (SGR), small cataclasites and diagenesis.

The third proposed seal is related to the Middle Triassic Muschelkalk Fm, containing sequences of claystones, marls and salt, deposited in a transitional shallow-open marine setting along with evaporitic precipitation in restricted areas (Dinoloket, 2016). The Muschelkalk caprock includes siliciclastics sediments, hence it can form an effective seal for Lower Triassic reservoirs of the Smith Bank Fm. Transgressive marine shales of the Fjerritslev Fm (Lower Jurassic) forms a good regional top seal for the underlying Middle-Upper Triassic reservoirs (Vollset and Doré, 1984).

5.2.4. Migration Pathways

Secondary migration from Paleozoic source rocks is possible all over the sedimentary basin, due to the buoyancy of hydrocarbons. The main hydrocarbon migration routes involve long-distance lateral and vertical migration along permeable fault planes and through salt windows in areas with grounded Triassic pods (Figure 43).

5.2.5. Sub- and supra-salt traps

The structural evolution of the NDB during the Permian-Triassic is the principal mechanism for generating sub- and supra-salt traps. Salt movement by reactivation of sub-salt faults is the primary mechanism of forming sub- and supra-salt traps, comprising a wide variety of structural and stratigraphic trapping regimes or complex combined traps (Figure 43).

Sub-salt traps are predominantly structural, defined by four-way closures and fault bounded two-way closures (Figure 27, Figure 30, Figure 43). Such traps are widely distributed in the Lista Fault Blocks area and adjacent in the Åsta Graben. Structural sub-salt traps were produced during the reactivation of Late Permian normal faults. Furthermore, stratigraphic traps are recognized within the Upper Paleozoic levels and classified as depositional pinch-outs in the Rotliegend Gp. Overall, combination traps are widely distributed in the basin, including complex associations involving salt or fault sealing and all above mentioned trapping styles (Figure 26). Hence, salt tectonics has a significant impact in determining complex traps and their geometries.

A wide variety of structural and stratigraphic supra-salt traps developed in the Triassic interval due to the halokinetic movements of the Zechstein salt (Figure 43). The majority of supra-salt traps, predominantly stratigraphic, are in the crests of turtle structures (Figure 28, Figure 29), up dip pinch-outs, occurring near salt structures due to facies change (Figure 26, Figure 27, Figure 28, Figure 29, Figure 37), and fluvio-channel traps, related to pod-intrapod sedimentation (Figure 28, Figure 31). Alternative trapping potential in the Triassic sediments above the salt are diapiric rock reservoirs and domal traps with and without associated faulting (Figure 26, Figure 31). These structural traps usually developed above salt diapirs and salt walls during the post-halokinetic stage. Other structural traps, widely distributed in the NDB, are four-way closures and fault traps, caused by halokinetic movements (Figure 27, Figure 30). Many traps are a combination of structural and stratigraphic traps with truncation against the salt bodies or fault planes (Figure 31). The final trapping regime recognized within the basin is a regional subcrop traplinked to the Lower Jurassic unconformity (Figure 37).

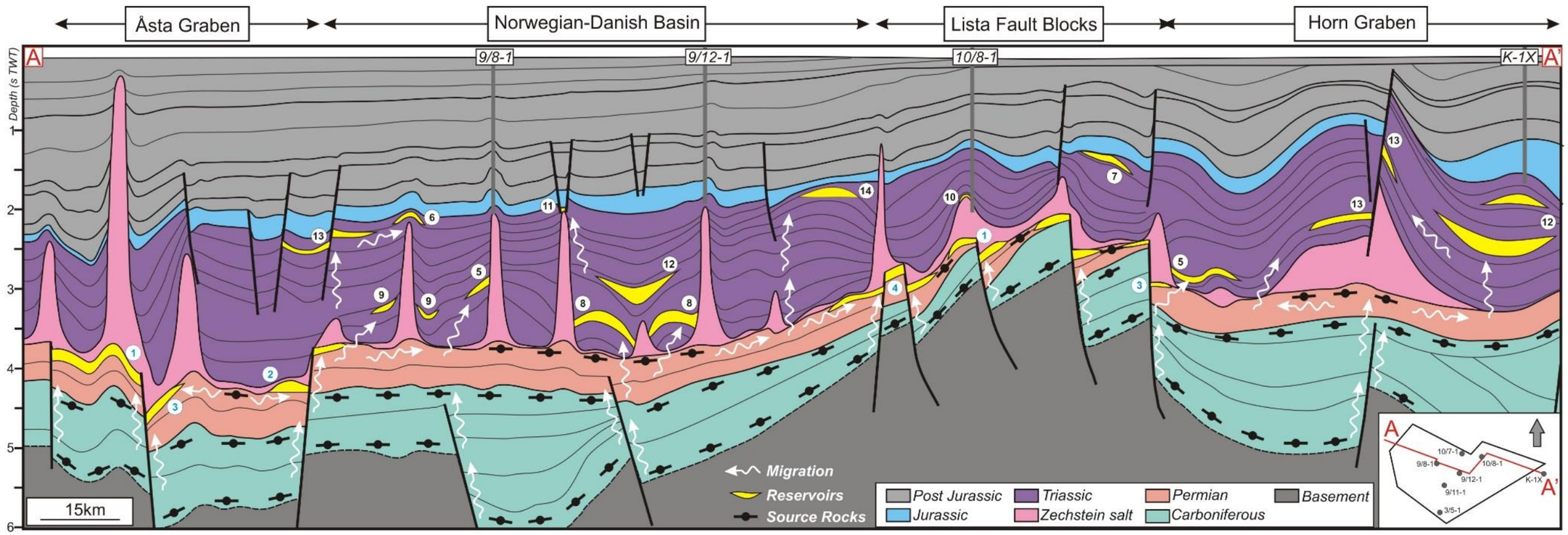

Source Rock:
- Upper Permian (Kupferschiefer Fm) organic rich shale;
- Upper Carboniferous (Namurian and Westphalian age) deltaic shale, carbonaceous shale and coal;
- Lower Carboniferous (Dinantian age) calcareous marine shale.

Reservoir:
- Upper Triassic (Skagerrak Fm) clastic continental deposits, mainly sandstone;
- Lower Triassic (Smith Bank Fm) clastic continental deposits, mainly sandstone;
- Upper Permian (Rotliegend) aeolian sandstone.

Seal:
- Fault sealing;
- Lower Jurassic (Fjerritslev Fm) marine shale;
- Middle Triassic (Muschelkalk Fm) claystone, marl and salt.
- Upper Permian (Zechstein Fm) salt.

Migration Pathways:
- Lateral and vertical migration;
- Aloung fault planes;
- Windows through grounded Triassic pods.

Sub-salt traps:
- Tilted fault blocks sealed by fault and salt (1)
- Four-way closure (2)
- Horst block traps (3)
- Stratigraphic pinch-out sealed by fault and salt (4)

Supra-salt traps:
- Reservoir truncated against salt (5)
- Domal trap above salt with no assosiated faulting (6)
- Subcrop trap related to Lower Jurassic unconformity (7)
- Turtle structures (8)
- Stratigraphic up dip pinch-out due to facies changes near salt structures (9)
- Diapiric cap rock reservoir (10)
- Domal trap above salt with assosiated faulting (graben structure) (11)
- Stratigraphic fluvio-channel trap (12)
- Fault trap (13)
- Four-way closure (14)

Figure 43. Conceptual geological section of the NDB, highlighting the Carboniferous-Triassic interval along with the sub-salt and supra-salt main petroleum systems and play elements.

6. Conclusions

6.1. Late Permian to Triassic tectono-stratigraphic evolution of the NDB

- In the Early-Middle Permian, the two major WNW-ESE trending interior sag basins with thick Rotliegend strata were formed in response to the pre-existing NE-SW Carboniferous rifting. The following rifting event with W-E extensional direction initiated in the eastern part of the NDB;
- The Late Permian is characterized by widespread rifting with a predominant W-E extensional direction, resulting in N-S oriented regional sub-salt fault and main tectonic domains within the NDB;
- Accumulation and distribution of the Zechstein salt interval was limited to the major Rotliegend depocentres as well as Late Permian extensional faults;
- Halokinetic movements within the NDB occurred due to the subsidence of Triassic sediments, differential loading and reactivation of sub-salt normal faults. As a result, it significantly affected salt movements along with the stratigraphic and structural architecture, described by the pod-intrapod model;
- The supra-salt normal faults formed in response to salt tectonics in the Late Triassic-Early Jurassic during the final tectonic stage in this period.

6.2. Halokinetic impact on play characterization and distribution

- Zechstein salt within the NDB provides a regional top seal for sub-salt plays;
- Halokinesis principally controls reservoir distribution, sealing mechanism, trap types and their distribution and allows just one possible charging mechanisms from subsalt source rock through salt windows in areas with grounded Triassic pods.

6.3. Sub- and supra-salt play potential

- Conceptual sub-salt Upper Permian and supra-salt Triassic plays cover an extensive area of the NDB. The supra-salt trapping mechanism is principally related to salt movements, comprising both structural and combined structural-stratigraphic types. Upper Permian play should be an important exploration target, due to presence of good quality aeolian Rotliegend sandstones as reservoir, and the Zechstein salt as an effective regional impermeable caprock. Supra-salt Upper and Lower Triassic plays have considerable exploration potential, comprising sandstone reservoirs from two

stratigraphic levels, Smith Bank Fm and Skagerrak Fm, and working seals such as theMuschelkalk evaporites and marls along with the Fjerritslev marine shales. Sub- and supra salt plays are charged by a working Paleozoic petroleum system, and migration is facilitated by pathways along fault planes and windows through grounded Triassic pods.

Appendix

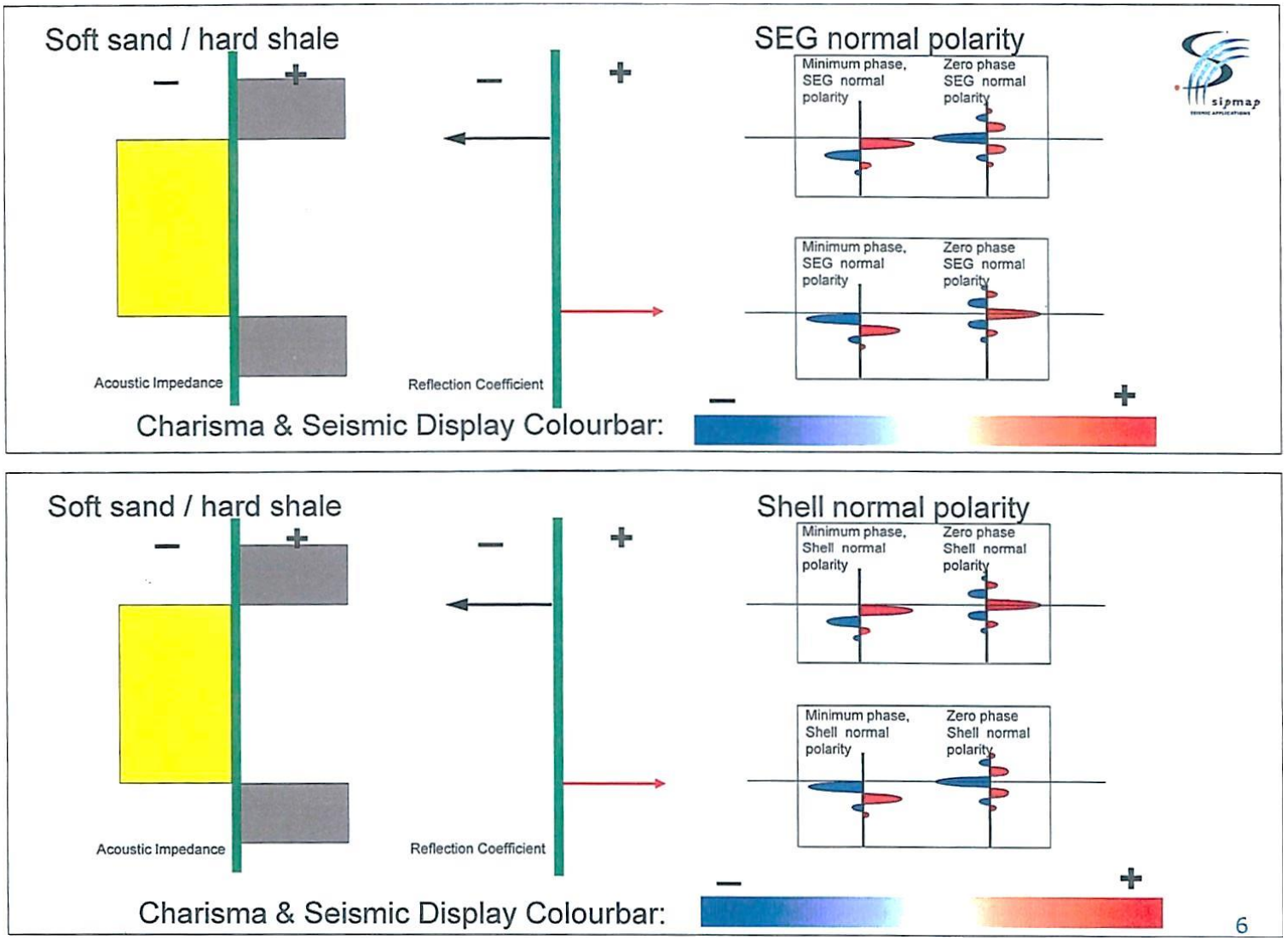

Appendix 1. Seismic polarity (from internal Shell seismic processing software SIPMAP).

Rotliegend Group	**Fault Group**	***First Fault Group***														
	Number of fault	**1**	**2**	**3**	**4**	**5**	**6**	**7**	**8**	**9**	**10**	**11**	**12**	**13**	**14**	**15**
	Strike ° (RHR)	239°	27°	164°	205°	206°	176°	201°	355°	358°	180°	175°	339°	167°	192°	179°
	Fault Group	***First Fault Group***												***Second Fault Group***		
	Number of fault	**16**	**17**	**18**	**19**	**20**	**21**	**22**	**23**	**24**	**25**	**26**	**27**	**28**	**29**	**30**
	Strike ° (RHR)	33°	18°	179°	177°	8°	178°	332°	2°	4°	305°	345°	159°	290°	287°	123°

Appendix 2. Measurements of strike directions of faults, penetrating Top of Rotliegend.

Salt structures	***Type 1. NW-SE trending salt walls***													
	Direction 1											***Direction 2***		
Number of salt structures	1	2	3	4	5	6	7	8	9	10	11	12	13	14
Strike °	124°-304°	118°-298°	141°-321°	149°-329°	154°-334°	129°-309°	144°-324°	141°-321°	137°-317°	132°-312°	129°-309°	12°-192°	23°-203°	13°-193°

Salt structures	***Tpe 2. NNE-SWW trending salt walls***						**Type 5. Salt rollers and anticlines**					**Type 6. Giant salt roller structure**
	Direction 1			***Direction 2***			***Direction 1***			***Direction 2***		
Number of salt structures	15	16	17	18	19	20	21	22	23	24	25	26
Strike °	17°-197°	19°-199°	4°-184°	136°-316°	135°-315°	117°-297°	22°-202°	161°-341°	174°-354°	147°-327°	156°-336°	107°-287°

Appendix 3. Measurements of salt structures alignment.

Skagerrak Formation	**Fault Group**	***First Fault Group***														
	Number of fault	**31**	**32**	**33**	**34**	**35**	**36**	**37**	**38**	**39**	**40**	**41**	**42**	**43**	**44**	**45**
	Strike ° (RHR)	291°	296°	277°	320°	133°	117°	334°	122°	314°	135°	311°	317°	139°	136°	319°
	Fault Group	***First Fault Group***					***Second Fault Group***									
	Number of fault	**46**	**47**	**48**	**49**	**50**	**51**	**52**	**53**	**54**	**55**	**56**				
	Strike ° (RHR)	6°	17°	56˚	54˚	234˚	29˚	354˚	175˚	208˚	341˚	163˚				

Appendix 4. Measurements of strike direction of faults, penetrating Top of Skagerrak.

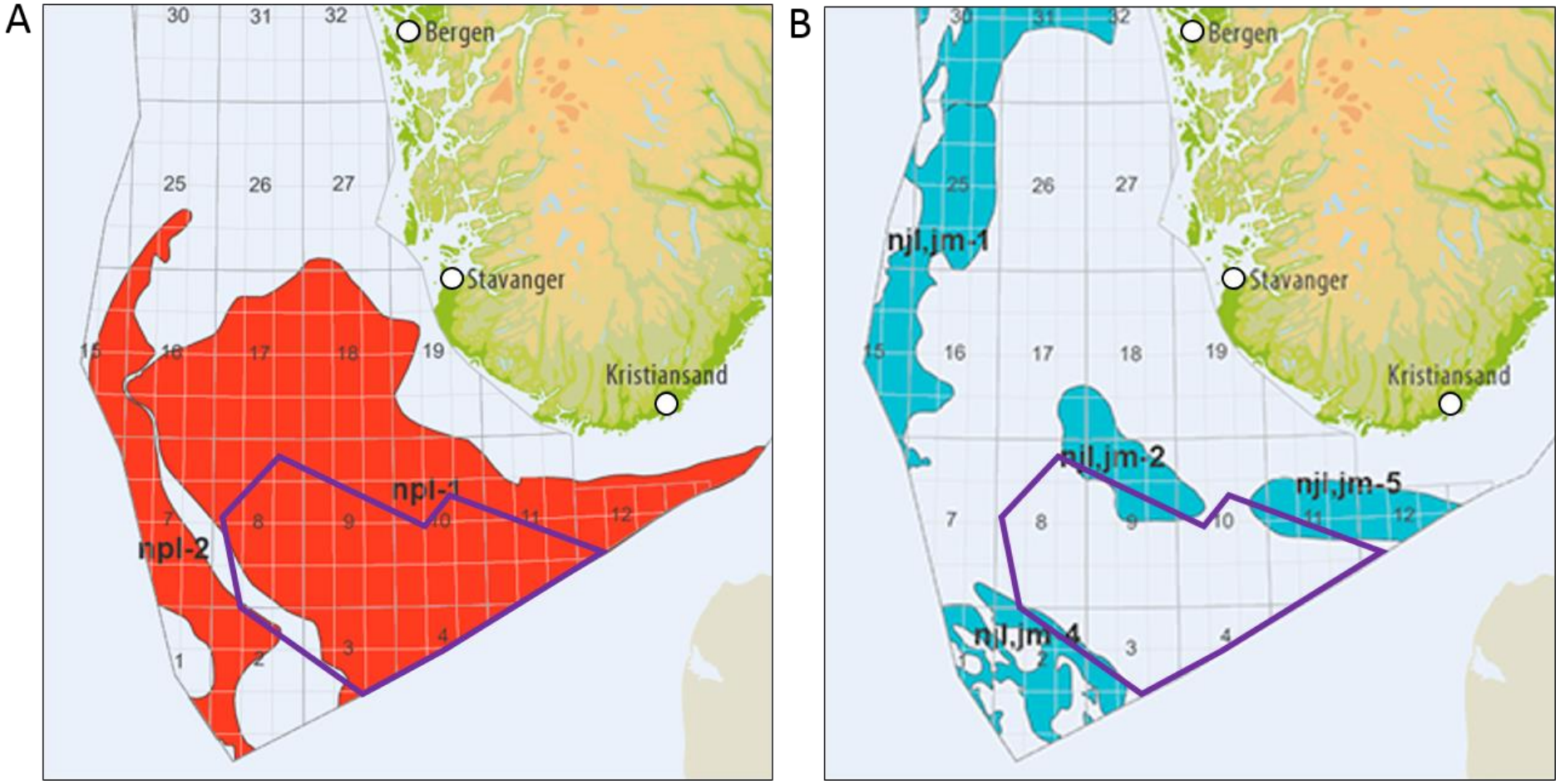

Appendix 5. (A) Carboniferous-Permian plays (NPD, 2015); (B) Upper Triassic, Lower to Middle Jurassic plays (NPD, 2015) with study area in violet.

	North Sea – Sub Triassic plays	North Sea – Upper Triassic, Lower to Middle Jurassic plays	
Name	npl- 1 (unconfirmed)	njl,jm-4	njl,jm-2
Group/ Formation	Rotligendes Gp and unnamed groups of Devonian and Carbonaceous age	Hegre Gp with Skagerak Fm, Gassum Fm, Vestland Gp with Bryne Fm	Gassum Fm, Vestland Gp with Bryne and Sandnes Fm
Age	Devonian, Carboniferous, Permian and possible Triassic	Rhaetian - Bathonian	Norian - Callovian
Area	Danish-Norwegian Basin, Egersund Basin, Ling Graben and Sele High	Central Graben	Egersund Basin
Reservoir rock	Sandstone	Sandstone	Sandstone
Depositional environment	Mainly continental	Fluvial, deltaic and shallow marine	
Trap	Rotated fault-blocks	Structural, rotated fault blocks, occasionally with stratigraphic component, sealing faults	
Source rock	Unknown source of PreTriassic age	Upper Jurassic shale (Draupne, Heather, Tau, Farsund and Mandal Fm) and Middle Jurassic shale and coal (Gassum, Bryne, Ness and Sleipner Fm, possible Drake Fm)	
Critical factors	Presence of mature source rock in the eastern area is not confirmed, migration, timing, reservoir quality due to reservoir depth	Mature source rock in Farsund Basin	
Examples of fields		Trym	Yme

Appendix 6. Combined information table regarding to identified geological plays within the North Sea (NPD, 2015).

References

Allen, P. A. and J. R. Allen, 2013, Basin Analysis: Principles and Application to Petroleum Play Assessment, Third Edition, Wiley-Blackwell, Oxford, 619 pp.

Bishop, D. J., 1996, Regional distribution and geometry of salt diapirs and supra-Zechstein Group faults in the western and central North Sea: Marine and Petroleum Geology 13(4), p. 355-364.

Bishop, D. J., P. G. Buchanan, and C. J. Bishop, 1995, Gravity-driven thin-skinned extension above Zechstein Group evaporites in the western central North Sea: an application of computer-aided section restoration techniques: Marine and Petroleum Geology 12, p. 115-135.

Buchanan, P. G., D. J. Bishop, and D. Hood, 1995, Development of salt related structures in the central North Sea: results from section balancing: Geological Society of London, Special Publications 100, p. 111-128.

Collinson, J. D., C. M. Jones, G. A. Blackbourn, B. M. Besly, G. M. Archard, and A. H. McMahon, 1993, Carboniferous depositional systems of the southern North Sea, in J. R. Parker, eds., Petroleum geology of northwest Europe: Proceedings of 4th Conference, Geological Society, London, p. 677–687.

Cornford, C., 1998, Source rocks and hydrocarbons of the North Sea, in K. W. Glennie, eds., Petroleum geology of the North Sea—Basic concepts and recent advances: London, Blackwell Scientific Publishers, p. 376–462.

Coward, M. P., 1995, Structural and geological setting of the Permo-Triassic basins of northwest Europe, in S. A. R. Boldy, eds., Permian and Triassic Rifting in northwest Europe: Geological Society, Special Publications 91, p. 7-39.

Deegan, C. E. and B. J. Scull, 1977, A standard lithostratigraphic nomenclature for the Central and Northern North Sea: UK Institute of Geological Sciences, Report 77/25, The Norwegian Petroleum Directorate, NPD-Bulletin No. 1, 36 pp.

Dinoloket, 2016, accessed May 1, 2016, https://www.dinoloket.nl/muschelkalk-formation-rnmu.

Evans, D., C. Graham, A. Armour, and P. Bathurst, eds., 2003, The Millennium Atlas: Petroleum Geology of the Central and Northern Sea: London, Geological Society of London, 389 pp.

Farmer, P., D. Miller, A. Pieprzak, J. Rutledge, and R. Woods, 1996, Exploring the Subsalt: Oilfield Review 8, no. 1, p. 50-64.

Fossen, H., 2010, Structural Geology: Cambridge, UK, Cambridge University Press, 463 pp.

Fraser, A. J., J. Farnsworth, and N. A. Hodgson, 1993, Salt controls on Basin Evolution - Central North Sea: Special Publications of the European Association of Petroleum Geoscientists 3, p. 59-68.

Grautier, D. L., 2003, Carboniferous-Rotliegend total petroleum system description and assessment results summary: US Geological Survey, Bulletin 2211, 24 pp.

Halland, E. K., I. T. Gjeldvik, W. T. Johansen, C. Magnus, I. M. Meling, S. Pedersen, F. Riis, T. Solbakk, and I. Tappel, 2011, CO2 Storage Atlas for the Norwegian continental shelf: Norwegian Petroleum Directorate (NPD), 163 pp.

Hamar, G. P., K. H. Jakobsson, D. E. Ormaasen, and O. Skarpnes, 1980, Tectonic development of the North Sea, north of the Central Highs, The sedimentation of the North Sea reservoir rocks, Norwegian Petreoleum Society, 11 pp.

Hodgson, N. A., J. Farnsworth, and A. J. Fraser, 1992, Salt-related tectonics, sedimentation and hydrocarbon plays in the Central Graben, North Sea, UKCS: London, Geological Society of London, Special Publications 67, p. 31-63.

Hospers, J., J. S. Rathore, F. Jianhua, E. G. Finnstrom, and J. Holthe, 1988, Salt tectonics in the Norwegian-Danish Basin: Tectonophysics, 149, p. 35-60.

Hudec, M. R. and M. P. A. Jackson, 2007, Terra infirma: Understanding salt tectonics, Earth-Science Reviews 82, p. 1-28.

Husebye, E. S., H. E. Ro, J. J. Kinck, and F. R. Larsson, 1988, Tectonic studies in the Skagerrak province: the 'Mobil Search' cruise: Norges Geologisk Undersokelse, Special Publication 3, p. 14-20.

Karlo, J. F., F. S. P. van Buchem, J. Moen, and K. Milroy, 2014, Triassic salt tectonics of the Central North Sea, Society of Exploration Geophysicists and American Association of Petroleum Geologists, Special section: Salt tectonics and Interpretation, Interpretation, Vol. 2, No. 4, p. 19-28.

Lewis, M. M., C. A.-L. Jackson, and R. L. Gawthorpe, 2013, Salt-influenced normal fault growth and forced folding: The Stavanger Fault System, North Sea; Journal of Structural Geology 54, p. 156-173.

Maystrenko, Y. P., U. Bayer, and M. Scheck-Wenderoth, 2013, Salt as a 3D element in structural modeling - Example from the Central European Basin System: Tectonophysics 591, p. 62-82.

McKie, T., 2014, Climatic and tectonic controls on Triassic dryland terminal fluvial system architecture, central North Sea, *in* A. W. Martinius, R. Ravnås, J. A. Howell, R. J. Steel and J. P. Wonham, eds, From depositional systems to sedimentary successions on the Norwegian continental margin: Special Publications of the International Association of Sedimentologists, 46, p. 19-58.

Norwegian Petroleum Directorate (NPD), 2015, Topics: Geology: Geological Plays: North Sea, accessed April 15, 2016, http://www.npd.no/en/Topics/Geology/Geological-plays/.

Norwegian Petroleum Directorate (NPD), 2014, Topics: Geology: Lithostratigraphy: North Sea, accessed April 15, 2016, http://www.npd.no/en/Topics/Geology/Lithostratigraphy/.

Pedersen, J. H., D. A. Karlsen, J. E. Lie, H. Brunstad, and R. Primio, 2006a, Maturity and source-rock potential of Paleozoic sediments in the NW European Northern Permian Basin: London, Geological Society of London, Petroleum Geoscience 12, p. 13-28.

Pedersen, J. H., D. A. Karlsen, K. Backer-Owe, J. E. Lie, and H. Brunstad, 2006b, The geochemistry of two unusual oils from the Norwegian North Sea: implications for new source rock and play scenario: London, Geological Society of London, Petroleum Geoscience 12, p. 85-96.

Petersen, H. I., L. H. Nielsen, J. A. Bojesen-Koefoed, A. Mathiesen, L. Kristensen, and F. Dalhoff, 2008, Evaluation of the quality, thermal maturity and distribution of potential source rocks in the Danish part of the Norwegian-Danish Basin: Geological survey of Denmark and Greenland 16, p. 1-66.

Rønnevik, H. C., W. van den Bosch, and E. H. Bandlien, 1975, A proposed nomenclature for the main structural features in the Norwegian North Sea, *in* K. G. Finstad and R. C. Selley, eds, Jurassic northern North Sea Symposium, Stavanger, Norwegian Petroleum Society, 12 pp.

Ramberg, I. B., A. Solli, Ø. Nordgulen, R. Binns, and P. Grogan, 2008, The Making of a land: geology of Norway: Trondheim, Norwegian Geological Association, 624 pp.

Ro, H. E., L. M. Stuevold, J. I. Faleide, and A. M. Myhre, 1990, Skagerrak Graben – the offshore continuation of the Oslo Graben: Tectonophysics 178, p. 1-10.

Skjerven, J., F. Rijs, and J. E. Kalheim, 1983, Late Palaeozoic to Early Cenozoic structural development of the south-southeastern Norwegian North Sea, *in* J. P. H. Kaasschieter and T. J. A. Reijers, eds., Petroleum Geology of the South-eastern North Sea and the Adjacent Onshore Areas: Geol. Mijnbouw 62, p. 25-45.

Sørensen, S., H. Morizot, and S. Skottheim, 1992, A tectonostratigraphic analysis of the Southeast Norwegian North Sea basin: Special Publications, Norwegian Petroleum Society, NPF 1, p. 19-42.

Stewart, S. A. and M. P. Coward, 1995, Synthesis of salt tectonics in the southern North Sea: UK, Marine and Petroleum Geology 12, p. 457-475.

Tvedt, A. B. M., A. Rotevatn, C. A.-L. Jackson, H. Fossen, and R. L. Gawthorpe, 2013, Growth of normal faults in multilayer sequences: A 3D seismic case study from the Egersund Basin, Norwegian North Sea: Journal of Structural Geology 55, p. 1-20.

Vollset, J. and A. G. Doré, 1984, A revised Triassic and Jurassic lithostratigraphic nomenclature for the Norwegian North Sea: NPD-Bulletin, 3, 53 pp.

Ziegler, P.A., 1981, Evolution of sedimentary basins in north-west Europe, *in* L. V. Illing, and D. C. Hobson, eds., Petroleum geology of the Continental Shelf of North-West Europe, Proceedings of the Second Conference, Heyden, London, p. 3-39.

Ziegler, P. A., 1982, Geological Atlas of western and central Europe: Shell Intern. Petr. Maatsch, 130 pp.

Ziegler, P.A., 1990, Geological Atlas of western and central Europe, Second edition: Shell Intern. Petr.. Mij, 239 pp.

Ziegler, P.A., 1992, North Sea rift system: Tectonophysics 208, p. 55-75.